Design and Process Optimization of a Hot Embossing Machine for Microfluidics with High Aspect ratios

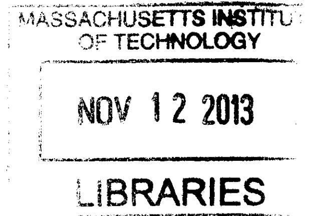
ARCHIVES
MASSACHUSETTS INSTITUTE OF TECHNOLOGY
NOV 12 2013
LIBRARIES

by

Viren Sunil Kalsekar
B.E. Honors, Mechanical Engineering, BITS Pilani, 2011

Submitted to the Department of Mechanical Engineering in partial fulfillment of the requirements for the degree of

Masters of Engineering

at

MASSACHUSETTS INSTITUTE OF TECHNOLOGY
September 2013

© Massachusetts Institute of Technology, 2013. All rights reserved

Author:..

Department of Mechanical Engineering

August 9, 2013

Certified by: ....

Dr. Brian Anthony
Thesis Advisor

Accepted by: ....

Dr. David E. Hardt
Ralph E. & Eloise F. Cross Professor of Mechanical Engineering,
Chairman, Department Committee on Graduate Students

This page intentionally left blank

Design and Process Optimization of a Hot Embossing Machine for Microfluidics with High Aspect ratios

By

Viren Sunil Kalsekar

Submitted to the Department of Mechanical Engineering on August 9, 2013
In Partial Fulfillment of the Requirements for the Degree of
Master of Engineering in Manufacturing

Abstract

Microfluidics is a growing technology in the field of medical diagnostics. Daktari Diagnostics is a startup located in Cambridge, MA that seeks to introduce a lab-on-a-chip device for monitoring HIV in patients. This work investigates hot embossing as a prototyping process for Daktari's microfluidic device. A hot embossing system was designed and built for the purpose of prototyping a critical feature of their microfluidic network. The machine was designed for an embossing area of 6 square inches, and was found to have a maximum positional repeatability of 43 microns.

The purpose of this research was to find the capabilities of the system used for hot embossing and optimize the process for maximizing the performance. The system was validated for alignment, measurement procedure and the process control. The measuring procedure was analyzed to find the best possible metric which could serve as a response variable for the performance of the process. The 'Fill ratio' of height and width were chosen as metrics for the experimental design which had precision to tolerance ratios of 0.44 and 0.33 respectively. An analysis of the factors affecting the hot embossing process was carried out using experimental design and the optimal parameters were identified. The tool temperature, pressure and the holding time were the most significant in that order. The C_p for the process with respect to the height fill was found to be 4.71 and for the width fill ratio was found to be 1.97. Using the optimal parameters the process variation of six standard deviations was found to lie within the specification limits. Hot embossing was recommended as a possible method for rapid prototyping of the assay channel and the complete cartridge at Daktari Diagnostics.

Thesis Supervisor: Dr. Brian Anthony
Title: Research Scientist

ACKNOWLEDGEMENTS

I want to thank my team mates and friends Nicholas Ragosta and Khanh Nguyen for their unbridled enthusiasm and support. It was great fun and a valuable experience working with them at Daktari Diagnostics.

Professor Brian Anthony, our advisor guided us through every phase of this project and his insightful advice helped us in channeling our ideas. I am grateful for the learning experience that he provided and he will always be an inspiration.

I would also like to thank Jennifer Craig for her help and advice on the technical writing throughout the semester.

I would especially like to thank Robert Etheredge, Aaron Oppenheimer, David Boccuti and Tony Sharma for the continual support and guidance throughout the project. I would also like to thank the whole Daktari team for the wonderful time we had at Daktari and I would take away a lot of knowledge and great experience.

Finally I would also like to thank my family and friends for being by my side and for their constant words of encouragement and support.

Table of Contents

1 Introduction 13
1.1 Background and Research Motivation 13
1.2 Problem Statement 14
1.3 Current Prototyping Processes 14
1.3.1 Photolithography 14
1.3.2 Micromachining 15
1.3.3 Injection Molding 15
1.4 Unmet Needs 15
1.5 The Hot Embossing Solution 16
1.6 Research Objectives 17
2 Background and Product Description 18
2.1 Microfluidics 18
2.2 General Card Features 20
2.3 Targeted Feature: The Assay Channel 21
2.4 General Channel Considerations 21
3 Review of Prototyping Processes 23
3.1 Photolithography 23
3.1.1 Process 23
3.1.2 Limitations 24
3.2 Micromachining 25
3.2.1 Process 25
3.2.2 Limitations 25
3.3 Injection Molding 27
3.3.1 Process 27
3.3.2 Limitations 28
4 Hot Embossing Process 30
4.1 Selection of substrate 30
4.1.1 Basic Properties of Thermoplastics 31
4.2 The Hot Embossing Process 31
4.2.1 Initial Heating Stage 33
4.2.2 Embossing Stage 33
4.2.3 Cooling Stage 33

4.2.4 De-Molding Stage ... 34
4.3 Consideration of Process Capabilities ... 34
4.3.1 Sharp Radii ... 34
4.3.2 Unfilled Extruded Features ... 35
4.3.3 Features Ending on Edges ... 36
4.3.4 Control of Tolerances and Variability ... 36
4.3.5 Abrupt and Variable Geometries ... 37
4.3.6 Surface Roughness ... 38
5 Machine Design Approach ... 39
5.1 General Effects of Operating Parameters ... 39
5.2 Design Requirements ... 40
5.2.1 Tool and Substrate Fixture Requirements ... 40
5.2.2 Force Requirement ... 40
5.2.3 Heating Requirements ... 41
5.2.4 Cooling Requirements ... 41
5.2.5 Alignment Requirements ... 42
5.3 Common Design Practices ... 42
6 Machine Design and Evaluation ... 44
6.1 Full Assembly ... 44
6.1.1 Operational Procedure ... 45
6.2 Load Bearing and Tilt Compensation ... 45
6.3 Tool and Substrate Fixturing ... 47
6.4 Heating and Cooling ... 48
6.5 Load Sensing ... 50
7 Methodology: Process Control and Capability ... 52
7.1 Process and System Validation ... 53
7.1.1 X & Y Repeatability ... 53
7.1.2 Parallelism ... 57
7.1.3 Measurement Validation ... 59
7.2 Process Evaluation & Performance Measurement ... 60
7.2.1 Selection of Features on Microfluidics Part ... 60
7.2.2 Evaluation Metrics ... 66
7.3 Process Parameters ... 67
7.3.1 Temperature ... 68

7.3.2 Force ... 68
7.3.3 Holding time ... 69
7.3.4 De-Embossing Temperature ... 70
7.3.5 De-Embossing Force ... 70
7.3.6 Embossing Velocity ... 71
7.3.7 Material of Part ... 72
7.3.8 Thickness of the Substrate ... 73
7.3.9 Material of the Tool ... 73
7.3.10 Noise Factors ... 73
7.4 Down selection of Parameters ... 75
7.4.1 Cause and Effect Matrix ... 76
7.4.2 Pre Design of Experiments Data ... 77
7.5 Design of Experiments (Fractional Factorial Model) ... 80
7.5.1 Controllable Factors ... 81
7.5.2 Uncontrollable Factors (Noise factors) ... 82
7.5.3 Response Variables: ... 82
7.5.4 Fractional Factorial Design ... 84
7.5.5 Experiments ... 86
8 Results ... 87
8.1 Analysis of Variance (ANOVA) and Significance of Effects ... 87
8.1.1 Width Fill Analysis ... 87
8.1.2 Height Fill ... 91
8.1.3 De-Embossing Defects ... 93
8.2 Response Optimization and Analysis ... 94
8.3 Confirmation Experiments to find Process Capability ... 96
9 Recommendations ... 101
10 Conclusion and Future Work ... 102
10.1 Conclusion ... 102
10.2 Future Work ... 103
10.2.1 Machine Improvements ... 103
10.2.2 Further Experimentation ... 105
Appendix A ... 107
Engineering Drawings: ... 107
Assembly Drawing: ... 107

Sub-Assemblies 108
Bill of Materials 112
PARTS 115
Data Sheets 124
Appendix B 131
References 138

List of Figures

Figure 1: Critical parameters in microfluidics 19
Figure 2: Schematic of a channel with a capillary stop 21
Figure 3: General channel dimensions 22
Figure 4 The positive mold (left) holds desired features and the negative mold (right) holds the opposite geometries of the features 24
Figure 5 Cross sectional depiction of burrs on the edge of a possible machined channel (left). An interferometer image of a machined feature showing tool marks and possible burrs. 26
Figure 6 The standard process for milling the outside radius (left) and inside radius (right) of corners. 26
Figure 7: Injection Molding Process 28
Figure 8: The master tool (top) and substrate (bottom) are heated up (1), then pressed together (2) and finally released (3) 32
Figure 9: General hot embossing temperature and force cycles. The process cycle begins from T = 0 to T = T3 32
Figure 10 The left image shows the dragging effect where the arrows indicate the direction of the tool and material movement. The right image shows air gaps which can reduce feature radius. 35
Figure 11 Cavities in the mold can be unfilled during the embossing process if temperature, pressure, and holding time are not adequate. 35
Figure 12: Substrate edge distortion 36
Figure 13 Schematic of a general cuvette feature 37
Figure 14: Schematic of 3-way junction 38
Figure 15: Depiction of misalignment 42
Figure 16 Full assembly view 44
Figure 17 Frame assembly and cross section views. 46
Figure 18 Visualization of misalignment air gaps. 47
Figure 19 Substrate fixture 48
Figure 20 Substrate heating assembly and cross section 49
Figure 21 The cooling profile of the top and lower heating platens over a period of 2.5 mins. . 50
Figure 22 De-coupling of force sensor 51
Figure 23 Fiducials used for x, y repeatability measurements 54
Figure 24 Distance between fiducials 54
Figure 25: Error Band for the three Locations 55
Figure 26: Central axis: ISO view 56
Figure 27: Central axis: top view 57
Figure 28: Measurement Locations for Estimating Platen Parallelism 58
Figure 29 Microscope Image of Channel Cross-Section 61
Figure 30: Microscope Image Close-up of Ridge 61
Figure 31: Channel Depth and Width 62
Figure 32 Ridge Height and Width 63
Figure 33: Channel Draft and Edge Radius 64
Figure 34: Scan of the Entire Length of an Embossed Channel 65
Figure 35: Along Channel Cross-Sectional Data Exhibiting Warping 65

Figure 36: Interferometer Scan of Tool Marks on a Micro machined Tool 66
Figure 37 Force Curve 69
Figure 38 Embossing Temperature and Velocity Impact on Depth of Channel [24] 71
Figure 39 Co-existing Operating Ranges 80
Figure 40 Experimental Design 81
Figure 41 Locations for Measuring Defects 83
Figure 42 Examples of De-Embossing Defects 84
Figure 43 Pareto Chart for Width Fill 88
Figure 44 Residual Analysis of the Width Fill 89
Figure 45 Main effect Plot 90
Figure 46 Interaction Effects 90
Figure 47 Main Effects Plot for Height Fill 92
Figure 48 Interaction Effects for Height Fill 92
Figure 49 Main effects for De-Embossing Defects 94
Figure 50 Response Optimization 96
Figure 51Run Chart for Confirmation Run 97
Figure 52 Process Capability Analysis of the Ridge Height 99
Figure 53 Process Capability Analysis of the Width fill 100
Figure 54 Assembly Drawing 107
Figure 55 Bottom Sub-Assembly 108
Figure 56 Top Sub-Assembly 109
Figure 57 Frame Sub-Assembly 110
Figure 58 Substrate Plate Sub-Assembly 111
Figure 59 Bottom Heating Plate 115
Figure 60 Bottom Plate 116
Figure 61 Sensor Block 117
Figure 62 Top Heating Plate 118
Figure 63 Middle Plate 119
Figure 64 Flange Shaft 120
Figure 65 Corner Insulation Block 121
Figure 66 Cold Plate 122
Figure 67 Top Plate 123
Figure 68 PDMS 124
Figure 69 PDMS 125
Figure 70 Epoxy Resin 126
Figure 71 Load Sensor 127
Figure 72 Temperature Controller 128
Figure 73 Bearings 129
Figure 74 Guiding Rods 130
Figure 75 Normal Plot for Width Fill 131
Figure 76 Normal Plot for Height Fill 132
Figure 77 Residual Plot for Height Fill 132
Figure 78 Pareto Chart for Height Fill 133
Figure 79 Normal Plot for De-Embossing Defects 134
Figure 80 Pareto Chart for De-Embossing defects 134
Figure 81 Residual Plot for De-embossing defects 135

Figure 82 Interaction Effects for De-Embossing Defects 135
Figure 83 Co-efficient for the regression model for De-embossing defects 136
Figure 84 Co-efficient for the regression model for Height Fill 136
Figure 85 Co-efficient for Regression Model for Width Fill 137

List of Tables

Table 1: Measurement Data ... 55
Table 2: Error Relation to Distance ... 56
Table 3 Parallelism Measurements ... 59
Table 4 Summary of Gage RR Results [34] ... 60
Table 5 Cause and Effect Matrix ... 77
Table 6 Pre-Design of Experiments Data ... 79
Table 7 Levels of Factors for the Fractional Factorial Design ... 81
Table 8 Aliasing Structure ... 85
Table 9 Fractional Factorial design parameters ... 85
Table 10 Fractional Factorial Design Of Experiments ... 86
Table 11 ANOVA for Width Fill ... 88
Table 12 ANOVA for Height Fill ... 91
Table 13 ANOVA for De-Embossing Defects ... 93
Table 14 Optimal Parameters for Confirmation Runs ... 96
Table 15 Confirmation runs ... 97
Table 16 Bill of Materials ... 112

1 Introduction

This thesis explores using hot embossing as a prototyping process of microfluidic channels for Daktari Diagnostics. The capabilities of the process were investigated with specific emphasis placed on reproducing a key feature of their current product.

1.1 Background and Research Motivation

Daktari Diagnostics is a startup company that is currently specializing in affordable and accurate Human Immunodeficiency Virus (HIV) diagnostics. HIV replicates in the human body by invading helper T cells (specifically the CD4+T cells). As the virus spreads, the patient's CD4 cell count declines and their ability to fight infection diminishes. Thus, CD4 cell count (cells/microliter of blood) correlates to the severity of the infection. A measurement of CD4 cells cannot be used to diagnose a patient as HIV positive; however, it is an effective and essential measurement for determining if a patient is responding to medication. Measurement of the CD4+ T lymphocytes is a critical part in the staging of the HIV-infected patients, determining need for antiretroviral medications and monitoring the course of their infection[1].

In developed countries, the CD4 count (CD4 cells per microliter of blood) is performed every three to six months using a method known as flow cytometry. This requires expensive ($30,000 to $150,000) equipment and trained operators. In resource poor countries, these assets are only available in the largest national hospitals. For many patients afflicted by HIV, this means that they must send blood out from a local clinic and wait days or even months for the results to return from the central hospital laboratory. These economic and technical limitations have made these instruments difficult to sustain in resource poor environments[2], where there are more than 35 million HIV-infected people, 6 million of which require urgent anti-retroviral treatment. The need for a low cost CD4 measurement technique is widely recognized[3].

Daktari is attempting to create a CD4 cell count system that is simple to operate, low cost and portable. Their product includes a microfluidic cartridge with a circuit of channels for

reagents and blood to flow. The CD4 cells are preferentially captured in a basin known as the assay channel, and then counted using impedance measurements[2]. CD4+ cell size is on average 8.5 microns in diameter, with 0.2% being above 12 microns[4]. The microfluidic device contains channels as shallow as 50microns and as deep as 1mm.

1.2 Problem Statement

To arrive at a functional design, it is necessary that Daktari Diagnostics take advantage of manufacturing methods that are capable of producing parts with features in this 10s of microns range. For commercial production, Daktari will use an injection molding process. However, for prototyping this method may not be the most efficient. Daktari is interested in other manufacturing processes that are capable of accurately and reliably creating aspects of their microfluidic card for prototyping purposes. This thesis evaluates hot embossing as a prototyping process.

1.3 Current Prototyping Processes

Currently, Daktari uses several processes in conjunction for the development stage of the product. These are: Photolithography and Polydimethylsiloxane (PDMS) molding, micromachining, and injection molding. Each of these processes has limitations that prevent them from being ideal prototyping processes. The processes and limitations are discussed in more detail in 3; a brief description of each process is below.

1.3.1 Photolithography

Photolithography is a technique used to produce very precise (nanometer resolution) patterns on a substrate. The general principle of the process is that a photosensitive material is selectively exposed to a UV light source. This exposure cures portions of the resist in the desired pattern while the remaining material is etched away. The technique is commonly used to make integrated circuits, but has recently been used as a method for producing molds for microfluidic applications. One major limitation of this process is the cost and complexity associated with making the mold. Another limitation, and Daktari's biggest concern, is that this process does not produce parts that are representative of production parts, meaning both the geometry of the parts produced and the material used differ from production specifications.

1.3.2 Micromachining

Micromachining directly into the substrate is another method that Daktari has used for prototyping microfluidic designs. Micromachining, either through micro milling, laser machining or micro-electrical discharge machining (micro-EDM) is a subtractive manufacturing process that affords great flexibility. This process is capable of producing complex micron scale features into almost any material desired. The major limitation here is the time required to produce a single part. It may take several hours to micro-machine one microfluidic design, and Daktari may need up to 50 parts made of a single design to fully evaluate it.

1.3.3 Injection Molding

Injection molding is the method currently used by Daktari for commercial production of their microfluidic card. Injection molding is a method in which a mold cavity is filled with a molten thermoplastic. It allows for highly complex parts to be rapidly produced. The major limitation of this process is the time and cost required to make a mold. A single mold cavity may take up to six months to design and manufacture. While this manufacturing process is desirable for volume production, it is not ideal as a prototyping process.

1.4 Unmet Needs

The processes described previously do not meet all of the requirements of an effective development tool for microfluidic devices. They are either prohibitively slow, prohibitively expensive, or produce parts that are not characteristic of parts produced with the production process. Therefore, there is a need for a more effective prototyping process.

The process must produce parts that are representative of production grade parts. This means that the behavior of flow through the channels in the prototyped parts must be similar to the flow that will occur in production parts. If this is not true, then the process cannot be realistically used as a development tool. The new development process must produce parts that have geometry representative of the final production parts. This includes tapers, surface roughness characteristics and material.

For the process to be an effective prototyping tool, it should take a relatively short amount of time to iterate on the design. This need translates to a requirement that has the entire process, from tooling to prototype production, be as short as possible.

1.5 The Hot Embossing Solution

Hot embossing is a viable solution for filling the prototyping gaps left by the previous processes[5]. It offers advantages in achievable feature replication[6], correct prototyping material, low process cycle time, and a variety of tooling options. Most features producible by injection molding and machining can be achieved by hot embossing, such as high aspect ratio features[7] and low surface roughness[8]. Mold tools for hot embossing can be produced through micromachining or lithography processes. The tools in hot embossing are used to transfer features over to substrate materials. The selection of substrate materials is very flexible and allows the correct material to be used for prototyping. The time in which it takes to make a single micro hot embossed part has been shown to be as low as 2min/part[9]. This bridges the gap between the fast process times of injection molding to the slow process time of micromachining. Hot embossing is able to bring prototype designs to production more quickly because the time required for tooling can be considerably less than that of injection molding where complicated features like ejection pins add to tooling time. Hot embossing also offers different materials for tooling that injection molding does not [8,10].

While there are many apparent benefits of using hot embossing, this technology is still an emerging manufacturing process that is not widely used commercially. The process exists primarily in academic and research settings and is still in the process of making a transition into commercial arenas. The true capabilities of the process will depend on the specific geometries of the parts being produced, and so this process must be evaluated for Daktari's particular needs.

1.6 Research Objectives

- To provide Daktari with a cost effective rapid prototyping technique with minimal lead time to enable manufacturing of the microfluidic backbone of the cartridge within tolerances.

- After selecting hot embossing as the process used for rapid prototyping, designing a machine capable to produce the microfluidic parts within specifications and analyzing that design to find out the capabilities of the device.

- Validation of the complete process to characterize the process variation and the system repeatability. Analysis of the machine capabilities and the characterization of the boundaries of the operational capabilities of the device.

- Analysis of the various controllable and uncontrollable factors affecting the system and the down selection of the factors according to their impact on the features to be embossed. Analysis of a particular metric as a response for the experimental design which can be a measure of the performance of the system.

- Setting up of an experimental design to analyze the effects of the factors on the system. Analysis and optimization of the responses to find the optimal factors for the best performance of the process.

- Analyzing the process capabilities and characterizing the process window to attain process control using the optimal parameters.

2 Background and Product Description

2.1 Microfluidics

The HIV diagnostic product developed at Daktari consists of a variety of parts but one of the most important and the critical part in the instrument is the microfluidic cartridge, which is manufactured using Poly methyl methacrylate (PMMA). The microfluidic cartridge is the component where the blood enters, mixes with different reagents in precise quantities and accurate measurements of the CD4 count of the blood are made. The important requirement for such a cartridge is having accurate quantities of the reagents and the blood flow at a precise rate through the channels. A microfluidic chip is suitable for this need.

Microfluidics has the potential to significantly change the way modern biology is performed. Using microfluidic devices we can work with smaller reagent volumes, shorter reaction times, and the possibility of parallel operation. They also hold the promise of integrating an entire laboratory onto a single chip (i.e. lab-on-a-chip)[11]. Apart from the traditional advantages of miniaturization, the greatest potential lies in the physics at the micro scale. By understanding and leveraging micro scale phenomena, microfluidics can be used to perform experiments which may not be possible on the macro scale which allows the introduction of new invention in functionality [12].

A microfluidic approach has been used for a wide range of applications which include analysis, diagnostics and synthesis [13]. Microfluidics is the analysis of accurate and precise flows through constrained routes or channels. Typically microfluidics is used to analyze fluids which flow, mix, separate and are processed otherwise. Some of the applications include passive fluid control using capillary forces, rotary drives applying centrifugal forces for the fluid transport on passive chips. Microfluidic chips can also be used to enhance rare cell capture and fractionation using biochemical interactions. Many of the microfluidic devices take advantage of the 3D structure of channels to increase the surface area available to be coated with the antibody [4].

There are a variety of ways in which the microfluidic chip can be manufactured which include soft lithography, micromachining and micro-injection molding. Some of the important parameters to be considered as shown in Figure 1 while producing the microfluidics part are:

1. Surface Finish: The surface finish plays an important role in the flow characteristics of the fluid and it depends on the process used for manufacturing.
2. Dimensional Tolerances on Features: The sides of the channel are important for the flow characteristics as well as the capture of any cells if relevant. The tolerance on these features like the width and length of the channels determines the flow characteristics. Also, the linearity of the features is an important along with the parallelism of the planes of the features.
3. Positional Tolerance: Parallelism and Perpendicularity with the outside boundary of the microfluidics may play an important role. Also, the positional tolerance of the features with respect to the outside boundary may be a crucial parameter.

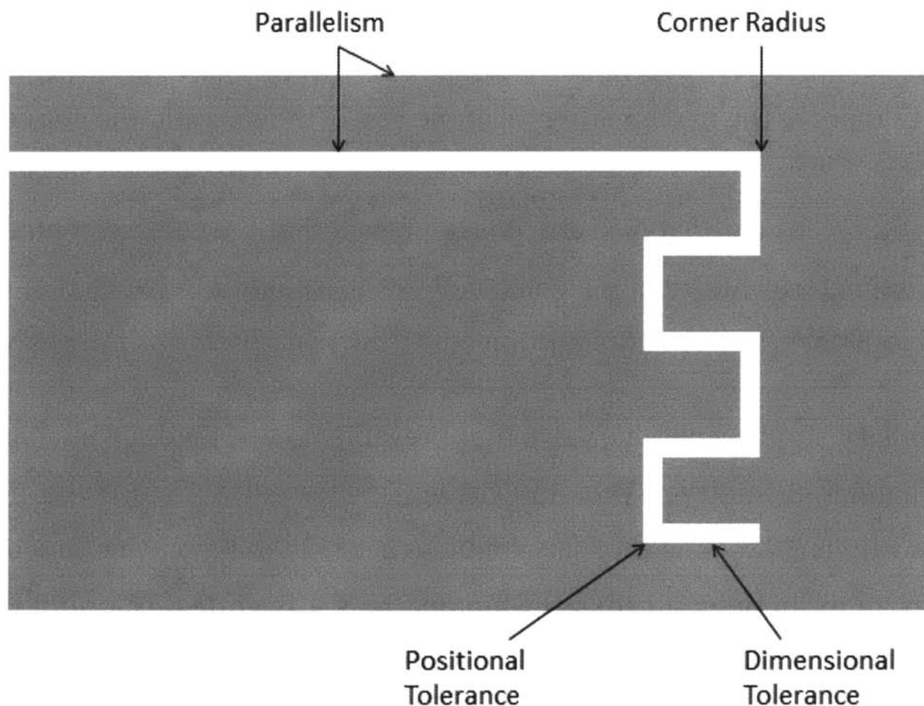

Figure 1: Critical parameters in microfluidics

Most of the crucial parameters can be further listed down according to the application of the microfluidic chip, which is in this case the microfluidic cartridge used at Daktari. The

critical features and parameters which are important to the performance of the device are enlisted the following section. These features in addition to the parameters listed above will be the basis for evaluating hot embossing as an appropriate prototyping process for Daktari Diagnostics.

2.2 General Card Features

Several parts of Daktari's microfluidic network have unique aspects that make them difficult to prototype. These features are also parts of the microfluidic network that need to be thoroughly iterated upon to reach a functional design. Therefore, it is necessary to demonstrate that hot embossing is a suitable manufacturing method for these key features before it can be declared an effect prototyping tool.

Blood is first introduced to Daktari's product through a feature known as the fill port. This is an inlet that is designed to allow blood to be pulled into the microfluidic network of the card through capillary action. The inlet resides on an edge of the card. It will be a channel of uniform depth. The fill port may have uniform width, or it may have a design with a wide opening that tapers to the narrower width of the rest of the microfluidic network.

After blood has entered the card, it is important that the volume of blood to be analyzed be known. The metering channel is a portion of the microfluidic network that takes in a precise quantity of blood for transfer to the portion of the card that performs the analysis.

A capillary stop is a passive valve that prevents flow of fluid. By having an abrupt, large change in channel geometry, a pressure barrier is created that stops the flow of fluid [14]. Daktari uses capillary stops in their microfluidic network to direct the flow of blood. Figure 2 below shows an example of a capillary stop and how it operates. The fluid flows in the main channel past the capillary stop. Some fluid enters the stop, but its motion is halted when it reaches the portion of the channel that has a sudden change in depth and width.

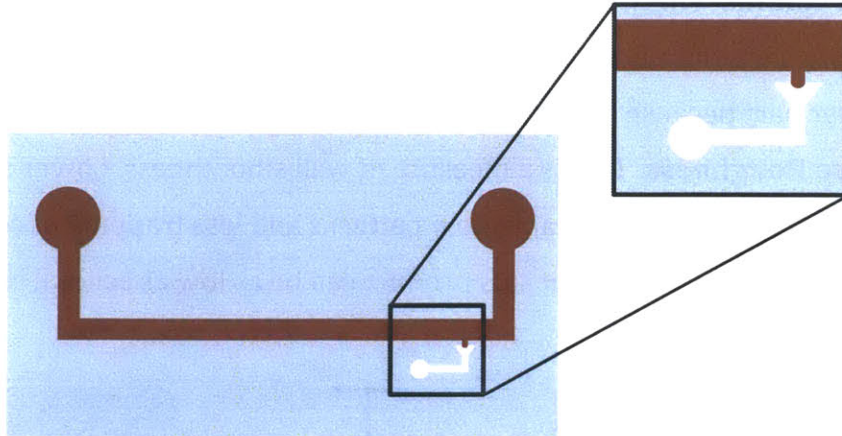

Figure 2: Schematic of a channel with a capillary stop

2.3 Targeted Feature: The Assay Channel

The most critical portion of the microfluidic system is a portion of the card known as the assay channel. This is the region in which a crucial analysis of the blood is performed. It contains a large collection of tight tolerances and dimensions that are both unique to this area and common to different features on the card. Therefore, prototyping of this feature will be a good indicator of hot embossing's capability to prototype various parts of Daktari's card.

2.4 General Channel Considerations

The microfluidic channels in Daktari's product are in general defined by six basic geometric parameters. These are:

1. **Depth**. Channel depth varies widely on Daktari's microfluidic network and can be as shallow as 50microns or as deep as 1 mm.
2. **Width**. Channels of widths at large as 2mm in span exist on Daktari's card.
3. **Draft Angle.** This is a measurement of the verticality of the channel's walls. Perfectly vertical walls are desirable, but not possible because of the molding process currently being used.
4. **Upper Radius.** This is the radius at the upper edge of the channel. In general this radius is governed by radius of the tool used to make the mold.

5. **Lower Radius**. This is the radius at the bottom edge of the channel. The tool can be made with essentially 0 radius at this point, however there may be a radius left on the polymer part because of the manufacturing process.
6. **Surface Roughness.** This is a measure of wall smoothness. Lower surface roughness is desirable, for more predictable flow patterns and less trapping of cells. Surface roughness requirements for this product can be as low as several tens of nanometers.

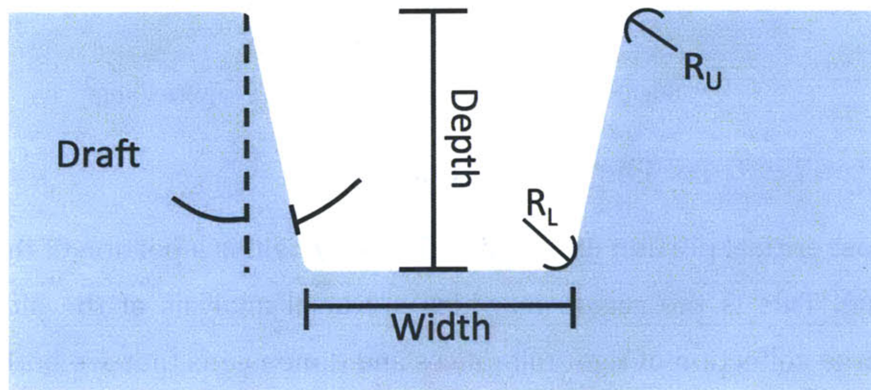

Figure 3: General channel dimensions

3 Review of Prototyping Processes

Many manufacturing processes can be used to produce parts with micro features. However, these micro features need to have a certain accuracy and fidelity. They need to satisfy the requirements of being biocompatible, corrosion-resistant and disposable etc. The manufacturing process needs to be viable with regards to the materials used and the feature size to be attained. Some of the potential manufacturing processes are discussed below based on the requirements listed above and manufacturing challenges. These processes are being currently used at Daktari for rapid prototyping the assay channel. Each of these processes has limitations that hot embossing will hopefully overcome.

3.1 Photolithography

Photolithography has been shown to be a cost effect and rapid way for producing micron scale features[15]. Additionally, photolithography in conjunction with Polydimethylsiloxane PDMS is commonly used as a means to prototype microfluidic channels[16].

3.1.1 Process

A positive mold containing the desired features is created using a photolithography process. The steps of the process are as follows and Figure 4 shows the differentiation of a positive and negative mold.

1. A photoresist resin is spin coated onto a silicon wafer
2. A mask is applied that covers some portions of the wafer and leaves other areas exposed
3. The wafer is exposed to UV light, this cures the resin not covered by the mask
4. The uncured resin is etched away leaving the completed silicon tool

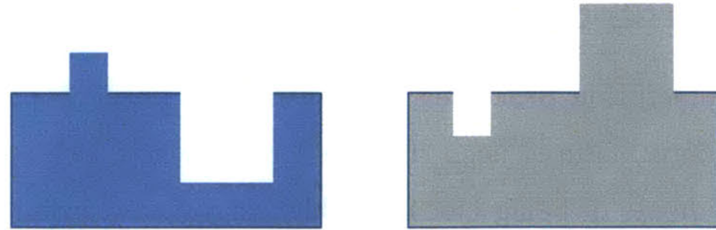

Figure 4 The positive mold (left) holds desired features and the negative mold (right) holds the opposite geometries of the features

Once this silicon positive mold is completed, PDMS parts can be produced from it. Liquid PDMS is poured onto the positive mold along with a hardener. Once the PDMS cures, it is removed from the silicon positive mold and creates a negative.

3.1.2 Limitations

This process can create parts quickly. It may take a couple weeks to receive the silicon positive mold from a semiconductor foundry. However, once the tool is made, PDMS copies can be produced rapidly and at low cost. The greatest problem with this process is that it produces parts that do not have geometry or properties that are entirely representative of the final production process. Photolithography results in parts that have nearly perfectly vertical walls and can produce corners with almost non-existent radii[17]. Conversely, injection-molding (the production process) produces parts with tapered walls and corners with radii. Additionally, this process produces fluidic channels in PDMS, which is not the production material. Material certainly has an effect on flow characteristics and because of this, results from testing PDMS parts may not be representative of how the design will perform with production material.

Another limitation of this process is that it is best suited for creating features with uniform height. Daktari's actual product is a microfluidic network with complex geometry with steps and ramping inclines. Therefore, this process is best for prototyping only portions of the design.

3.2 Micromachining

Micromachining can be used to produce parts with microfluidic applications because of the available working materials, machinable geometries, achievable feature sizes and surface roughness[18].

3.2.1 Process

Like traditional milling, a micro mill uses endmills with sizes as small as five microns that can cut into metals and softer materials. During the milling process, the endmill is moved relative to the work piece. This allows features to be cut directly into the thermoplastic substrate. In micromachining, the microfluidic channels are cut directly into the thermoplastic substrate. This process allows for complete control of the end part and is capable of producing many types of geometries.

3.2.2 Limitations

An advantage of micromachining is the flexibility afforded by the process. Once a micro mill is acquired, designs can be quickly iterated on. However, the benefit of not requiring custom tooling for each design is balanced by the relatively long cycle time of this process when compared to injection molding or producing PDMS parts from a silicon tool. Daktari anticipates needing 20-50 of any given prototype design for testing. This requirement makes the cycle time of micromachining each part undesirable.

A potential problem with micromachining is that tool marks left by the process may produce surface roughness characteristics that are undesirable. As mentioned previously, the cells of interest for Daktari are on the order of 1-10 microns. It is possible to achieve a surface roughness several orders of magnitude lower than this [18], however if the process is not carefully controlled then this characteristic might be problematic. Another artifact and problem with machining is the introduction of burrs which could have an impact on the performance or assembly of microfluidic devices. Burrs are introduced when material is not fully removed or becomes welded on the edges of a corner. Figure 5 depicts a cross sectional view of burrs and shows tool marks and potential burrs left by micro machining on aluminum.

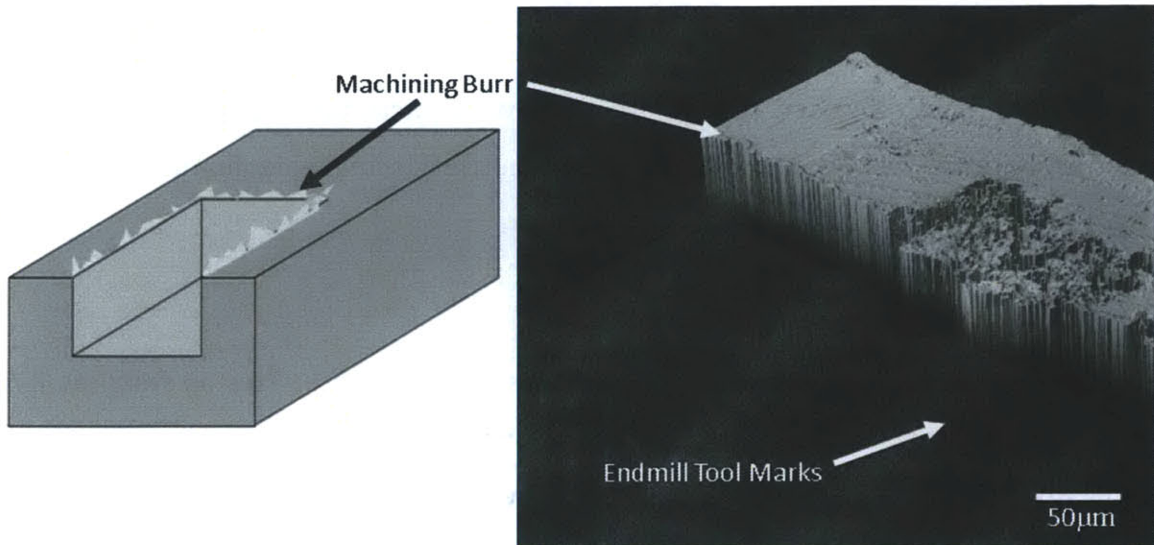

Figure 5 Cross sectional depiction of burrs on the edge of a possible machined channel (left). An interferometer image of a machined feature showing tool marks and possible burrs.

Micromachining also limits features such as sharp convex corners which are sometimes used in microfluidic devices to control fluid flow. An example of this use of sharp corners is to control capillary action where the sharp corners can be used to stop fluid flow. The radius of the endmill usually dictates the achievable radius on the interior of a corner, but usually not the exterior. Control and prediction of the corner milling resolution has also been seen as an issue in automated machining for mass production [19]. Figure 6 shows the common process for milling a corner.

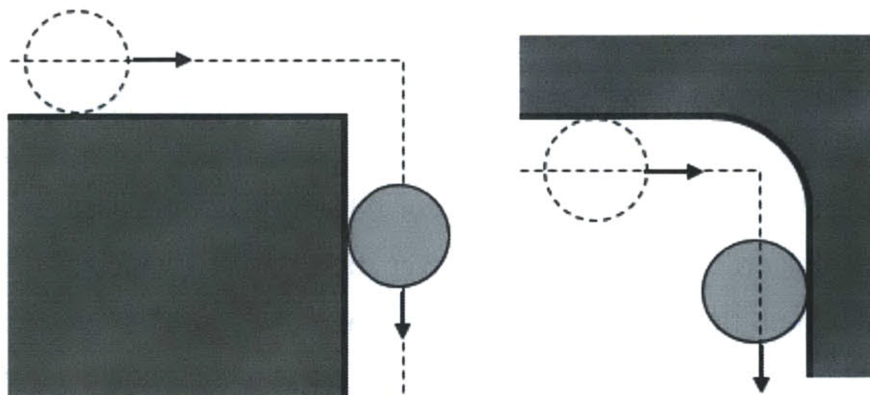
Figure 6 The standard process for milling the outside radius (left) and inside radius (right) of corners.

3.3 Injection Molding

Injection molding is a common process used to make parts containing micro-features. It offers the ability to use a wide variety of thermoplastic materials, many of which are biocompatible.

3.3.1 Process

Micro-injection molding is a process of transferring a thermoplastic material in the form of granules from a hopper into a heated barrel so that it becomes molten and soft. The material is then forced under pressure into a mold cavity where it is subjected to holding pressure for a specific time to compensate for material shrinkage as shown in Figure 7. The material solidifies as the mold temperature is decreased below the grass transition temperature of the polymer. After sufficient time, the material freezes into the mold shape and is ejected. This cycle continues to produce a number of parts. A typical cycle lasts between few seconds to few minutes [20]. The process has a set of advantages that make it commercially applicable. Advantages include the wide range of thermoplastics available and the scope for complete automation with short cycle times [21,22], cost effectiveness for mass-production process, especially for disposable products, very accurate replication and good dimension control, low maintenance cost of the capital equipment, when compared to the lithographic methods and applicability of the large amount of industrial information and technical know-how available for the traditional injection molding process. Also, because the working materials are injected into the cavities at a quasi-liquid state, the high mobility of the material makes making high aspect ratio, larger than 10, devices possible [23]. The process requires relatively inexpensive equipment and a metal mold to be produced. Additionally, the complexity of geometry possible is only limited by mold making capability. The dimensions of the injected parts fall into a region from 500 nm to several hundred micro meters.

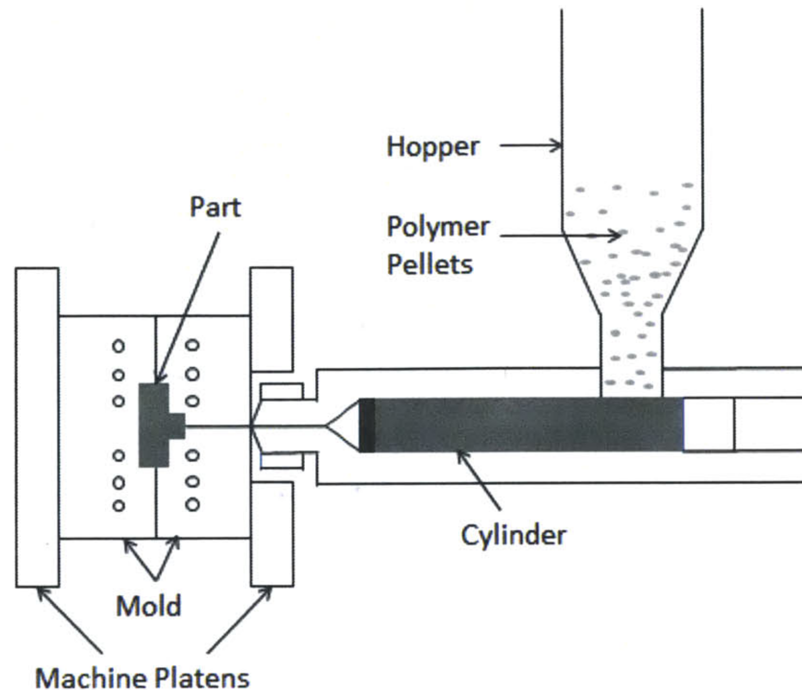

Figure 7: Injection Molding Process

3.3.2 Limitations

However, because the working materials are processed under wide temperature range, from the room temperature to 10 to 20 degrees above the polymer melting temperature, the shrinkage of the material is large, and hence good uniformity in the walls with different thickness is hard to achieve[24].

Daktari will finally use the injection molding process for the manufacturing of the device on a mass-level. Once tooling is completed, their contract manufacturer is able to produce their backbone (cartridge) in a high volume and at relatively low cost per unit. If Injection molding is used as a prototyping tool, then parts produced are completely representative of what the parts will be like from a production run.

The major limitation of this process is the monetary and time investment required to make the mold. Lead times for precision micro molds can be in excess of 6 months, and changes to the mold design can take weeks to complete. While the fidelity achievable through injection molding is desirable, the time required to make tooling is too long for this process to

be an effective development tool. Daktari needs a prototyping tool which gives them a part which has the same material properties as the final part, which is made out of PMMA, be robust and function like the final product in a short period of time. This will enable reiterations of the design at a faster rate with a prototype, which is actually similar to how the product will work.

4 Hot Embossing Process

Hot embossing is a promising technique for manufacturing micro-fluidic devices due to its excellent feature transfer capabilities from master molds, with high aspect ratios and low roughness, onto polymers[7,25]. This meets the requirement for prototyping microfluidic devices that have varying feature sizes, surface roughness and complex geometries. It has also been shown that hot embossing has the capability for producing Poly methyl methacrylate (PMMA) parts with microfluidic features and low cycle times[9,26].

The cost associated with creating the hot embossing master tool can be equal to or lower than injection molding in most cases [11]. On the other hand, the cost for the embossing equipment and materials are relatively low in comparison due to lesser heat and force requirements. Hot embossing requires much less force and heat in comparison to casting or injection molding. The working substrate is normally only heated to, or a little above, its glass transition temperature (Tg) and needs only a few MPa of pressure to transfer features from a master mold onto the substrate[27]. Hot embossing is a very flexible process that often only requires the change out of the master tool between prototype designs. The simplicity flexibility of the system drives engineering, material and energy costs down.

4.1 Selection of substrate

Daktari currently uses PMMA as the primary material for their diagnostic chip for many reasons. PMMA is used for the purpose of hot embossing and injection molding at Daktari because it is an economical alternative to polycarbonate, especially when extreme strength is not necessary. Also, PMMA does not contain the potentially harmful bisphenol-A subunits found in the polycarbonate. PMMA is often preferred as the polymer because of its material properties, easy handling and processing and low cost. The glass transition temperature (T_g) of atactic PMMA is 105 C (221 F). The forming temperature starts at the glass transition temperature and goes up from that point. PMMA is a strong and lightweight material with a density of 1.17-1.20 g/cm^3, which is less than half of that of glass and has an ignition temperature of 460 C and burns forming carbon dioxide, water, carbon monoxide and low-

molecular weight compounds including formaldehyde. PMMA is the least hydrophobic of all the common plastic materials. Moreover, its optical clarity is also a significant benefit for the testing purposes. PMMA will be the primary material used in this work since it is commonly used in hot embossing and is the material used for Daktari's diagnostic chip.

4.1.1 Basic Properties of Thermoplastics

A thermoplastic is a thermo-softening polymer that becomes pliable with an increase in the temperature and returns back to the original solid state with cooling. Most of the thermoplastics have a high molecular weight and its massive molecular chains have high intermolecular forces binding them together. These forces help in the binding of the material once the temperature cools down and hence the polymer can set back into its solid state. Above its glass transition temperature T_g and below its melting point T_m the physical properties of a thermoplastic change drastically without an associated phase change. Within this range, the thermoplastic is a rubbery mass due to alternating rigid crystalline and elastic amorphous regions approximating random coils. This makes hot embossing of these thermoplastics possible without working in a broad temperature range like in case of injection molding. Brittleness might be a deterring factor for the hot embossing process and this can be reduced with the addition of plasticizers, which interfere with the crystallization to effectively lower the T_g. Modification of the polymer through co-polymerization or with the addition of non-reactive side chains to monomers before polymerization can also reduce the T_g.

4.2 The Hot Embossing Process

Hot embossing is the process in which a substrate is impressed with features from a master tool. The master tool holds the negative of the desired features so that the positive of the features may be transferred. It is also very common to heat up the master mold and usually results in better feature transfers and lower cycle times[25]. Figure 8 depicts the process overview with the master tool and substrate.

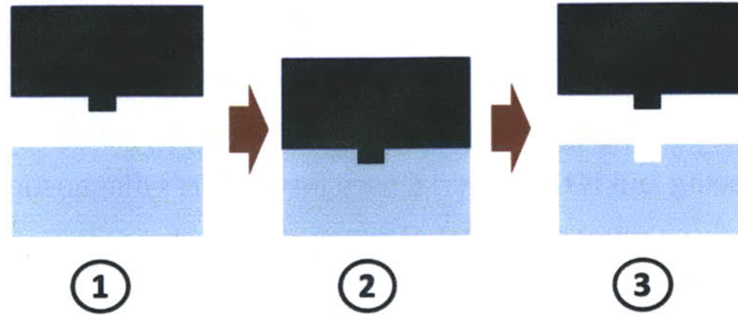

Figure 8: The master tool (top) and substrate (bottom) are heated up (1), then pressed together (2) and finally released (3)

Figure 9 shows the force and temperature cycle of the hot embossing process. The process cycle starts when the substrate begins heating up to or past its glass transition temperature, T_g, from T_0 to T_1. At T_1, the master tool is pressed into the substrate and held for a period of time at a constant molding force. The holding time lasts until T_2, at which time the substrate is set to cool. At T_3 the substrate temperature reaches below its T_g to a desired de-molding temperature and the molding force is released, ending the process cycle.

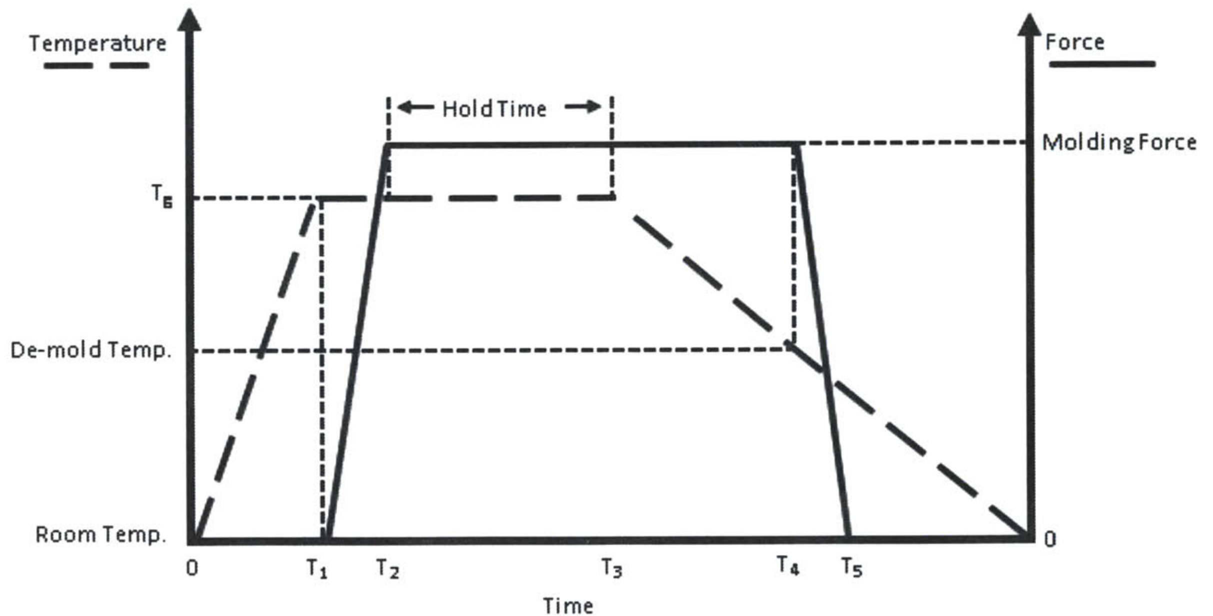

Figure 9: General hot embossing temperature and force cycles. The process cycle begins from T = 0 to T = T3

4.2.1 Initial Heating Stage

Referring to Figure 9, the heating stage occurs between T_0 to T_1. During the initial heating stage, the substrate is heated up to or a little past its T_g. It is also very common to heat the tool up at this time to the same temperature of the substrate or a bit cooler[28]. This initial heating prepares the substrate to be malleable and less viscous for the embossing stage. The higher the substrate temperature is, the less force is required. Also, a higher replication accuracy is correlated with better material flow[29]. Uniform heat distribution is preferable because it can dictate the quality of the part and complexity of process control and analysis. Control and repeatability of the temperature during this stage is desired for quality and process control purposes.

4.2.2 Embossing Stage

The embossing stage spans from T_1, the time in which the master tool and substrate come into contact, to T_4, when the tool and substrate start to separate. The embossing stage initiates from T_1 to T_2, during which time the tool and substrate come into contact and force begins to be applied and ramped up to a desired load. Once a desired force is reached, it is kept constant from T_2 to T_4. Constant force as well as constant position can be kept during this time, depending on the types of features required. For example, a part may have to be made to a certain thickness. This would only be achieved under constant position holding and not force. The holding time occurs between T_2 to T_3 and defines the amount of time that the substrate is placed under constant force and heat, or position and heat.

4.2.3 Cooling Stage

Cooling happens after T_3 and is the stage that brings the substrate below its T_g. De-molding temperature plays a large role in the final shape of the embossed part and is usually set well below the substrates T_g. Releasing the molding force at too high of a temperature may cause the substrate material to flow and fill in the features that were created[29]. Cooling rates also has an effect on thermal stresses, which would affect part quality[30,31]. For the purposes of this work, the cooling rate does not have to be rapid and can be kept such that the best quality parts are produced. A long cooling time (~10mins) would be acceptable.

4.2.4 De-Molding Stage

De-molding begins at T_4, at which point the substrate has been cooled below its T_g to a desired de-molding temperature. Force application is released at this point and the tool and substrate are pulled apart until there is no longer contact, at T_5. De-molding can require a considerable amount of force depending on the size of the part, features, and amount of friction between the tool and substrate[5]. Materials such as mold release may be used in order to facilitate the de-molding process, but could potentially yield undesirable part quality, especially for a feature that requires tight tolerances. The de-molding process has been shown to contribute greatly to the quality of the part, especially when friction and substrate shrinkage are considered. Parts have been seen to have poor quality because of high friction and shrinkage[32]. Control of how the tool and substrate separate can also have an effect on the part quality. It has been recommended that the tool and substrate be separated initially at a single location or edge, then "peeled" away from one another[5].

4.3 Consideration of Process Capabilities

To consider hot embossing as a viable rapid prototyping process for Daktari, it must have capabilities in replicating a wide range of features. This section will provide an overview of some of the features that may be challenging for hot embossing to accurately and precisely produce. These features include many of the channel parameters introduced in chapter 2, as well as features that are specific to the assay channel.

4.3.1 Sharp Radii

Many features such as the assay channel require a sharp radius on raised edges. During the hot embossing process, the substrate exhibits a "dragging" behavior where the sidewalls, near the tip of the tool feature, "drags" the substrate as pressure is applied between the tool and substrate. This dragging process can wear the tip of the tool out while creating air gaps. Figure 10 shows a cross section of a channel and how air gaps can increase the radius on the raised edge. These air gaps can be reduced by increasing forming temperature so that the

substrate can more easily flow and fill the gaps[33]. Increasing pressure and embossing hold time can also help reduce these gaps.

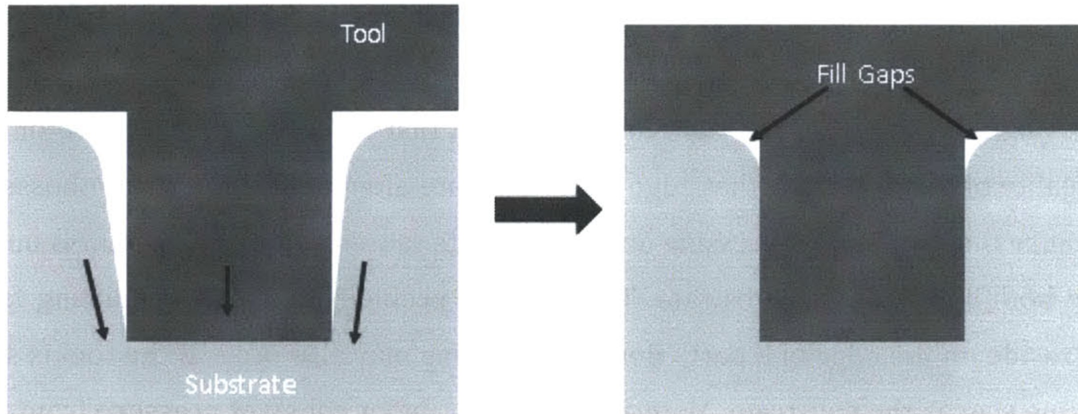

Figure 10 The left image shows the dragging effect where the arrows indicate the direction of the tool and material movement. The right image shows air gaps which can reduce feature radius.

4.3.2 Unfilled Extruded Features

The filling of high aspect ratio cavities can be difficult and can depend on the temperature, pressure, and hold time. The effects that cause incomplete filling in corners may also contribute to this incomplete filling of extruded features. Figure 11 shows an unfilled cavity during the embossing process. The substrate is pushed into the cavity, but if the hold time, pressure and temperature are not adequate, then the substrate may not be able to flow and fill the cavity.

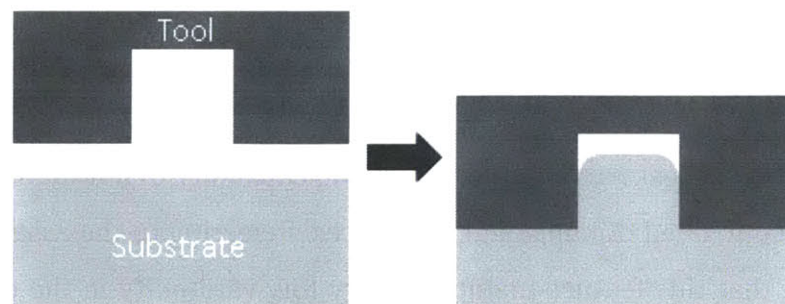

Figure 11 Cavities in the mold can be unfilled during the embossing process if temperature, pressure, and holding time are not adequate.

4.3.3 Features Ending on Edges

It may be necessary to have features that reside directly on the edge of an embossed card, such as a fill port. Producing features that reside on the edge of an embossed part may be difficult for the hot embossing process. Figure 12 displays a possible fill port design, which can be referenced back in section 2.2. The image on the left is the ideal part produced through hot embossing. The image on the right displays a part that is more representative of the process. The reality of the process is that edge distortions are often present on the embossed part. This is because the heating and pressing on the substrate causes material flow that is unconstrained at the boundaries of the substrate. This may be problematic when producing features that must reside on the edge of a part. Boundary bowing may also occur if the tool is smaller or of the same size as the substrate. Material that is not under constant pressure from the tool will deform with random warping during cooling.

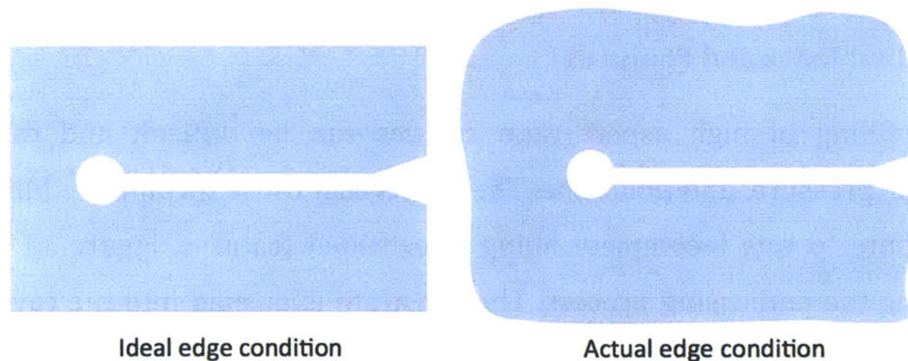

Figure 12: Substrate edge distortion

4.3.4 Control of Tolerances and Variability

It will be necessary to demonstrate the capability of hot embossing to produce features with tightly controlled dimensional tolerances. Referring to the assay channel in section 2.3, it is important that this feature maintains very low variability in the dimensions of the channel card to card and that the dimensions are precise as possible. The assay channel is a straight rectangular channel with a defined ridge around its perimeter. Figure 13 below shows what the assay channel may look like. The two holes represent inlet and outlets for a fluid.

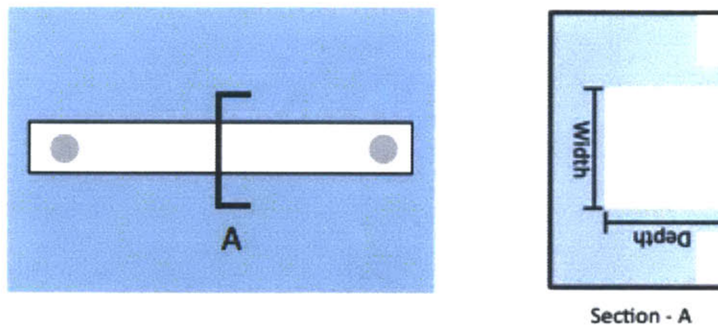

Figure 13 Schematic of a general cuvette feature

For hot embossing to be an effective method of producing this channel it is necessary that the variability of the process be well understood. This feature will also test the capability of hot embossing to fully transfer the mold onto the substrate. It will be critical to know what percentage of the mold geometry is transferred into the substrate. For example, if the mold has a feature with a cross section that is 10 microns deep and 10 microns wide, it will be important to know how closely the corresponding feature on the embossed part matches these dimensions.

4.3.5 Abrupt and Variable Geometries

Another common feature for this microfluidic network are areas where multiple channels come together at a junction. These junctions may bring channels together that have different depths and different widths. The hot embossing process must be capable of producing features of variable depth, either with a gradual incline at the bottom of the channel or with a step. The process must also be capable of producing features with variable width. Figure 14 below displays one possible design for a junction of multiple channels. Notice the change in channel width from the left to the right. This sudden change in width may be a necessary aspect of Daktari's product. It will be necessary to investigate the capability of the hot embossing process for producing channels with sharp corners, like those seen at the junction. Another variable dimensional control would be in the depth of channels. The channels should be a constant depth along the length and width so that their functionality can be more predictable.

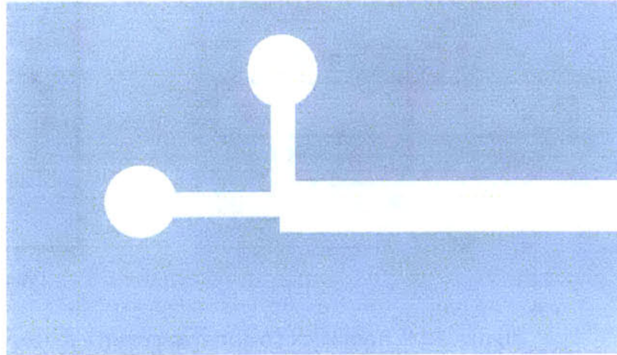

Figure 14: Schematic of 3-way junction

4.3.6 Surface Roughness

The cuvette feature requires not only tight tolerances, but also a low surface roughness. This feature is a wide and very shallow basin (roughly 50 microns in depth). Therefore, tight dimensional tolerance of the channel depth and width are critical. Additionally, surface roughness of the bottom surface is of paramount importance in the assay channel. The CD4 cell counting is occurring in this channel; therefore surface roughness must be maintained at a level that does not cause unwanted trapping of cells. The assay channel will also challenge the capability of hot embossing to produce large and smooth surface area features.

5 Machine Design Approach

This chapter will outline the design requirements needed for an embossing machine that is capable of making Daktari's assay channel. The general effects of different operating parameters will be described so that a basic idea of how different components and their operating ranges can work together to make parts. Design requirements will then be discussed. Current design practices that are in-line with this study will then be highlighted to help with the design.

5.1 General Effects of Operating Parameters

Hot embossing feature replication is largely dependent upon three factors; embossing temperature, pressure, and embossing time. The combination of values of the three settings effects not only the cycle time of the embossing process, but the achievable quality of the embossed substrate. For example, low embossing temperatures would require high pressures in order to achieve the same results as high embossing temperature and low pressures [1]. The lower embossing temperature would decrease the heating and cooling time resulting in a possible decreased cycle time. This assumes that the embossing time is equal for both settings.

The tradeoff between these different settings would be in equipment size, cost, process cycle time, and achievable feature resolution. It is important for this design to be flexible with embossing temperature and pressure in order to accommodate future tool designs. Embossing and cycle time is not as important because it has been decided that low volume (20-50) production is required for prototyping.

5.2 Design Requirements

The following design requirements help guide machine design so that it may be able to hot emboss Daktari's microfluidic feature.

5.2.1 Tool and Substrate Fixture Requirements

It was decided that the embossing system should be able to accommodate the master tool and substrate material with surface sizes ranging from 25mm x 90mm to 65mm x 100mm. All sub features of the microfluidic device are able to fit on a 25mm x 90mm area, which provides flexibility in designing and testing of such features. The microfluidic device is able to fit into the 65mm x 100mm area, allowing for prototyping of the entire device. The substrate normally has the same surface size as the master tool, so the fixture holding the substrate should be positioned and orientated in the same manner as the tool. Repeatable placement of the substrate is not critical as long as the tool is able to emboss all features onto the substrate without deformation. The substrate can be reworked after embossing so that deformed edges can be taken off, so long as features do not reside on them. The fixture should also be able to hold down the substrate during the de-embossing phase so that the tool and part can be separated.

5.2.2 Force Requirement

Daktari has chosen PMMA to be the working material for the microfluidic device. Forming pressures as low as 1MPa can be used for high temperatures and long embossing times, but on average, 2MPa is used for embossing micro features on PMMA, and 4MPa being a rare case [2]. 2MPa is used as the standard requirement, hence with the entire microfluidic chip measuring 63mm x 100mm, a working force of 12.60kN would be required. It should be noted that the working force could be lower than 12.60kN since increasing embossing temperature or time could achieve the same results as working with this load. Also, pressure is the least sensitive variable in the embossing process because it normally only needs to be above a certain threshold [3]. The machine should also be able to meet de-molding forces, which could be high for large parts. It was determined that the machine did not have to initially

meet 12.60kN of force since the largest embossing area that would be tested initially would be 22.50cm^2. For a 2MPa application pressure, a working force of 4.5kN would have to be met.

5.2.3 Heating Requirements

Commercially available PMMA has a T_g of between 85 to 165^oC, thus the embossing temperature must be able to reach above this temperature. The specified maximum operating temperature was chosen to be 200^oC in order to accommodate any future changes in plastic selection for prototyping. Popular plastics such as polycarbonate, polystyrene, and Zeonex have, on average, T_gs below 200^oC. It should be noted that hot embossing can tolerate embossing temperature tolerances of +/- 3^oC, so the accuracy of temperature control is defined by this tolerance [2]. Heating rate is not as important because the entire process is not aimed to be rapid and is allowed to take up to half an hour. The substrate only needs to be brought to a desired temperature and kept there. Uniform heating should be considered in order to increase process control and part quality.

5.2.4 Cooling Requirements

It has been shown that the de-embossing temperature has an effect on not only the cycle time, but also on the quality of the embossed substrate [3]. The cycle time, in the case of prototyping 20-50 microfluidic parts, is not as important as the quality of the part itself. A cycle time of up to 30 minutes is acceptable in this case. Although cooling rate has an effect on part quality, the system does not require precision control of this parameter as long as it is consistent with every embossing run and fits within the 30min process window. As noted earlier, cooling over a longer period of time typically provides for better parts that suffer less from thermal stresses.

5.2.5 Alignment Requirements

Alignment of the heating platens is important because part planar uniformity is dependent upon this. Figure 15 shows how platen alignment can affect a part.

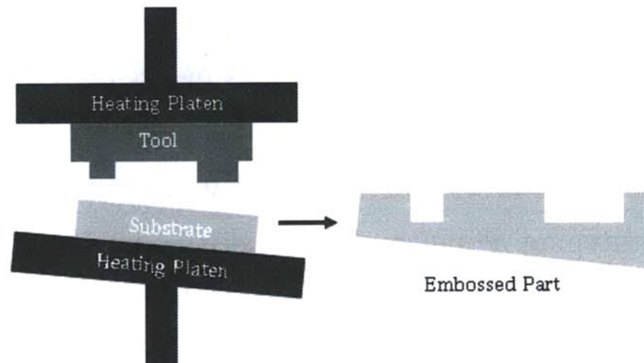

Figure 15: Depiction of misalignment

Alignment requirements, defined primarily by Daktari's microfluidic chip, concern planar x and y travel, angular rotation and vertical parallelism. Daktari has expressed interest in possibly embossing features on both the top and bottom surfaces of a substrate. This double embossing would require features from one side to line up with features on the opposite side. Unfortunately, there is currently no specified high precision x, y and angular alignment requirements because of a lack of understanding on how top and bottom features will perform together under misalignment. However, planar alignment and vertical parallelism should be designed to as high tolerance as possible while considering costs and time.

5.3 Common Design Practices

Simple thermocouples and liquid cooling systems have been shown to be an effective way to measure and facilitate in temperature control[9]. Effective cooling and heating systems help to drastically reduce the process cycle time. The cost associated with this system is associated with the desired cooling rate, accuracy, and thermal mass to be cooled. Temperature control has been shown to be an important parameter in reducing embossed part defects[5].

Force application and control can be achieved using different motors or hydraulics/pneumatics. Servo motors allow for great position control, but can be limited to the amount of force they can apply. Hydraulics and pneumatics offer much greater forces, but can be challenging in position controlling. Constant force application is generally more common and important than constant position, so pneumatics and hydraulics are generally used. It should also be noted that in most embossing cases there is a force threshold, that once achieved, most embossed features do not change drastically in quality, from process to process, beyond this threshold [9].

In most cases, two heated platens are used for heating up and controlling the temperature of the substrate and master tool. The cost and effectiveness of the platens are related to the size and material used. Platens are normally not sized much larger than the master mold and would only require the increase in size to accommodate a heating source. Aluminum and brass are common materials used due to their low cost, machinability, and effective thermal conductivities.

6 Machine Design and Evaluation

This chapter will provide an over view of the machine design and describe its operating parameters and procedures. Important operations performed by subcomponents and the characteristics of the machine will then be discussed.

6.1 Full Assembly

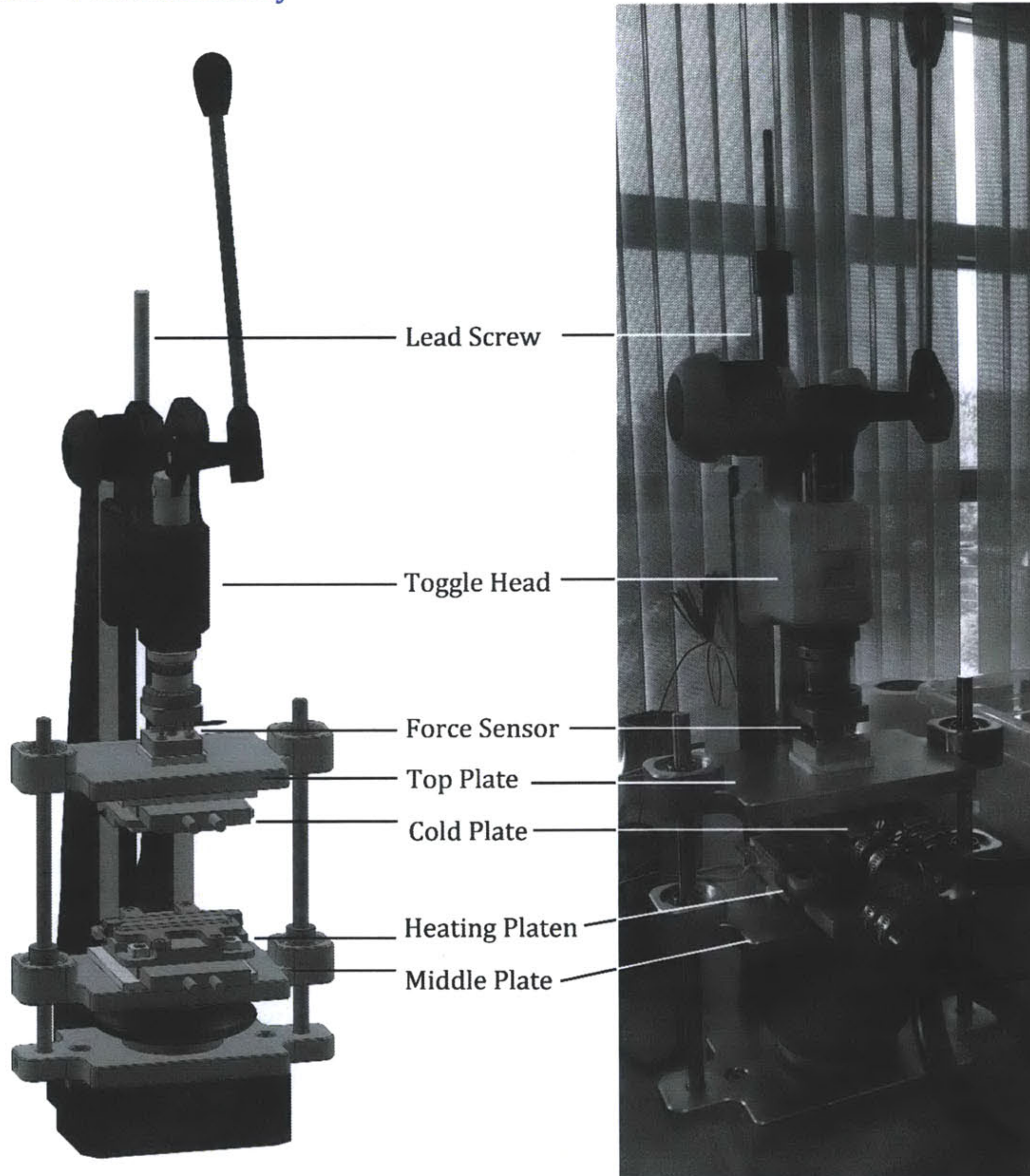

Figure 16 Full assembly view

6.1.1 Operational Procedure

a. The toggle is not engaged
b. The top and middle stacks are set to their starting positions by rotating the linear traveling lead screw that moves the toggle head
c. The master tool and substrate are loaded onto the top and middle fixtures, respectively
d. The heating platens are then raised to their desired temperatures
e. Once the desired temperature of both platens are reached, the embossing head is moved down using the lead screw
f. The force sensor indicates when contact is made by the output voltage reading begins to change
g. The lead screw is turned until the desired force is indicated by the sensor
h. The hold time begins and the temperature and force are kept constant (the force can be allowed to decrease slightly because of substrate flow)
i. After the holding period, heating is shut off and the liquid cooling system is turned on
j. The toggle head can be raised using the lead screw once the platens reach a temperature below the substrates T_g

6.2 Load Bearing and Tilt Compensation

The embossing system frame handles the loading application as well as the alignment between the tool and substrate. The definition of what the frame consists of can be seen in Figure 17. This system uses a Schmidt model 15F toggle head and frame capable of applying 12.00kN of force. The tool and substrate can be brought into contact using either the toggle action, which has a working stroke of 34.8mm, or the linear traveling lead screw, with a working range from 80mm-325mm.

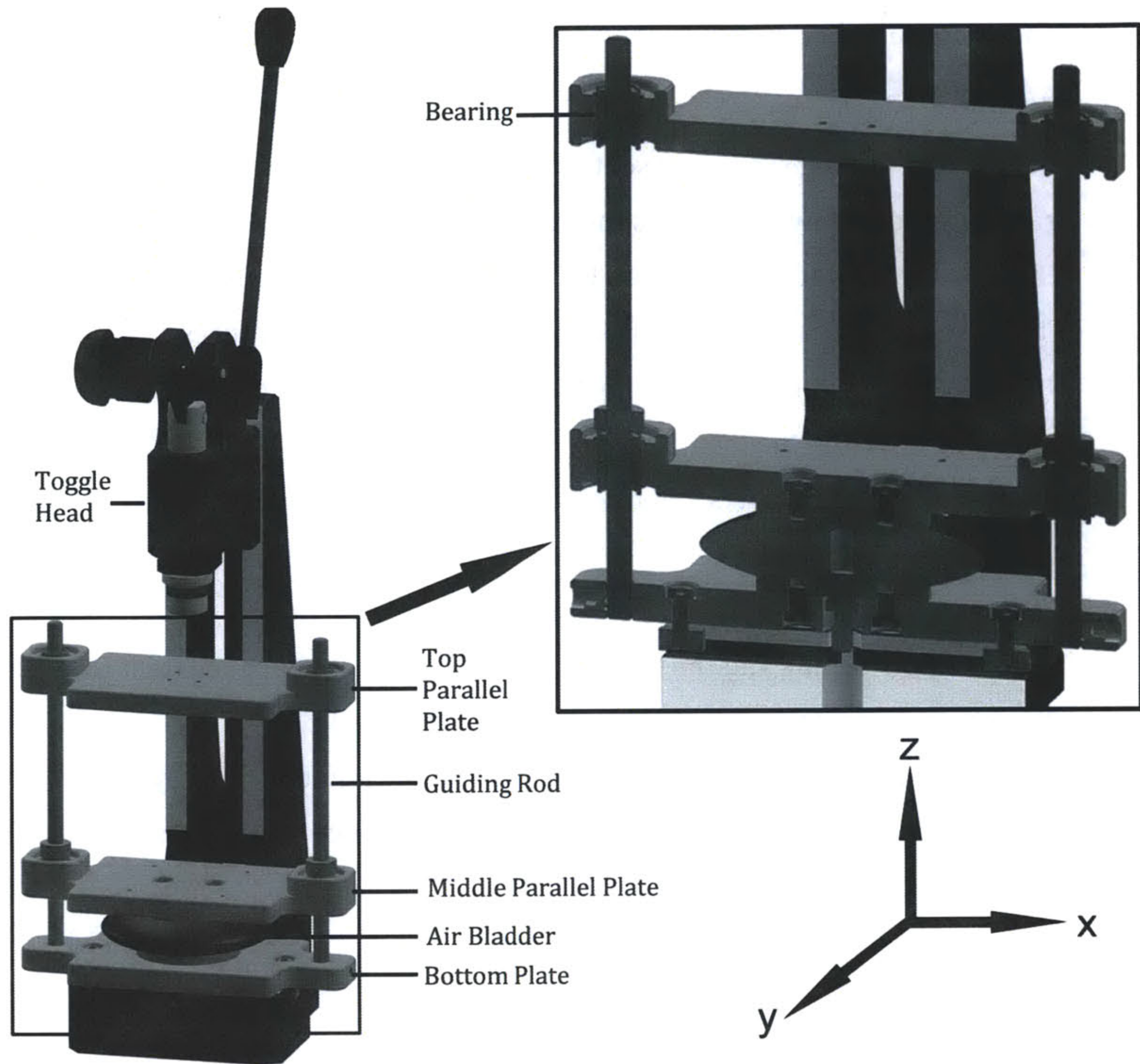

Figure 17 Frame assembly and cross section views.

Referring to Figure 17, the top and middle plates ride on guide rods using linear roller bearings. The bearings have individual inner bore diameter tolerances of 12.7mm+0.0/-6.35μm and tilt allowances of 15 minutes. The guiding rods have a diameter of 12.7mm+0.0000/-5.08μm. Maximum tilts of the stacks are dictated by the allowable tilt of the bearings. The frame also consists of an air bladder, rated for 6.67kN at 100psi, which couples the bottom plate to the middle plate, allowing for tilt compensation and equal pressure distribution between the tool and substrate. When the tool and substrate contact, the air spring distributes pressure evenly, theoretically making the top and middle plates parallel. Tilt may have an effect on feature quality by introducing gaps into the substrate during the initial

stages of embossing. Figure 18 shows how such gaps may form. The figure also shows how repeatability of feature location, relative to a locating point, could be affected by tilt. During the tilting process, the top and middle plates may be misaligned since they can move relative to one another.

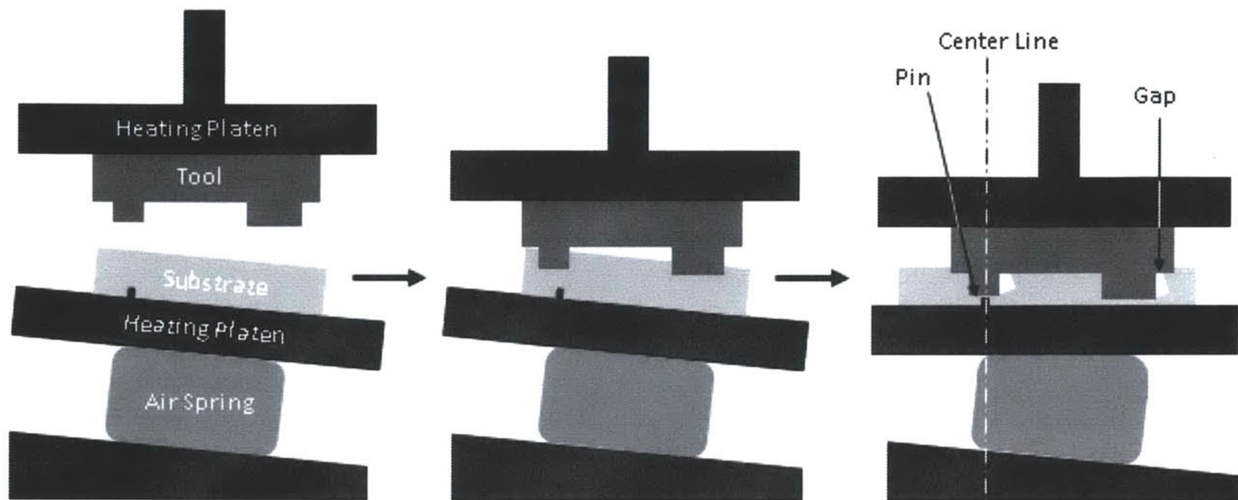

Figure 18 Visualization of misalignment air gaps.

6.3 Tool and Substrate Fixturing

The embossing tool was mounted directly to the heating platen and did not require a fixture because it was not removed in between experiments. The tool and substrate were positioned in line and orientated with one another. A fixture was designed so that the general placement of the substrate could be somewhat repeatable. The substrate fixture has three outer locating pins that rest on the perimeter of the PMMA. This fixture also has three secondary inner pins that are embossed onto the backside of the PMMA. These embossed pin features were used to assess the machines x, y and angular repeatability, and as locating features for attachment to a measurement fixture. The PMMA is held down using side clamps, which in the event of substrate shrinkage onto the tool, helps to hold down the PMMA as the tool is lifted upwards and de-embossed. This fixture is mounted directly to the heating platen through four bolt patterns. Figure 19 shows how the substrate was fixtured.

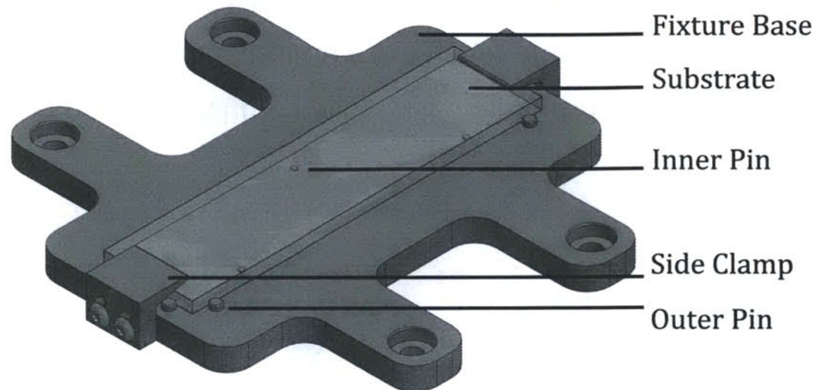

Figure 19 Substrate fixture

6.4 Heating and Cooling

Both the tool and substrate had dedicated heating platens and cooling plates. Figure 20 shows the tool and substrate assemblies. A single 150W-heating cartridge was inserted into each platen and was oriented in the direction of the tool and substrate lengths. These cartridges were used because of their rated heating temperature of 538°C and low cost. They are aligned in the same direction as the tool and substrate to provide uniform heating from the mid line. An Omega CN7500 series temperature controller capable of maintaining 2°C accuracy and a 200°C rated adhesive thermocouple were used to control the heating of each platen. The thermocouples were placed on the surface of the heating platen. Precise control of heating rate was not considered to be an important aspect of the machine because of the allowable 30 minute embossing process time window. Ceramic Macor insulation was used to reduce thermal transfer to the frame components through conduction. Convection and radiation heating were assumed to be negligible in comparison to conduction. Figure 20 shows the conduction path blocked by the insulation at the top of the bolt heads and bottom of the cold plates.

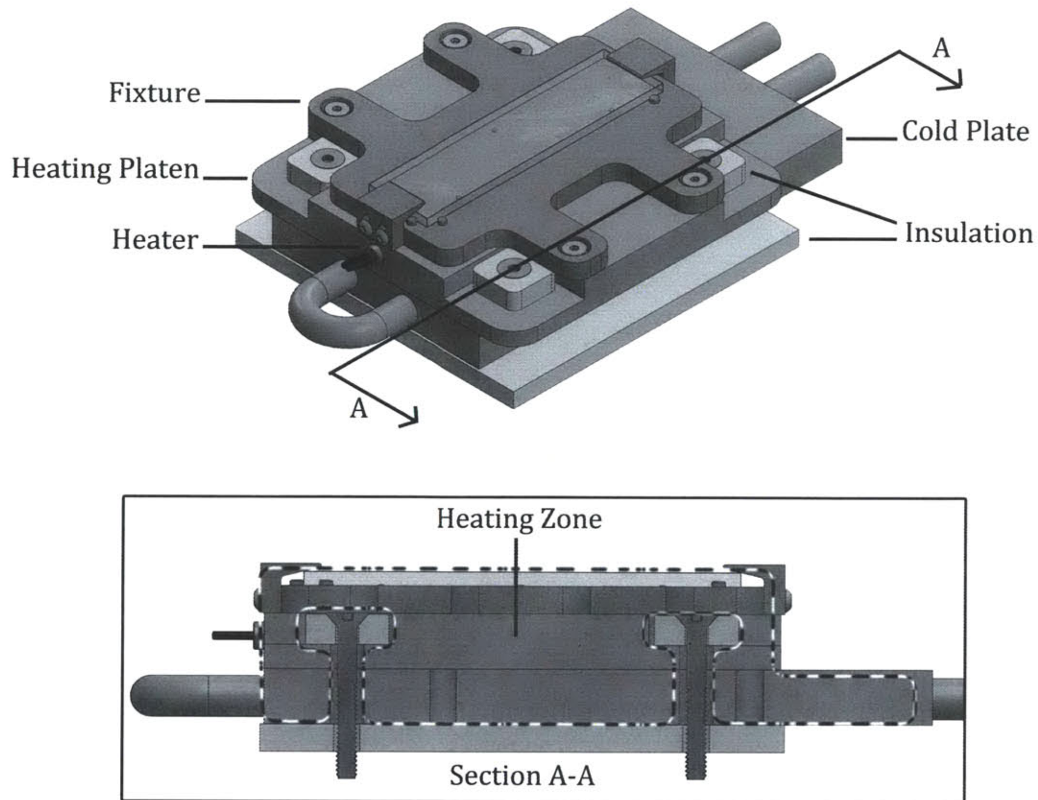

Figure 20 Substrate heating assembly and cross section

Cooling was achieved by using cold plates placed directly in contact with the heating platens. The cold plates ran a double loop, with 11L of recirculating room temperature water as the acting fluid. A pump provided flow of 38L/min over 1.83m of head (47L/min at 1.5m of head). This system was able to cool each platen from 140C to 40C in 2 minutes. Figure 21 shows experimental cooling data. The top plate was designed with the same configuration setup, minus the substrate fixture, and was bolted directly onto the heating platen.

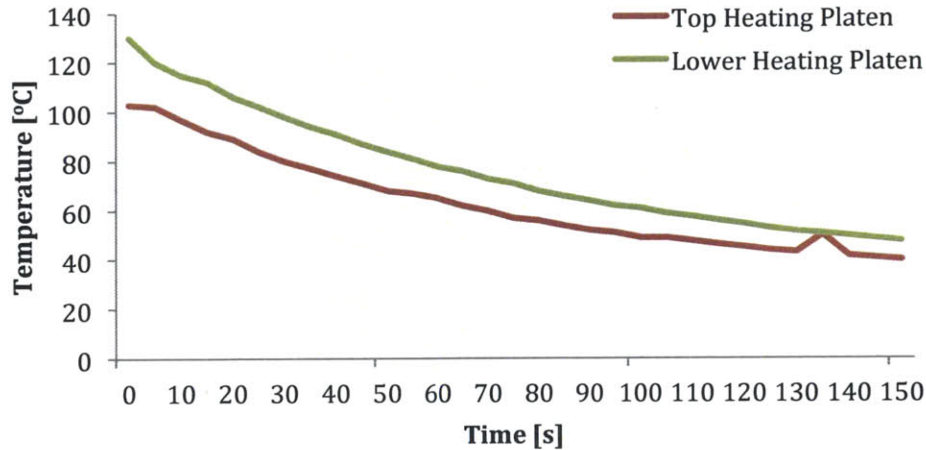

Figure 21 The cooling profile of the top and lower heating platens over a period of 2.5 mins.

6.5 Load Sensing

The load sensor was used to determine the amount of force applied between the substrate and tool. A Futek LCM200 sensor was chosen based on its size, 4.45kN sensing capacity and in line mounting option. The sensor limits force application to 2MPa since the embossing area is 22.50cm^2. The sensor is bolted to the top parallel plate and de-coupled from the toggle head. De-coupling the sensor from the toggle head allows for the frame assembly to be unconstrained from top to bottom. This allowing for any vertical misalignment at the point of the toggle head to be resolved after the toggle head applies pressure on the force sensor. The alignment correct was thought to help reduce any errors that could occur in constraining the frame assembly and having the load sensor pick up stresses such as shearing. Figure 22 shows the placement and mounting of the sensor. De-coupling was achieved by providing a gap between the flange that connects the toggle head to the force sensor and the top aluminum block that the sensor was screwed into.

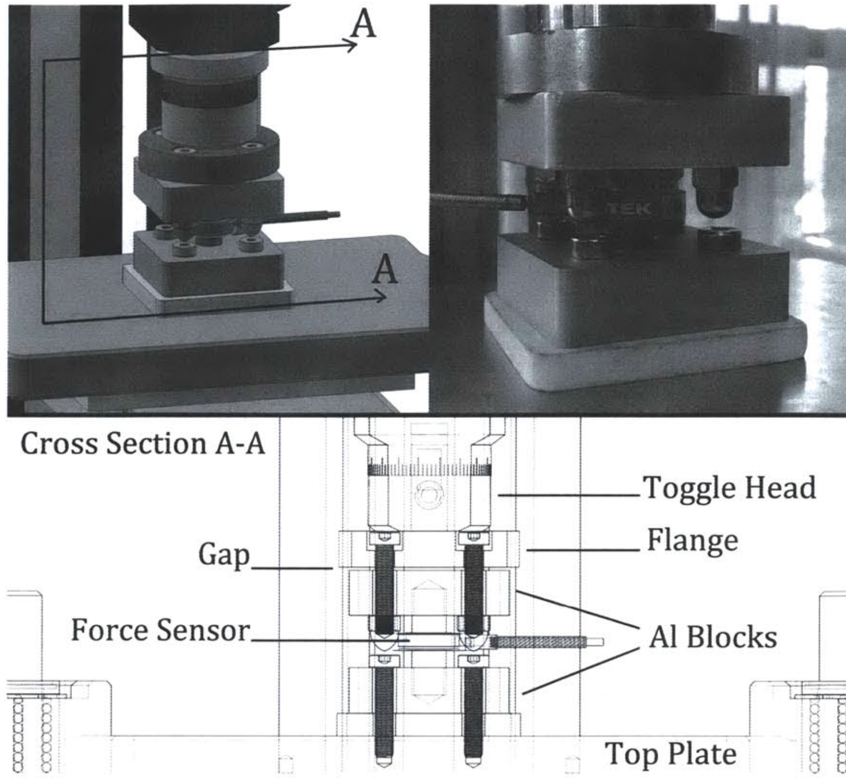

Figure 22 De-coupling of force sensor

7 Methodology: Process Control and Capability

The objective of this research is to validate the system and the process, characterize the process window for hot embossing and understand the capabilities of the hot embossing process to manufacture the microfluidics backbone cartridge part at Daktari Diagnostics. This entails the analysis of the capability of the machine designed for hot embossing and its limitations towards the manufacturing of particular part features and size. It also includes the optimization of the process using statistical process control techniques to find the optimal settings for the most significant factors.

The system validation includes the analysis of the alignment, process variation and the validation of the measurement system. The alignment validation is a study of the repeatability and reproducibility of the system to manufacture multiple parts. This is one of the measures to evaluate and characterize the process. This analysis helped in gaining more knowledge of the capability to hold specific position and dimension tolerances when making multiple parts using the particular system. The system used for measurement of the critical features at critical locations has to be characterized for its repeatability and the reproducibility using the Gage Repeatability and Reproducibility (Gage R&R) analysis. The analysis evaluates the performance metrics or dimensions according to their ability to be replicated. These metrics validated by the measurement system analysis are later used as the response variables in the experimental design.

The process is optimized using the appropriate model for the design of experiments using factors which affect the process the most. The aim of these experiments was to characterize the response of the significant factors and find the capability of the process using these optimal factors.

7.1 Process and System Validation

The process for the rapid prototyping at Daktari using the hot embossing process is liable to a number of sources of imperfections which can bring inaccuracies into the process. This section aims at gaining more knowledge of the capabilities of the process and validating the measurement procedure used for evaluating and quantifying the system capability.

7.1.1 X & Y Repeatability

Referring to Figure 17, the alignment system consists of the top and middle plates, air spring, guiding rods and bearing. To evaluate the x and y positional repeatability of the embossing system, the distance between fiducials that resided on the back and front of embossed parts were measured. By measuring the variability of these distance measurements over 10 parts, an estimate of the positional repeatability could be calculated. This positional repeatability was then decomposed into purely x and y planar slip, and rotational error.

The fiducials used were marks left by the 3 locating pins embossed onto the back of parts and surface features on the fronts of these parts left by the embossing tool. Figure 23**Error! Reference source not found.** shows the three embossed pin fiducials, on the top images, with their corresponding embossing tool fiducials, directly below. The planar distance between corresponding fiducials were taken for the three locations and used to estimate planar misalignment. Figure 24 shows a sample of how the planar distance between corresponding fiducials was measured.

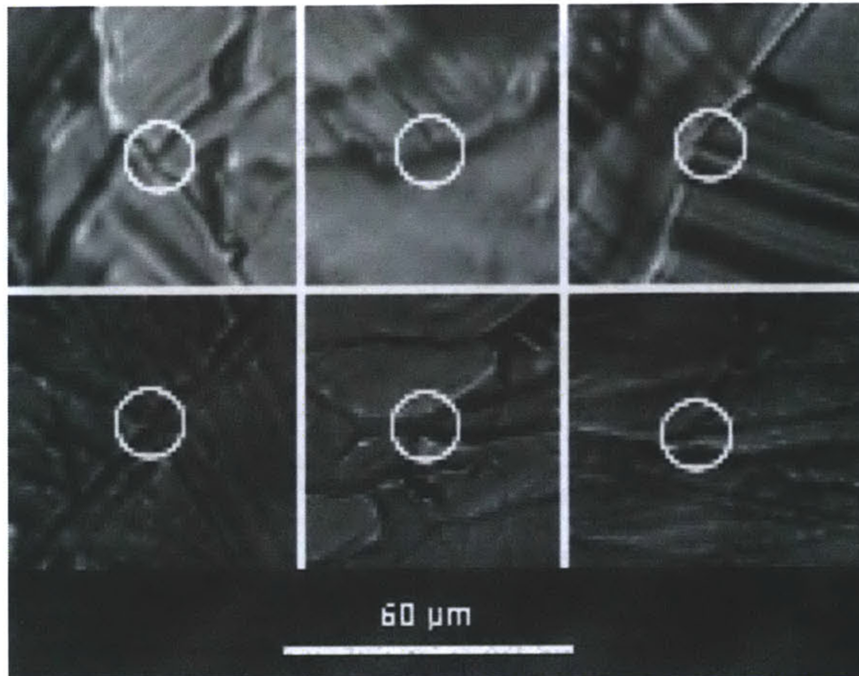

Figure 23 Fiducials used for x, y repeatability measurements

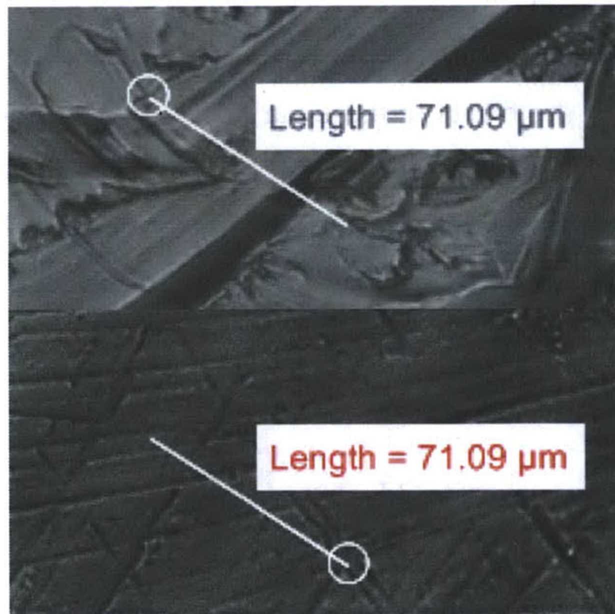

Figure 24 Distance between fiducials

Table 1 shows the measurements taken at the three locations for the 10 samples. All the parts had the same set of parameters with the tool temperature being at 140 C, the substrate temperature at 120 C, pressure of 600 lbs, holding time of 10 minutes and the de-embossing

temperature of 30 C. The measurements were taken on a Nikon Eclipse Ti-SR optical microscope with a magnification of 10X.

Table 1: Measurement Data

	L1_M1	*L1_M2*	*L1_M3*	*L1 Avg*	*L2_M1*	*L2_M2*	*L2_M3*	*L2 Avg*	*L3_M1*	*L3_M2*	*L3_M3*	*L3 Avg*
R1	139.30	139.58	139.30	139.39	79.00	78.86	79.23	79.03	71.09	71.42	70.42	70.98
R2	129.77	129.77	128.33	129.29	98.37	97.21	96.93	97.50	78.01	76.49	76.58	77.03
R3	126.83	128.81	128.25	127.96	81.52	81.66	83.33	82.17	58.30	58.84	58.10	58.41
R4	138.64	140.40	138.79	139.28	93.57	95.08	96.48	95.04	73.24	72.90	74.32	73.49
R5	144.61	143.15	143.69	143.82	66.06	65.17	67.82	66.35	39.27	39.69	40.29	39.75
R6	127.91	128.32	128.59	128.27	76.49	77.28	75.69	76.49	53.66	52.92	53.80	53.46
R7	138.70	139.51	139.00	139.07	73.94	74.80	72.95	73.90	76.71	76.72	76.71	76.71
R8	153.38	152.53	152.54	152.82	58.09	57.29	57.95	57.78	80.40	80.30	80.29	80.33
R9	151.12	152.52	151.68	151.77	58.93	59.29	58.21	58.81	79.23	78.67	78.36	78.75
R10	148.06	147.50	146.70	147.42	56.62	56.96	58.58	57.39	76.74	77.79	77.07	77.20

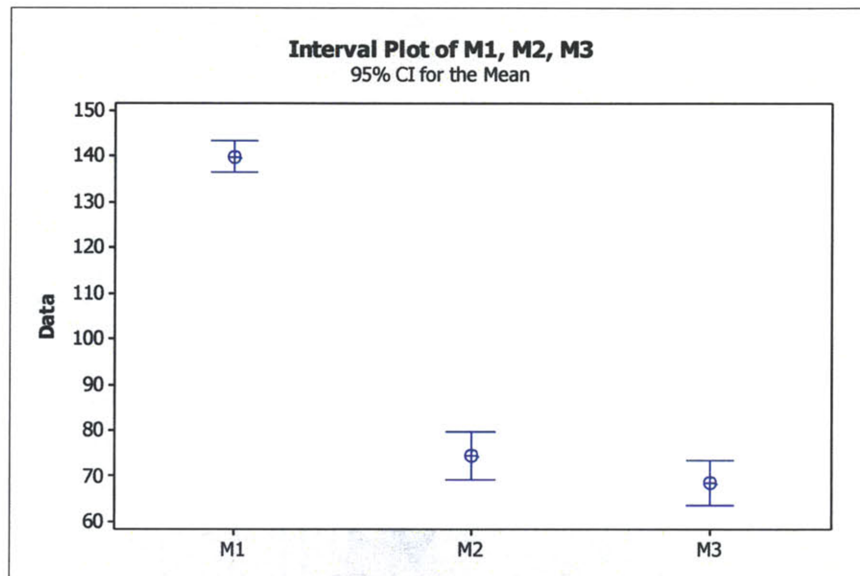

Figure 25: Error Band for the three Locations

Figure 25 depicts a plot of the 95% confidence interval on these fiducial measurements. The width of this confidence interval is what was used to estimate positional repeatability. If there was no angular component to this repeatability, then all three measurement positions should have confidence intervals of similar widths. However, the confidence interval on the measurements taken at position 1 is visibly narrower than the intervals for positions 2 and 3. This difference is attributable to angular misalignment, and indicates that location 1 is located closer to the central axis of the press than the other two locations.

A summary of these error bands (95% confidence intervals on measurement) is seen in Table 2. Calculated error band for the three locations and the distances of these locations from the central axis are as follows:

Table 2: Error Relation to Distance

(All values in microns)	*Location 1*	*Location 2*	*Location 3*
Error Band	26.55	41.75	41.13
Center Distance	8690	33448.559	33448.559

To decompose the measurements summarized in the above table into errors attributable to pure x and y planar slip and angular error, the equation (1) was used.

$$E = e + \alpha l \tag{1}$$

E is the total positional error, e is the static x and y error component, and the αl term is angular error. Angular error is a function of distance from the central axis of the press, α is a constant describing the severity of this error, and l is the radial distance from the central axis. The axis that l is measured from can be seen in Figure 26 and Figure 27. The axis runs down the toggle head, along the center of force application.

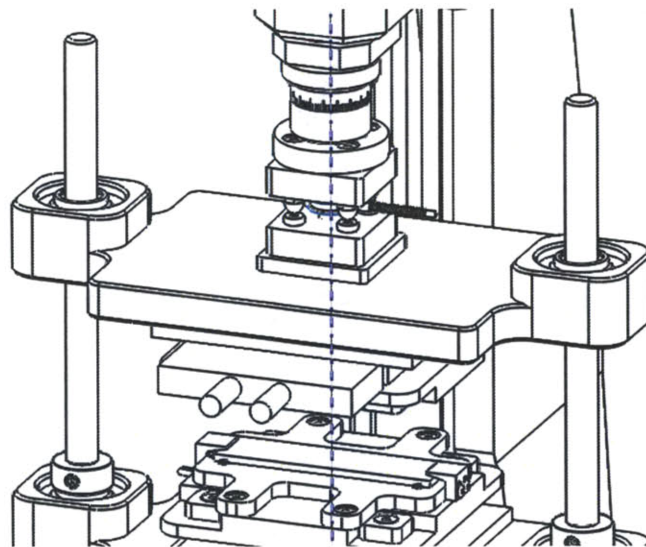

Figure 26: Central axis: ISO view

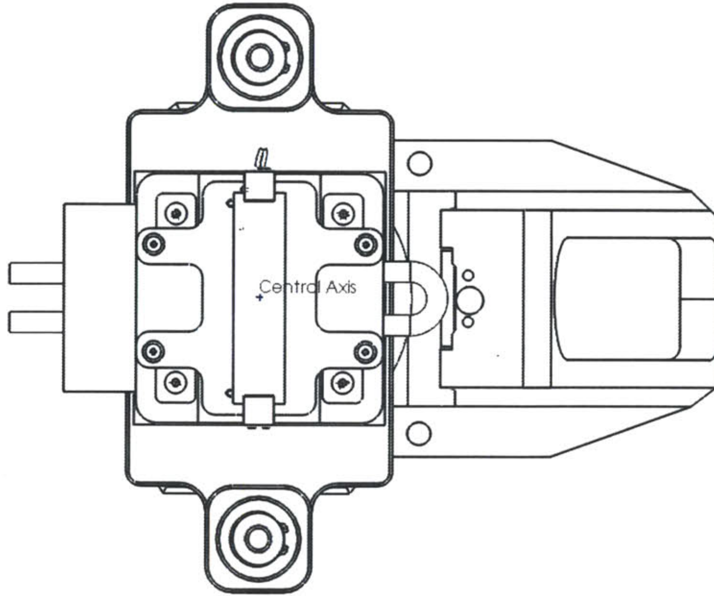

Figure 27: Central axis: top view

The x and y planar slip (e) was found to be 21 microns. The constant describing angular error was found to have a value of 0.000614. Using this data, the maximum positional error for embossing with our tool was calculated. With the spatial error remaining constant at 21 micron, the angular error at a distance of 3.6 mm (maximum distance of a feature embossed from the center for the cuvette) is equivalent to 22 microns. Hence, the total XY repeatability is equivalent to 43 microns. This is the positional error located at the via furthest from the center of the tool.

7.1.2 Parallelism

As shown in Figure 17 the setup includes the three plates, with the guiding rods and the air bladder as a subsystem for the purpose of alignment. The bearings used are linear roller bearings with re-circulating stainless steel balls and a ceramic cage. For attaining greater accuracy in the parallelism between the plates, the plates were precision manufactured with 12.5 micron (0.0005 inch) tolerance for parallelism.

The guiding rods are used with linear roller bearings (AISI 52100 Steel balls and DURACON M90 cage), which allow an angular misalignment of 0.25^0 that incorporates a 43 micron clearance (allowable wiggle room for the air bladder) across the width of the cuvette at a distance of 10 mm from the center. The air bladder (*Single-Tire Style Air Spring rated @1500lbs*) is used to absorb the inaccuracy in parallelism to make the plates parallel. For analysis of the capability of the system to provide absolute parallelism, two methods were shortlisted as options:

- Use of the Nikon Eclipse Ti-SR optical microscope to focus on one fiducial on one side of the part produced and then recording the z direction travel to focus on a different fiducial on the other side of the part.
- Use of a Vernier Callipers with a precision of 10 microns to measure the 4 corners of the part to find out the parallelism accuracy across the length and the width of the part.

The Nikon Eclipse Ti - SR optical microscope was tested for repeatability for the z travel measurement and it was repeatable with a precision of 25 micron. The Vernier Callipers instrument with precision of 10 micron was the better of the two options.

To analyze the parallelism of the parts the method used was the measurement of the thickness at four locations on the part. The positions of these measurements are shown in the Figure 28. These measurements were used to find the parallelism across the length of the part and across the width of the part. Ten parts were measured at these 4 locations to find out the tolerance of the system for parallelism. Table 3 shows the results of the analysis.

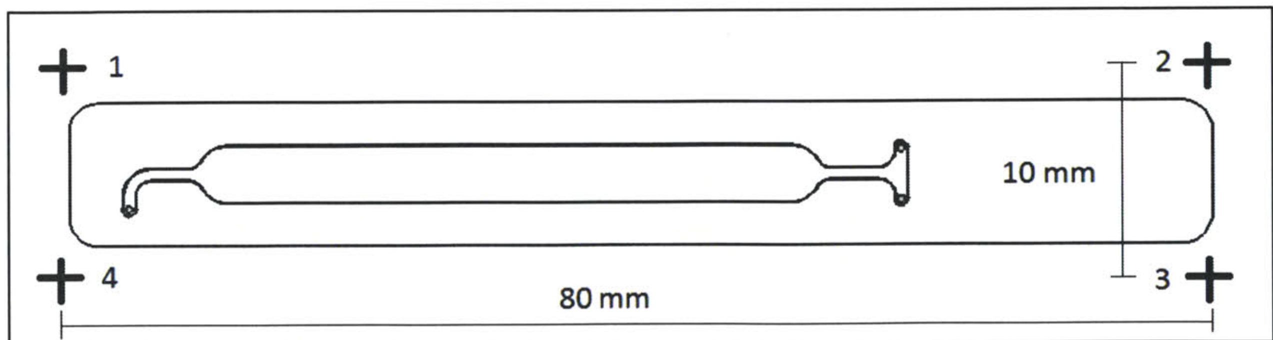

Figure 28: Measurement Locations for Estimating Platen Parallelism

Table 3 Parallelism Measurements

(all values in mm)	*M1*		*M2*		*M3*		*M4*		*Along the length*	*Across Width*
R1	3.05	3.04	3.04	3.05	3.07	3.07	3.08	3.08	0.00	0.03
R2	3.02	3.01	2.99	2.99	3.01	3.01	3.04	3.05	0.03	0.02
R3	3.01	3.01	3.04	3.05	3.05	3.06	3.04	3.04	0.03	0.02
R4	2.95	2.94	2.93	2.92	2.96	2.98	2.99	3	0.02	0.05
R5	2.97	2.97	2.99	2.99	2.99	2.98	2.96	2.98	0.02	0.00
R6	2.93	2.93	2.95	2.95	2.96	2.95	2.96	2.95	0.01	0.01
R7	2.97	2.95	2.97	2.98	2.98	2.99	2.98	2.97	0.01	0.01
R8	2.9	2.89	2.89	2.88	2.94	2.92	2.95	2.95	0.02	0.05
R9	2.95	2.95	2.93	2.93	2.95	2.94	2.95	2.98	0.02	0.02
R10	2.94	2.95	2.93	2.93	2.98	2.98	2.98	2.98	0.01	0.04
R11	2.98	2.98	3	3	3.01	3.01	3.02	3.02	0.00	0.02
									0.02	0.03

The parallelism achievable with this system was found to be 30 microns across the width of the part and 20 microns across the length.

7.1.3 Measurement Validation

We need to validate the measurement procedure to verify the accuracy of the measurements and also the capabilities of the measurement procedure. For this purpose, a Gage R&R technique was used to find the precision to tolerance ratio for each of the dimensions measured. This would also give us an idea of which of the dimensions could be measured precisely and could be used as a metric for the system performance [34].

The precision of measurement consists of two terms which are the reproducibility and the repeatability. Repeatability is the measurement variability present in measuring the same sample multiple times while reproducibility is the measurement variability under different conditions. The precision to tolerance ratio (P/T) is a measure of the capability of the measurement system. Generally, a P/T ratio of 0.1 is ideal and 0.3 is in the acceptable range [34].

Table 4 shows the P/T ratio of the various dimensions of the cuvette and we can see that the ridge width and the ridge height have the least P/T ratios. We can use these feature dimensions as the metrics in the experimental design as validated by the Gage R&R analysis.

Table 4 Summary of Gage RR Results [34]

	Channel Depth	***Ridge Height***	***Ridge Width***	***Cuvette Width***	***Surface Roughness***	***Radius***	***Channel Draft***
Tolerance Band	2.00	2.00	10.00	20.00	N/A	6.00	2.00
Units	Micron	Micron	Micron	Micron	Nanometer	Micron	Degree
Gage Variance							
Total	0.1228	0.0292	0.4187	8.9237	57.7034	1.6850	4.2344
Repeatability	0.1106	0.0162	0.4187	5.4495	13.6782	0.3417	0.6242
Reproducibility	0.0121	0.0130	0.0000	3.4742	44.0252	1.3433	3.6102
Precision	1.80	0.88	3.33	15.38	39.12	6.69	10.60
Precision/ Tolerance	0.9022	0.4399	0.3333	0.7692	N/A	1.1142	5.2988

7.2 Process Evaluation & Performance Measurement

For the purpose of gauging the performance of a process or the analysis of the capabilities of a process, evaluation of the process with set metrics and using them to measure the performance is one of the crucial steps of process control. It involves selection of critical locations and deciding the metrics to evaluate performance, measuring the parts at these critical locations and quantifying these metrics to use them as a gauge for performance. This helps in acquiring quantifiable data to make a decision on the effectiveness of different settings and parameters.

7.2.1 Selection of Features on Microfluidics Part

To evaluate the capability of hot embossing as a prototyping process for Daktari, the assay channel of their microfluidic network was chosen for replication. This specific feature was selected because it represents a location that has undergone extensive iterative design, and therefore would likely benefit from the ability to be prototyped with greater speed and fidelity. Additionally, this feature contains some of the tightest tolerances and smallest dimensions on the microfluidic product and so represents one of the most difficult features to replicate.

The assay channel is a rectangular channel that has a high aspect ratio. The depth of this channel is 50 microns, while its width is 4 mm. A microscope image of the complete channel cross section can be seen in Figure 29. Immediately adjacent to the channel, is a 10-micron high ridge that runs around the assay channel. A microscopic image of this ridge is seen in Figure 30. This ridge poses one of the largest challenges for the embossing process. It is a tightly toleranced feature with small dimensions, which is adjacent to a zone of high material displacement.

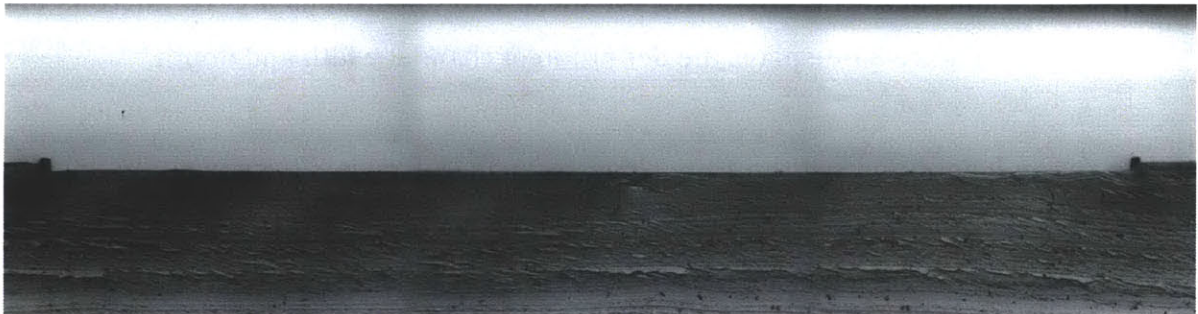

Figure 29 Microscope Image of Channel Cross-Section

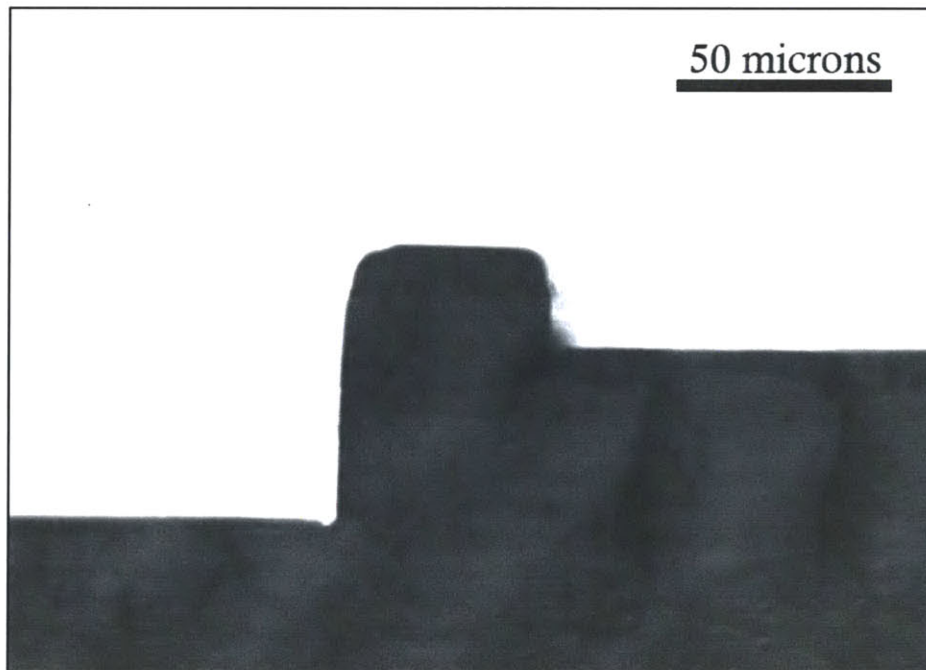

Figure 30: Microscope Image Close-up of Ridge

Several critical dimensions of this channel can be described as 2-dimensional measurements taken from a cross-section of the channel. These dimensions are the depth and width of the channel, the height and width of the ridge, the draft on the channel walls, and the radius of the inner edges of the ridge. We list down all the possible measurements of the assay channel which could be used a metric for the evaluation of the process.

7.2.1.1 Width and Depth

Correct depth and width of the channel are critical for proper performance of this device. As mentioned previously, the specification for the width of this channel is 4mm and the depth is 50 microns. The tolerances for these two dimensions are 10 microns and 1 micron respectively. Figure 31 displays the definition of channel width and depth.

The height and width of the ridge, as seen in Figure 32 are also dimensions of critical importance. The specification for this ridge height is 10 microns and its width is 50 microns. This ridge feature presents a particularly difficult challenge for replication with hot embossing, and its dimensions will likely be a clear indicator of the quality of finished parts.

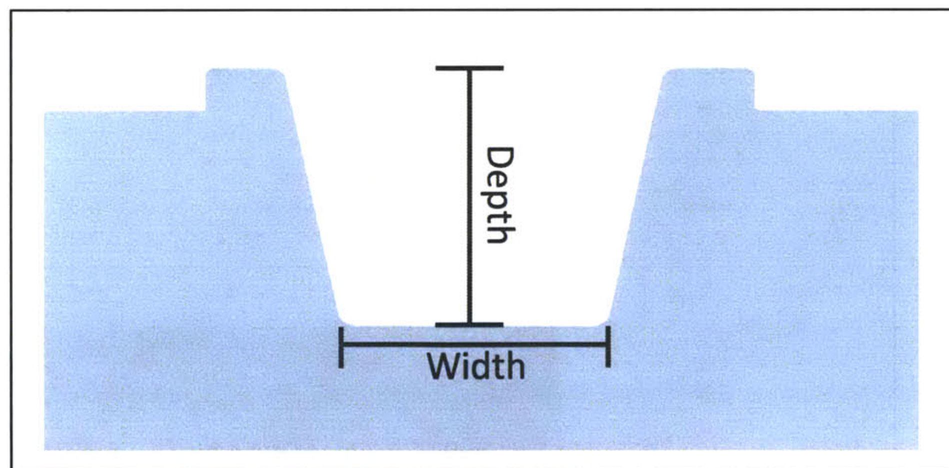

Figure 31: Channel Depth and Width

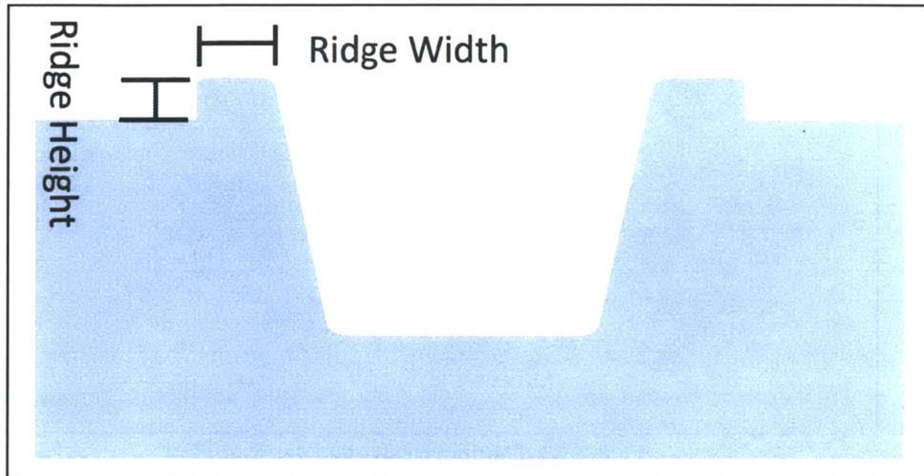

Figure 32 Ridge Height and Width

7.2.1.2 Edge Radius and Draft

A cover will be attached over the top of the channel. Therefore pinch points exist at the location of the upper edges of the channel. The radius of these edges must be minimized in order to limit the possibility that cells are trapped in these pinch points. A smaller radius at this edge is also indicative of more complete filling of the mold cavity. Figure 33 shows the location of this upper edge. Ideally, this radius would be non-existent, and the corner would be perfectly sharp.

Draft of the channel wall is another dimensional quality of the channel that can affect the performance of the embossed part. The production parts are injection molded and therefore have a designed in draft. The parts produced with hot embossing are being made with a tool that has vertical walls. Draft should be essentially absent from fully formed parts. In the future, Daktari may design embossing tools that have a designed in draft. If this were the case, measuring this draft angle would be critical to examining the quality of embossed parts.

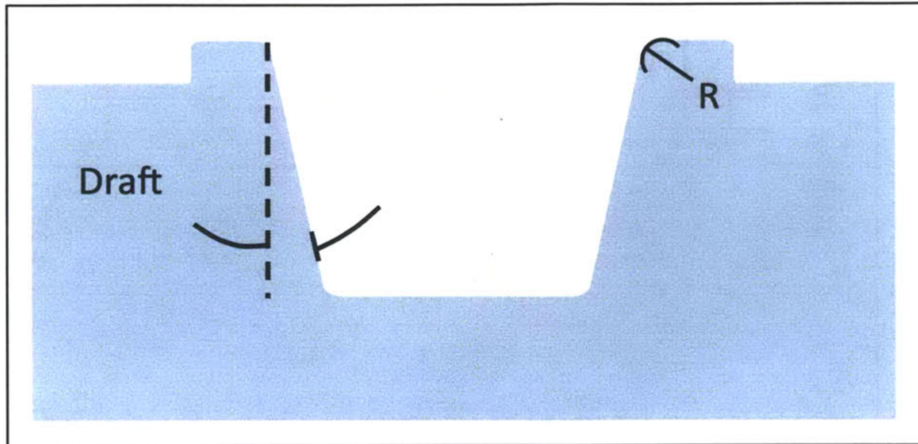

Figure 33: Channel Draft and Edge Radius

7.2.1.3 Channel Uniformity

Channel uniformity is a measure of within part variability. This metric will be used to measure how constant the cross sectional dimensions of a channel are along the length of a channel. The uniformity of channel width and depth are very important for the performance of this product, as variations in these dimensions can cause anomalous flow of fluid through the assay channel. Taking cross-sectional measurements at several locations along the length of the channel and reporting the standard deviation of this sample of measurements will measure uniformity of these dimensions. An ideal channel, with perfect uniformity would have identical width and depth measurements at all points along the channel.

7.2.1.4 Warping

Card bow is a measure of warping that occurs during the hot embossing process. After the load applied during the embossing process has been relaxed, it is possible for uneven cooling rates to cause the part to warp. Allowing the part to cool more thoroughly before removing the embossing load can reduce warping. However, this will lock residual stresses into the part and could make the part more difficult to de-emboss from the tool.

Bowing or warping of the embossed part is undesirable and should be measured as a quality metric. Bowing will be measured by scanning the entire length of an embossed channel. The height data of a cross section along the length of the channel, as seen in Figure 34 is obtained from the interferometer scan. This height data is then cropped to only include the

data points that reside on the bottom of the channel. The resulting data should ideally be a flat line. Any large regular deviation away from flat can be attributed to general warping of the part. Figure 35 depicts measurement data of a channel that exhibits warping. The warping metric will be measured in microns and will be calculated as the maximum difference in height data from a set that should represent a flat plane.

Figure 34: Scan of the Entire Length of an Embossed Channel

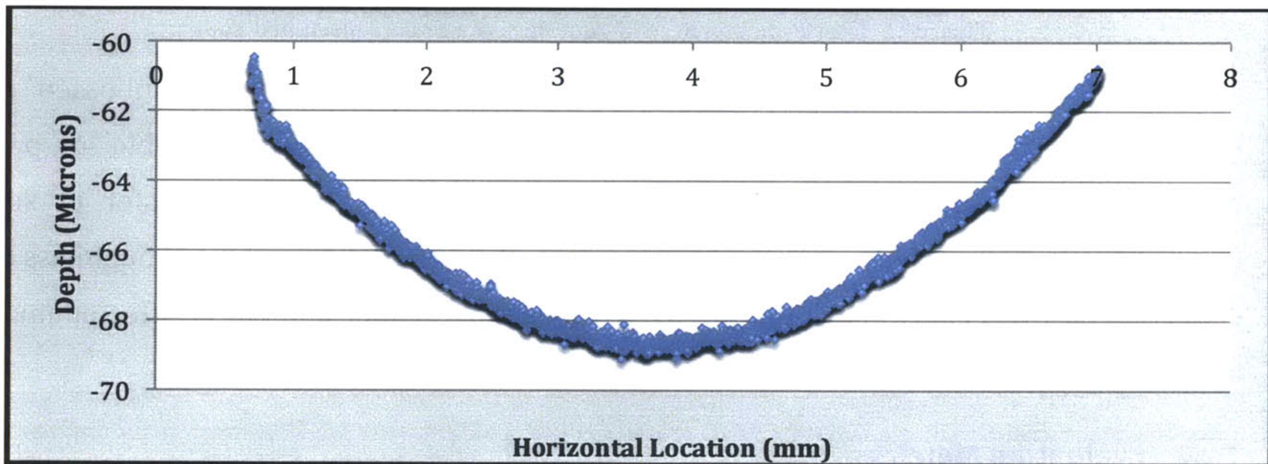

Figure 35: Along Channel Cross-Sectional Data Exhibiting Warping

7.2.1.5 Surface Roughness

As mentioned previously, achieving low surface roughness in microfluidic channels is necessary for proper performance of the device. Surface roughness must be minimized in order to reduce wall drag, ensure smooth flow and limit cell capture on channel walls. Surface roughness will be measured by scanning the bottom of an embossed channel using the procedure described previously. Figure 36 shows an image obtained from scanning the flat surface of a micro-machined hot embossing mold with an interferometer. The tool marks produced by the machining operation can be clearly seen.

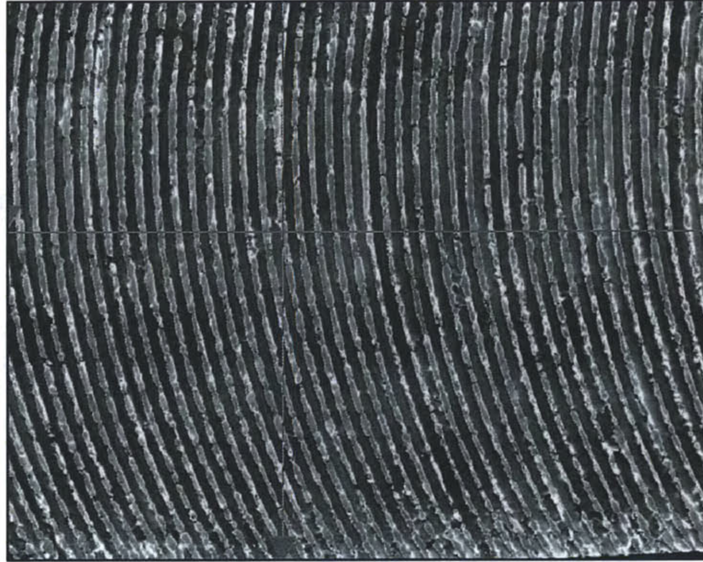

Figure 36: Interferometer Scan of Tool Marks on a Micro machined Tool

It is important to characterize the surface roughness of embossed parts; however, surface roughness will likely not be chosen as the response variable for process optimization. The hot embossing process accomplishes high fidelity transfer of surface features between the mold tool and the embossed part. Therefore, the surface roughness of the embossed part will likely match the surface roughness of the tool, and not be affected much by the process parameters.

7.2.2 Evaluation Metrics

For the purpose of gauging the performance of a part, a few of the dimensions from the list above need to be set as metrics for the evaluation of the process. These metrics will then be further used in experimental design and need to be an accurate measure of the performance of the part and should be suitably sensitive to it.

Measurements indicate that the ridge on the cuvette is one of the more sensitive features to the embossed part quality. Hence, the ridge dimensions of width and height would be a good indicator of the part quality. In comparison to the results of the Gage R&R (Reproducibility and Repeatability) for the radius and the draft angle the results for the width and height indicate that ridge width and height dimensions can be used a metric for the performance of the part [34].

The ridge width and the height are a definite indicator of the filling of the material in the intricate corners. For the purpose of using a metric for the experiments to measure performance a ratio of the height of the ridge on the part to the height of the ridge on the tool was used as one metric.

$$Height\ Fill = \frac{Ridge\ Height}{Tool\ Height} \tag{2}$$

Another metric which was used is the width fill which is a ratio of the width of the ridge on the part to the width of the ridge on the tool. Apart from being an indicator of the fill ratio of the part made this metric was also useful in giving an approximate idea of the forming of the radius as well as the draft angle[34].

$$Width\ Fill = \frac{Ridge\ Width}{Tool\ Width} \tag{3}$$

7.3 Process Parameters

The process of hot embossing is affected by a number of parameters which have a correlation with the process performance. The method followed to find out the optimal parameters was to first consider all the parameters which may remotely affect the process and then down select from these parameters according to preliminary analysis to find the parameters which are critical to this process. These critical parameters are used as factors for the design of an experiment to find the most significant factors affecting this process and also quantify the significance of each factor to the process.

The factors which may affect the hot embossing process are listed and explained as below. Also, we list down the possible noise factors which may play a major part in this process.

7.3.1 Temperature

Temperature is a critical factor affecting the hot embossing process. The factor temperature relates to the temperature of parts being embossed. The temperature of the part decides the width, the depth as well as all the dimensional components of the micro feature. With increasing temperature the depth of imprint of the micro feature increases in a direct correlation [35]. As a temperature gradient is involved, the difference in the temperature co-efficient of the embossed part and the tool have to be taken into account to avoid the creation of additional forces due to the large shrinkage of the polymer material in comparison to the tool material [7].

The glass transition temperature of the material being used for the experiments was calculated to be 110 C on an average of 10 samples. The regulation of this factor is achieved using the cartridge heater in the top and bottom plate. These plates are in direct contact with the part to be embossed and the tool (mold). The temperature profile over time of these plates and in turn the hot embossed part and the tool can be controlled using the heater and the cooling system in place. An OMEGA 520323 temperature controller was used to measure and control the temperature of the plates heated by the cartridge heaters..

7.3.2 Force

Force is another very important factor which affects the hot embossing process directly. The force directly affects the dimensions of the micro features embossed. Prior research suggests that the force plays a major part in case of hot embossing but there is a particular threshold, beyond which the force doesn't play a major role towards the performance of the part [36]. It is observed that the force used in the process directly affect the fill ratio (Ratio of the most critical feature transferred to the original feature on the mold). Also, excessive force does cause the material to bottom out or make a through hole. This also depends on the temperature of the material and the tool.

At Daktari, a SCHMIDT press (Rated at 3000lb force) was used in conjunction with a load cell for pressurizing the platens together. A FUTEK load sensor (See Appendix A) with a controller was used as a force-readout. For the purpose of the experiment the load range used

was from 2000N to 4000N. Figure 37 Force Curve shows an example of the loading and unloading data of a part.

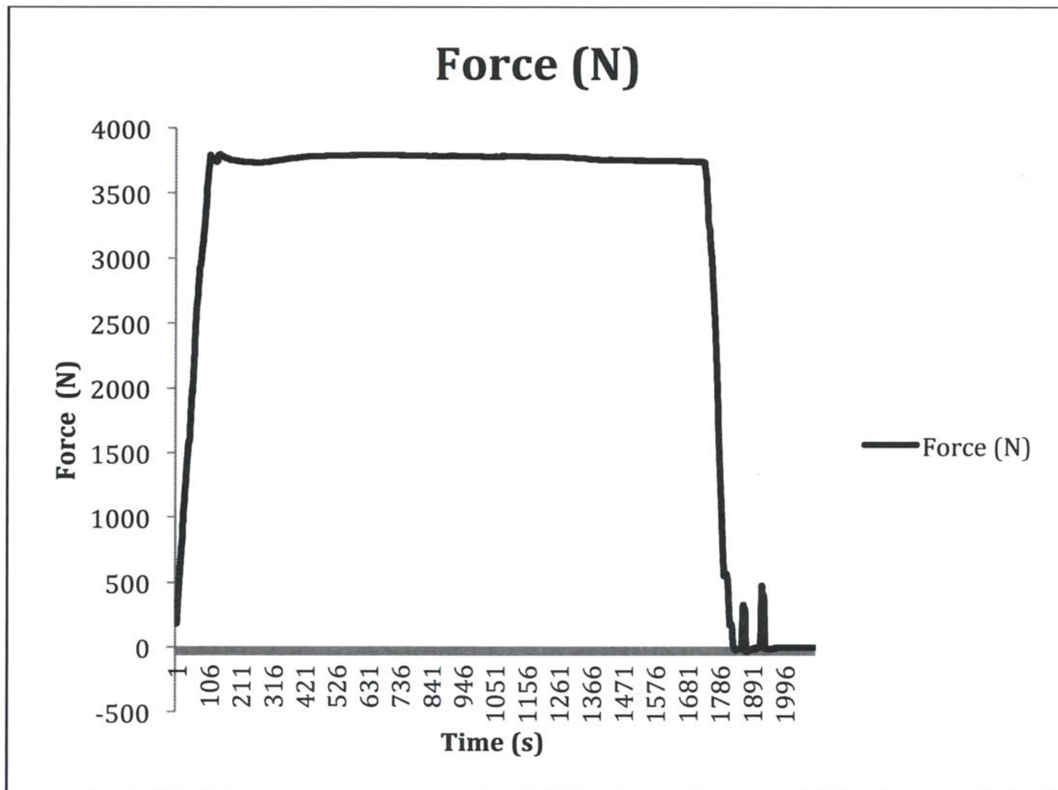

Figure 37 Force Curve

7.3.3 Holding time

One of the important parameters to be considered is the holding time used for hot embossing. The holding time is the time for which two plates are pressed together with constant force (Assuming that the system is force-controlled). The holding time is a critical parameter for the hot embossing process as the material flows into the micro-features over this time and mates with the tool which is the negative of the profile of the feature. The holding time plays an important role in the filling of the features while embossing. The radius and the draft angle of the feature on the final also depend on the holding time because of the same reason [37].

In the current setup, holding time is measured using a stop watch and for the purpose of the experiments the range of the experiments is from 5 minutes to 30 minutes. For the length of this holding time, the force on the part does relax as the material of the part being embossed is above its glass transition temperature and hence begins to flow [7]. As the press in the current setup is displacement-controlled as opposed to force-controlled, force does relax over the holding time.

7.3.4 De-Embossing Temperature

The De-Embossing temperature is one of the most crucial and important parameters in the hot embossing process. The De-Embossing temperature plays a part in the material contraction when it is lower resulting in a part which is out of specification. The contraction depends on the length of the feature contracting and varies accordingly.

The De-Embossing temperature is also a major factor for the defects in the parts formed because of the shearing of the material while de-embossing. At a lower temperature the material contracts on to the tool and is difficult to separate. A higher de-embossing force is required to separate the part from the mold and in the process the part is damaged [38].

The de-embossing temperature is controlled in the current system using an OMEGA 52023 controller (See Appendix A) and a cooling system with a recirculating pump.

7.3.5 De-Embossing Force

The de-embossing force has an inverse co-relation with the de-embossing temperature. Higher the de-embossing temperature lower is the de-embossing force required as the material tends to contract minimally around the tool at the higher temperature. But at a lower temperature, the contraction is much more and de-embossing defects may be seen on the part when a higher de-embossing force is applied [39].

The de-embossing defects are seen on a higher scale if the part is de-embossed with a central upward force compared to prying it off at one end and then propagating the de-embossed region along the length of the part [38]. For the purpose of controlling this factor on

the current setup we use the substrate flanges on the press. But the use of the substrate flanges which are at either end of the substrate uses a central force to de-emboss and causes the part to bend upward and snap back in place which causes further damage to the part. For this reason, the substrate flanges were discarded and a method to manually pry off the part at one end and then propagate that crack along the length of the part was used.

7.3.6 Embossing Velocity

One of the factors identified as a possible parameter affecting the process was the velocity with which the embossing was done. Embossing velocity is defined as the velocity at which the top platen attached to the press is displaced downwards to inflict the required force. It is measured in terms of the Newtons of force applied per minute [24]. For temperatures lower than the glass transition temperature the embossing velocity has a significant impact on the channel depth (for example PMMA glass transition temperature is 95C to 110C) and slower the velocity, the deeper the channel tends to be. When the temperature reaches above the glass transition temperature, around 110C to 120C, the embossing velocity doesn't make obvious impact on the channel depth. Figure 38 shows the impact of the embossing velocity and temperature on the Depth of the feature.

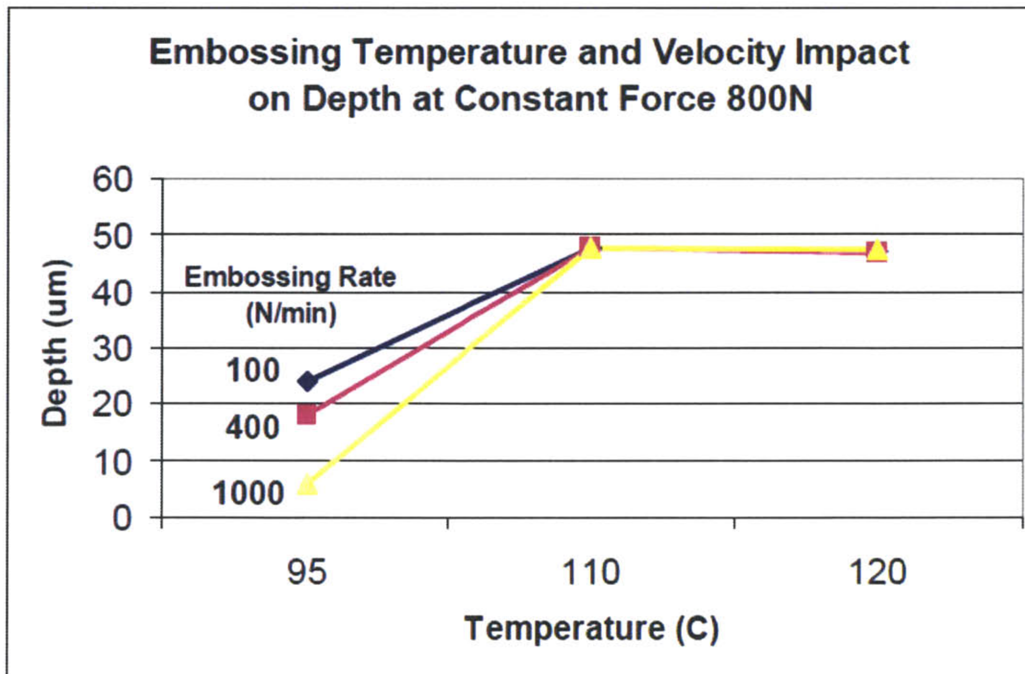

Figure 38 Embossing Temperature and Velocity Impact on Depth of Channel [24]

The embossing velocity may have a direct correlation to the material and may cause a significant change in the performance of the final part. Due to the lack of capability of force control of the current hot embossing setup at Daktari, we do not have a control over this parameter. This parameter does not directly affect the final design of experiments as the temperature range is above the designated threshold of glass transition temperature of the PMMA.

7.3.7 Material of Part

The material of the part is also an important parameter for the purpose of the hot embossing process. Daktari is using the poly methyl methacrylate (PMMA) for the microfluidic cartridge and intends to use the same material for the purpose of rapid prototyping. The material properties do play a significant part in the hot embossing process like the viscosity of the material, the behavior of the material to the temperature change, the glass transition temperature, the thermal co-efficient and so on. As Daktari is only concerned with the material PMMA the focus of this thesis will be using cast or extruded PMMA.

Extruded PMMA was used for the experiments which had higher tensile strength and lower glass transition temperature compared to the cast PMMA. Apart from the high tensile strength of 8,100-11,030 psi another advantage of using the extruded PMMA was the low glass transition temperature which helped in ruling out the Embossing Velocity parameter (The experiments were all above the glass transition temperature of 105 C). The Hardness for the material used was M68 and the impact strength was 0.7 ft.-lbs/in as shown in Appendix A For the purpose of uniformity in the material properties of the PMMA substrate, bulk PMMA sheets were procured to reduce part to part variability.

7.3.8 Thickness of the Substrate

The material thickness may be one of the important factors in the case of hot embossing as a higher thickness helps the material to flow and the reaction forces on the substrate from the base are different because of the lack of proximity to the base. The dynamics of the material flow while embossing might change with the thickness of the material.

To reduce the variability in the thickness of the PMMA bulk sheets of thickness 0.25 inch and 0.125 inch were procured with a tolerance of 0.05 inch. The PMMA substrate was cut into rectangular pieces of 25 mm X 100 mm for use in experiments.

7.3.9 Material of the Tool

The material of the tool or the mold in question may also be a critical factor as the material properties such as the melting point and the coefficient of expansion may play a significant role in the part performance. Apart from the direct impact on the dimensions on the final part the material of the tool is one of the factors in the degree of tool wear.

For the purpose of the experiment, a Brass (Ultra Machinable Brass Alloy 360) was used to make the tool using micromachining. A total of three Brass tools were used for the set of preliminary experiments and the experimental design.

7.3.10 Noise Factors

Noise factors are the parameters in the experiment which are not possible or difficult to control during the manufacture or use but can be set at fixed levels in the experiment and varied jointly with the design factors.

7.3.10.1 Ambient Temperature

One of the possible noise factors is the ambient temperature which may affect the cooling rate and the heating rate of the process. These are important parameters to the process and they may change drastically due to the ambient temperature being different.

7.3.10.2 Part to Part dimensions

This is another important noise factor introduced into the system which might play a major part in the embossing process. For example, the dimensions may vary for each part or follow a trend. Each lot of the PMMA may have a different thickness according to the tolerance of the manufacturing process used. Also, the parallelism between the two surfaces may be varying from lot to lot. Such variations in the dimensions of the part may affect the process.

7.3.10.3 Part to Part material properties

The manufacturing process involved in processing of the PMMA does cause the material properties like the tensile strength, specific heat, thermal co-efficient to vary from part to part which may be very critical to the process. The thermal co-efficient is of particular significance as it may affect the loading of the plates directly and may lead excessive force or insufficient force. Also, the tensile strength of the material as a function of the temperature is of significance because if the profile of the tensile curve does vary from part to part then the embossed parts may not be uniform and may create a lot of defects.

7.3.10.4 Tool Wear

The tool wear is another important parameter which may be a cause of defective parts being produced. It may be important to the process that this parameter be quantified and kept under check. The quantification of this parameter may be done as the number of parts produced before the tool wears out which means that the parts processed after that number are out of specification limits. Further analysis of the tool wear is carried out by Khanh Nguyen [40].

7.3.10.5 Parallelism of the Platens

This may be the single most critical factor affecting the part quality. The platens are mounted on the press and are guided using two guiding rails. The parallelism between the two platens is of importance because with misalignment the part and the features will be imprinted at an angle. With the change of angle the thickness of the material in that direction changes, the

embossed parts may be off center, the part to part variation may increase and also the features may have a defect due to low forces in a particular direction.

7.4 Down selection of Parameters

The different parameters listed in 7.3 are the list of parameters which could be instrumental in deciding the performance of the rapid prototyping process. For further analysis of these factors and their effects on the performance of the system they first need to be down selected into a smaller group according to the importance of their effects. The purpose in reducing the number of factors is to reduce the number of experiments needed to be carried out.

The relation between factors (n) considered in a design to the number of experiments in a design of a model is given by:

$$no.\,of\ runs = 2^{n} - Full\ Factorial\ Model \tag{4}$$

$$no.\,of\ runs = 2^{n-a} - Fractional\ Factorial\ Model \tag{5}$$

Where, a is dependent on the fraction confounded by the design.

The critical parameters were analyzed in a cause and effect matrix to find out the most critical ones and to eliminate the ones which don't affect the process significantly. This was followed by a PRE-DOE (Preliminary Data or Pre-Design of Experiments) to find out the levels at which the factors can be operated for the design of experiments. The PRE-DOE data was used to find the levels to design a fractional factorial design which was partially confounded by half a fraction. The fractional factorial model with two replicates was used to find the most significant factors affecting the performance of the hot embossing process.

7.4.1 Cause and Effect Matrix

We use a cause and effect matrix to find out the significant factors from the complete array of factors which could be associated with the process. The cause and effect matrix uses the metrics as discussed by Nicholas Ragosta [34] and selected as the best estimate to characterize the performance of the process. The cause and effect matrix has the process inputs as the rows and the tests and the performance measures as columns. Importance points are given to each test and measure for the corresponding parameter and the factor being used.

An importance on a scale of 1 to 10 is given to each performance or metric used to gauge the parameter. These importance numbers for each of the factors are given on a scale of 1 to 10 but on an exponential scale such as 1, 3 and 9. With this a clear divide is achieved between the importance of the parameters and the significant parameters can come to the surface. For the purpose of reducing the number of factors to be analyzed a threshold was selected for the total points. Table 5 shows the importance values assigned to each of the dimensions and the ratings given to each of the factors.

To select the importance and the rating given to each of the parameter, prior research on hot embossing and their impact on these metrics used in conjunction with the importance of each metric according to the tolerances required on each of the metrics for Daktari [24].

Table 5 Cause and Effect Matrix

	Radius	*Draft*	*Filling*	*Dimensional Control*	*Total*
IMPORTANCE	**8**	**5**	**10**	**10**	
All Factors					
Ambient Temperature	1	1	1	1	33
Cooling rate	9	3	9	3	207
Cooling temperature	3	3	9	3	159
Holding Time	9	3	9	9	267
Material of Tool	3	1	1	1	49
Substrate Properties (thickness)	9	3	9	3	207
Parallelism of the platens	1	1	1	3	53
Part to part dimensions	1	1	1	1	33
Part to part material properties	3	1	3	3	89
Pressure	9	9	9	9	297
Temperature	9	9	9	3	237
Tool Wear	3	3	1	3	79
Velocity	3	3	9	3	159

In the cause and effect matrix, we choose a threshold of 150 separating 7 of the most important factors. These factors are the Pressure Applied, Temperature of Tool, Temperature of Substrate, Holding Time, Cooling Rate, Embossing Velocity, De-Embossing Temperature (Final Cooling Temperature) and substrate properties (thickness). As we discussed earlier, the de-embossing velocity cannot be controlled with the current setup but operating over the glass transition temperature does help in eliminating it as a significant factor [24]. The cooling rate for the current system cannot be controlled and is set at a particular level of 1.24 C/s.

7.4.2 Pre Design of Experiments Data

The Pre Design for Experiments Data was aimed to find a rough estimate of the possible ranges of operation for the most important factors. For the purpose of this experiment the output response variable was the fill ratio. (Ratio of the cross section embossed to the cross section of the tool)

As discussed by Nicholas Ragosta [34] the critical location to be measured for the Pre-DOE data was the ridge around the cuvette (the lip) which was one of the most critical dimensions with respect to the functionality, the size of the feature and its high aspect ratio which is one of the challenges to the hot embossing capabilities. The lip has the cross sectional dimensions of 10 microns in width and 50 microns in depth. The metric Total Fill rate used was a multiplication of the individual Height and Width Fill ratio.

A series of experiments was carried out with the aim of finding the lowest possible levels at which a part could be made with acceptable accuracy (fill ratio) and the highest possible levels for the same. An effort was made to find out the lowest and highest levels for each of the main factors identified which could co-exist. For example, the system is capable of attaining a temperature range of 100C-160C and a pressure range of 0 to 4000N. But for a range of 120C-150C a range of pressure possible for the system is from 0 to 3500N for a holding time of 30 minutes. This was because of the bottoming out of the part and the tool head touching the substrate locating pins. Hence, a range of force and temperature which can co-exist has to be found out.

For these experiments the factors considered were selected according to section 7.4.1. These factors were the Top Plate Temperature (Tool temperature), the bottom plate temperature (Substrate temperature), the holding time for embossing, the pressure used to emboss, and thickness of the input substrate part as the substrate property and the de-embossing temperature of the part.

The experiments were carried out as given in Table 6 with resulting metric as the fill ratio which could help in making a preliminary guess towards the optimal range of the various factors involved in the process. The purpose of these experiments was to find an operating range for all the factors according to the system capability.

Table 6 Pre-Design of Experiments Data

	Temp Top Plate (C)	*Temp Bottom Plate(C)*	*Force (N)*	*Holding Time*	*De-Embossing Temperature(C)*	*Thickness (inch)*	*Fill Rate*
Experiment 1	100	100	250	10 min	30	0.1195	0.1234
Experiment 2	140	120	2700	10 min	20	0.1195	0.2236
Experiment 3	120	120	2700	10 min	50	0.12	0.0932
Experiment 4	140	120	2700	20 min	20	0.1205	0.4076
Experiment 5	140	140	3500	20 min	70	0.1195	0.7492
Experiment 6	140	140	4000	20 min	40	0.245	0.9853
Experiment 7	140	120	2700	15 min	20	0.1195	0.5534
Experiment 8	140	120	2700	15 min	60	0.1195	0.8956
Experiment 9	140	120	2700	15 min	80	0.1195	0.3456
Experiment 10	140	120	3500	15 min	40	0.12	0.8465
Experiment 11	140	120	4000	5 min	40	0.177	0.6048
Experiment 12	140	120	4000	15 min	40	0.177	0.8424
Experiment 13	140	120	4000	10 min	40	0.177	0.5332
Experiment 14	150	150	4000	20 min	40	0.177	0.9113
Experiment 15	140	140	3500	30 min	40	0.2	0.9387
Experiment 16	120	120	1800	5 min	40	0.115	0.0182
Experiment 17	150	150	3500	30 min	40	0.12	0.9978
Experiment 18	140	120	4000	5 min	40	0.12	0.6928

The data gave an estimate of the levels to be implemented for the fractional factorial model. Some of the parts were analyzed for the cross section using two methods: one was the analysis of the cross section using the PDMS cast and then cutting it and the other was freezing the PMMA embossed part itself and breaking it along a score to propagate a crack along the cross section.

Results suggested that the Experiment 6 was the best of all parts made with a fill ratio very close to 1. The PDMS cast and the breaking of the PMMA part itself revealed that the walls were well formed with minimal draft and no visible and quantifiable defects. The PRE-DOE data suggested using the levels for the Tool Temperature as 120 and 140, substrate temperature as 120 and 140, pressure at 2500N and 3800 N, holding time at 10 minutes and 20 minutess, de-embossing temperature at 30 C and 70C. Figure 39 shows the ranges of all the factors and the range for which all the factors can co-exist to produce an acceptable part.

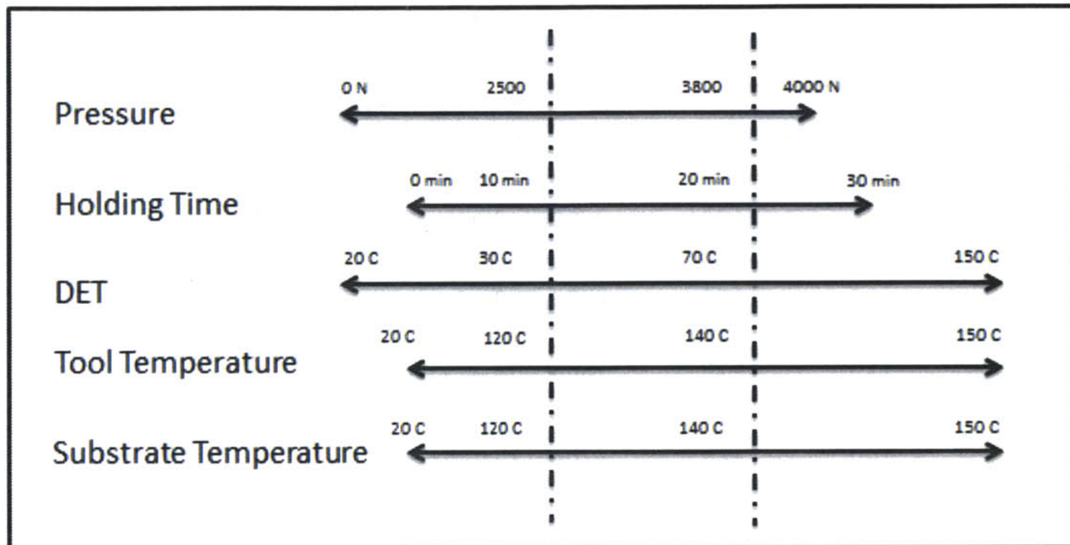

Figure 39 Co-existing Operating Ranges

7.5 Design of Experiments (Fractional Factorial Model)

Design of experiments or experimental design is a test or a series of tests in which purposeful changes are made to the input variables of a process so that we may be able to observe and identify corresponding changes in the output response [41]. As shown in Figure 40 the process can be a combination of machines, methods and people that transforms an input material into an output product. Some of the process variables are controllable and some of them are not controllable and are called the noise factors. The objectives of the design of experiments include:

- Determining which of the variables are the most influential on the response variable.
- Determining where to set the process variables so that the response variable is near its optimal value.
- Determining where to set the influential process variables so that variability in the response variable is at a minimum.

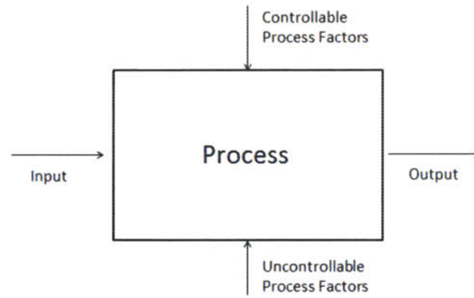

Figure 40 Experimental Design

7.5.1 Controllable Factors

As discussed in 7.4.2 with the help of the Pre-Design of Experiments data, we get an estimate of the levels at which acceptable quality parts can be made. The factors chosen to be included in the model are:

- Tool Temperature
- Substrate Temperature
- De-Embossing Temperature
- Force Applied
- Holding Time

The factors with their upper and lower levels for the design of experiments are shown in the Table 7 as analyzed in the prior sections.

Table 7 Levels of Factors for the Fractional Factorial Design

LEVELS	***High***	***Low***
Temperature Top Plate	120 C	140 C
Temperature Bottom Plate	120 C	140 C
Pressure	2500 N	3800 N
Holding Time	10 min	20 min
De-Embossing Temperature	30 C	70 C

7.5.2 Uncontrollable Factors (Noise factors)

As discussed in 7.3, we see that the noise factors which are significant for the hot embossing process are the Ambient Temperature, part to part variability and tool wear.

To neutralize the effects of the ambient temperature, the experiments were conducted in a controlled environment with an ambient temperature of 20 C and a humidity of 55% RH. The noise factor of variability in part to part dimensions and material properties was reduced using a bulk procurement of PMMA extruded sheets of 0.25 inch and 0.125 inch thickness (Tolerance in thickness: 0.0125 inch).

The tool wear analyzed by Khanh Ngyuen [40] may be a noise factor of concern but the tool wear is negligible and the tool remains fairly consistent in dimensions over the complete series of experiments.

7.5.3 Response Variables:

The analysis of the hot embossing process using a design of experiments involves the selection of certain response variables. These variables should be able to rightly depict the performance of the process and be a gauge of the system capability.

7.5.3.1 Height Fill Ratio

As discussed in 7.1.1 and 7.2.2, one of the most suitable metrics as a measure of the performance used for the experimental design was the Height fill ratio as given in equation (2). The height fill is the ratio of the height of the part produced to the height of the tool used for the embossing process.

7.5.3.2 Width Fill Ratio

As discussed in 7.1.1 and 7.2.2, one of the most suitable metrics used as a measure for the performance used for the experimental design was the Width fill ratio as given in equation (3). The Width fill is the ratio of the height of the part produced to the width of the tool used for the embossing process.

7.5.3.3 De-Embossing Defects

De-embossing of the part after it has been embossed is one of the important steps in the process to get parts complying with specifications. The de-embossing temperature directly affects the contraction of the dimensions and creates the smearing (shearing of the sides) of the walls which leads to defects seen on the final part. These defects may vary in their intensity according to the force applied for de-embossing and the temperature at which it is de-embossed. Therefore, de-embossing defects were chosen to be one of the response variables.

In the design of experiments, to quantify the de-embossing defects, which is an attribute rather than a measurement, an importance scale was used from 1-3 at 6 locations on the cuvette which were critical with respect to the performance of the part. Figure 41 shows the six locations at which the parts were inspected for the defects and given a rating. The six locations are the three holes, the two sides of the cuvette and the two curvatures at both ends of the cuvette. The "de-embossing defect" response variable was the addition of these ratings given to each location. Some of the examples of the defects seen on the parts are shown in Figure 42.

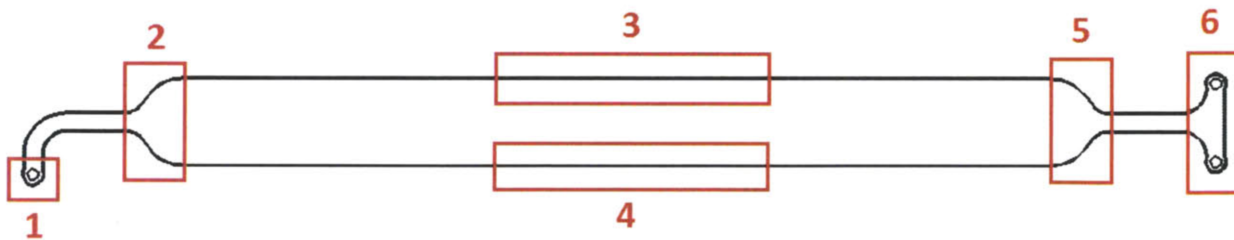

Figure 41 Locations for Measuring Defects

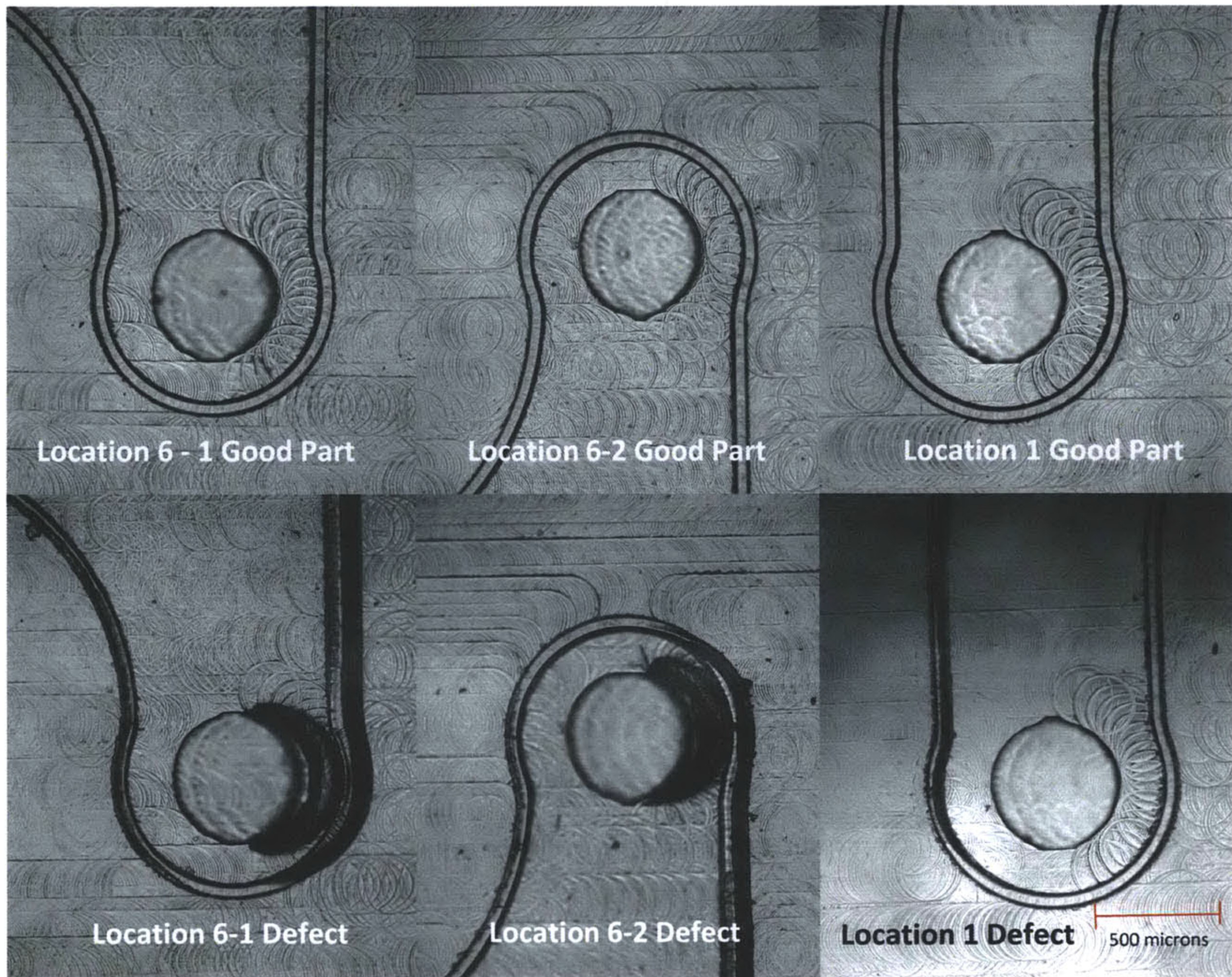

Figure 42 Examples of De-Embossing Defects

7.5.4 Fractional Factorial Design

For the purpose of reducing the number of experiments to be carried out, a fractional factorial model can be implemented with introducing a confounding between the factor interactions with different aliasing structures. In this particular research, we have five factors to be analyzed for three response variables which would need 32 runs for a full factorial model (2^5) with no replicates according to the equation (4). Alternatively, the fractional factorial model confounded for half a fraction will involve 16 runs (2^{5-1}) according to equation (5) which allows us to use two replicates for 32 samples and does not lose accuracy of results as it is a Resolution V design. The comparison between the two designs reduces to the confounding of half a fraction against the two replicates.

For the fractional factorial model 2^{5-1} the resolution is V with the design generator as *I=ABCD* which is involves the aliasing of the main effects with the four-way interaction effects, the two-way interaction effects aliased with the three-way interaction effects as shown inTable 8. The number of experiments in the model is 32 and the degrees of freedom for the experiment are 31 which allow the estimation of the main effects, the two way interaction effects and the three way interaction effects to some degree. We can safely assume that the three-way interaction effects are not significant. As the main effects are not aliased with the three way interaction effects, the fractional factorial model with resolution V can be safely used for the design of experiments. An advantage of using this model with confounding is that we can have two replicates for the same number of experiments as in case of the full factorial model, which reduces the variability in the data and neutralizes the effect of the noise factors to a greater degree.

Table 8 Aliasing Structure

I	ABCDE	AC	BDE
		AD	BCE
A	BCDE	AE	BCD
B	ACDE	BC	ADE
C	ABDE	BD	ACE
D	ABCE	BE	ACD
E	ABCD	CD	ABE
AB	CDE	CE	ABD
		DE	ABC

The fractional factorial model chosen had the parameters in Table 9. The five factors are assumed to have approximately linear relationships with the responses and no center points are added to the system. Since the model supports both the main effect estimation and the two-way interaction effect estimation some protection against curvature is already inherent in the system.

Table 9 Fractional Factorial design parameters

Fractional Factorial Design

Factors:	5	Base Design:	5, 16	Resolution:	V
Runs:	32	Replicates:	2	Fraction:	1/2
Blocks:	1	Center pts (total):	0		

7.5.5 Experiments

The experiments were carried out using a standard operating procedure with a single operator to reduce variability. The experiments were carried out in a controlled environment with set ambient temperature and humidity and did not change through the complete series of experiments. Table 10 shows the fractional factorial model (2^{5-1}) of experiments with the specific levels of the factors for each experiment and the recorded responses.

Table 10 Fractional Factorial Design Of Experiments

Tool Temp (C)	*Substrate Temp (C)*	*De-Embossing Temp (C)*	*Force (N)*	*Holding Time (min)*	*Height fill*	*Width fill*	*De-Embossing Defects*
120	140	70	2500	20	0.9904	0.5841	16
120	120	30	12	20	0.8985	0.7787	9
120	140	70	12	20	0.8932	0.6902	16
140	140	30	18	10	0.9206	0.8761	10
140	140	30	12	20	0.9062	0.8761	14
140	120	30	18	20	0.9254	0.7965	10
140	140	70	18	20	0.9176	0.9026	17
140	120	30	12	10	0.916	0.8761	15
140	140	30	18	10	0.8983	0.9203	8
140	120	70	18	10	0.9059	0.9115	17
120	140	30	18	20	0.9683	0.7699	12
140	140	30	12	20	0.8979	0.8938	9
120	140	30	12	10	0.8824	0.5487	10
140	120	70	18	10	0.8965	0.8672	16
120	140	30	12	10	0.7252	0.2035	9
120	120	70	12	10	0.8971	0.4248	16
120	120	70	18	20	0.9191	0.8849	17
140	140	70	12	10	0.9085	0.8584	16
140	120	30	18	20	0.9003	0.8672	8
120	140	70	18	10	0.9079	0.823	16
120	140	70	18	10	0.9075	0.7522	15
140	140	70	12	10	0.9202	0.8761	14
140	140	70	18	20	0.9195	0.9115	15
120	120	70	18	20	0.9225	0.8761	18
140	120	70	12	20	0.9164	0.8849	17
120	120	70	12	10	0.8916	0.6372	16
120	120	30	18	10	0.914	0.8141	9
120	120	30	18	10	0.9248	0.8584	11
140	120	70	12	20	0.9173	0.8672	18
140	120	30	12	10	0.9048	0.9115	9
120	120	30	12	20	0.878	0.823	10
120	140	30	18	20	1.0906	0.646	8

8 Results

In this chapter, we will analyze the results of the experimental design to find the optimal parameters for the hot embossing process used for rapid prototyping of the microfluidic cartridge at Daktari. The optimal parameters are according to the response variables chosen and the importance given to each of the responses. These optimal parameters were used in a confirmation run of experiments to analyze the quality of the parts and the capability of the process.

8.1 Analysis of Variance (ANOVA) and Significance of Effects

The MINITAB version 16 was used for the analysis of these experiments. The analysis of variance of the 2^{5-1} design with two replicates provides us with the data for the three response variables.

8.1.1 Width Fill Analysis

The Analysis of Variance (ANOVA) data for the Width fill in the Table 11 shows us that the tool temperature, Pressure (Force), Holding time have a p-value less than 0.05 which indicates that these main effects are significant in a 95% confidence interval. Apart from these main effects, the two-way interaction effects of Tool Temperature-Substrate Temperature, Pressure (Force)-Holding Time, Tool Temperature-Holding Time and Tool Temperature-Pressure (Force) are also significant within a 95% confidence interval. The R squared value for the model is 75.80% which indicates that the model is well utilized for the significant effects. To find the magnitude of the significance of each factor, we use the equation 6, which comes out to be 32% for Tool Temperature, 13.86% for Pressure (Force) and 4.11% for Holding Time.

$$\%\ Magnitude\ of\ Significance = \frac{Sum\ of\ Squares\ of\ Factor}{Total\ Sum\ of\ Squares}\% = \frac{SSa}{SSt}\% \tag{6}$$

Table 11 ANOVA for Width Fill

Analysis of Variance for Width Fill						
R-Sq(adj) = 75.80%						
Source	***DF***	***Seq SS***	***Adj SS***	***Adj MS***	***F***	***P***
Main Effects	5	0.418785	0.418785	0.083757	13.69	0
Tool Temp	1	0.25572	0.25572	0.25572	41.81	0.000
Substrate Temp	1	0.02128	0.02128	0.02128	3.48	0.081
De-Embossing Temp	1	0.000907	0.000907	0.000907	0.15	0.705
Pressure	1	0.108671	0.108671	0.108671	17.77	0.001
Holding Time	1	0.032207	0.032207	0.032207	5.27	0.036
2-Way Interactions	10	0.266833	0.266833	0.026683	4.36	0.005
Tool Temp*Substrate Temp	1	0.037183	0.037183	0.037183	6.08	0.025
Tool Temp*De-Embossing Temp	1	0.000068	0.000068	0.000068	0.01	0.917
Tool Temp*Pressure	1	0.10663	0.10663	0.10663	17.43	0.001
Tool Temp*Holding Time	1	0.045753	0.045753	0.045753	7.48	0.015
Substrate Temp*De-Embossing Temp	1	0.026095	0.026095	0.026095	4.27	0.055
Substrate Temp*Pressure	1	0.008444	0.008444	0.008444	1.38	0.257
Substrate Temp*Holding Time	1	0.000112	0.000112	0.000112	0.02	0.894
De-Embossing Temp*Pressure	1	0.003771	0.003771	0.003771	0.62	0.444
De-Embossing Temp*Holding Time	1	0.000399	0.000399	0.000399	0.07	0.802
Pressure*Holding Time	1	0.038378	0.038378	0.038378	6.27	0.023
Residual Error	16	0.097871	0.097871	0.006117		
Pure Error	16	0.097871	0.097871	0.006117		
Total	31	0.783489				

The Pareto chart in Figure 43 depicts the standardized effects and the significant factors. It also portrays the magnitude of the effects of each of the significant factors.

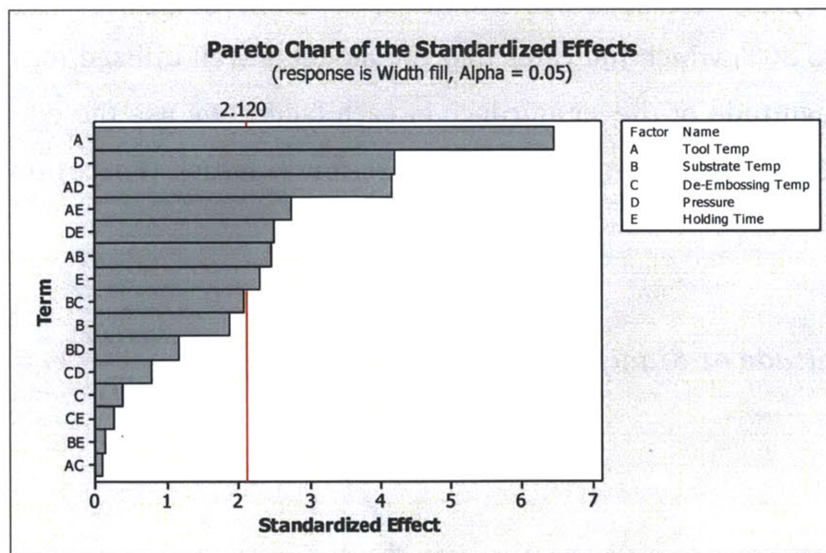

Figure 43 Pareto Chart for Width Fill

The residual Plots in Figure 44 for the width fill do indicate that there is some variability in the variance of the different parameters but we assume the variances to be equal to use the results for the Design of Experiments.

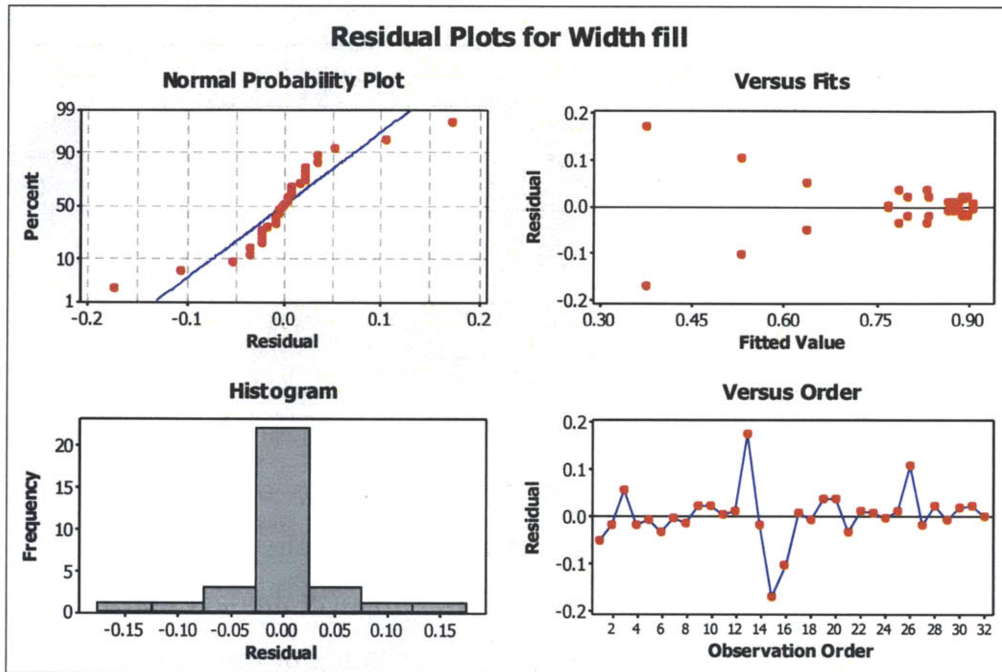

Figure 44 Residual Analysis of the Width Fill

Figure 45 shows us the main effects and how they affect the Width Fill response variable. We can clearly see that the de-embossing temperature does not affect the width fill as the slope is negligible and it is a similar case for substrate temperature and holding time. The Width fill is very sensitive to both the Pressure (Force) and Tool Temperature and we can see that they have the same correlation with the width fill where it increases with an increase in either of the two factors. The substrate temperature affects the response with a negative correlation which means that a lower substrate temperature corresponds to a higher response.

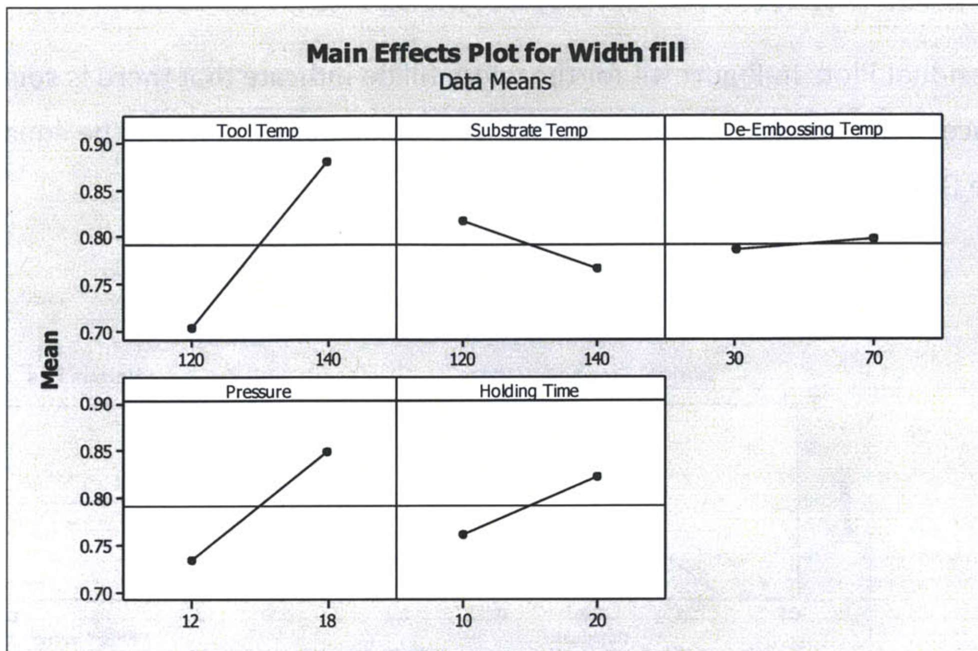

Figure 45 Main effect Plot

Figure 46 gives us information about the interaction effects and how they affect the Width Fill. The graphs show us how the interactions behave with respect to changes in individual factors. The response is the maximum when the tool temperature and the substrate temperature are at their higher levels, which supports the fact that the material flows much more at a higher temperature allowing a higher filling of the corners. The response is higher when the pressure and the holding time are at their high levels. Also, the response is more at a higher tool temperature and a longer holding time.

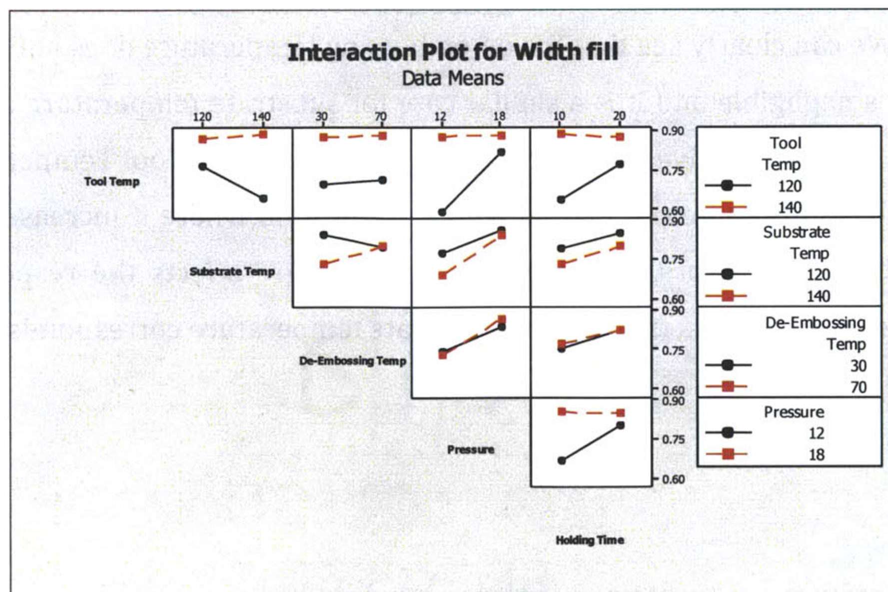

Figure 46 Interaction Effects

8.1.2 Height Fill

The Analysis of Variance (ANOVA) data for the Width fill in the Table 12 shows us that holding time has a p-value less than 0.05 which indicates that this main effect is significant in a 95% confidence interval. Apart from these main effects, the two-way interaction effect of Pressure (Force)-De-Embossing Temperature is also significant within a 95% confidence interval. The R squared value for the model is 31.76% which indicates that the model isn't utilized to full capacity for the significant effects. We run the model again considering only the significant effects to get a well-utilized model and find the magnitude of each factor which affects the response. To find the magnitude of the significance of each factor, we use the equation 6, which comes out to be 10% for Holding Time and 12% for the interaction effect of Pressure (Force)-Holding Time.

Table 12 ANOVA for Height Fill

Analysis of Variance for Height Fill						
R-Sq (adj) = 31.76%						
Source	DF	Seq SS	Adj SS	Adj MS	F	P
Main Effects	5	0.011199	0.011199	0.00224	1.97	0.138
Tool Temp	1	0.000227	0.000227	0.000227	0.2	0.66
Substrate Temp	1	0	0	4E-08	0	0.995
De-Embossing Temp	1	0.001312	0.001312	0.001312	1.16	0.298
Pressure	1	0.00428	0.00428	0.00428	3.77	0.07
Holding Time	1	0.005379	0.005379	0.005379	4.74	0.045
2-Way Interactions	10	0.022178	0.022178	0.002218	1.96	0.112
Tool Temp*Substrate Temp	1	0.000004	0.000004	3.99E-06	0	0.953
Tool Temp*De-Embossing Temp	1	0.000613	0.000613	0.000613	0.54	0.473
Tool Temp*Pressure	1	0.00443	0.00443	0.00443	3.91	0.066
Tool Temp*Holding Time	1	0.003945	0.003945	0.003945	3.48	0.081
Substrate Temp*De-Embossing Temp	1	0.001197	0.001197	0.001197	1.06	0.32
Substrate Temp*Pressure	1	0.001158	0.001158	0.001158	1.02	0.327
Substrate Temp*Holding Time	1	0.004079	0.004079	0.004079	3.6	0.076
De-Embossing Temp*Pressure	1	0.00623	0.00623	0.00623	5.49	0.032
De-Embossing Temp*Holding Time	1	0.000272	0.000272	0.000272	0.24	0.631
Pressure*Holding Time	1	0.000249	0.000249	0.000249	0.22	0.646
Residual Error	16	0.018149	0.018149	0.001134		
Pure Error	16	0.018149	0.018149	0.001134		
Total	31	0.051525				

Figure 47 shows the impact of the main effects on the response and we can see that holding time and pressure (12 mV : 2500 N and 18 mV: 3800N) both have a direct impact on the response with the same correlation. Higher pressure or holding time results in a higher Height Fill.

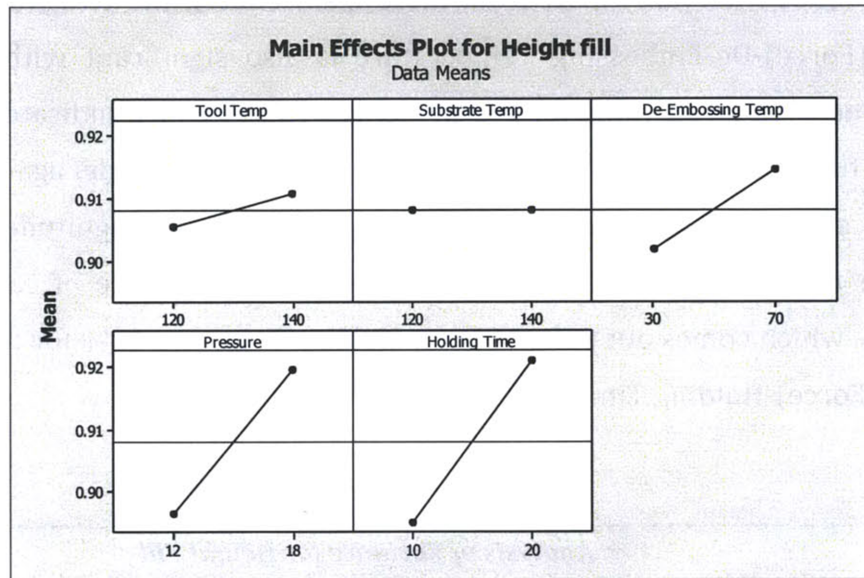

Figure 47 Main Effects Plot for Height Fill

Figure 48 shows the interaction effects and we can see that the Pressure and De-Embossing Temperature interaction is highly significant because their higher slopes. A low de-embossing temperature and a higher Pressure does give the maximum Height Fill. But an important observation is that a condition with high de-embossing temperatures with lower pressure also gives a higher Height Fill.

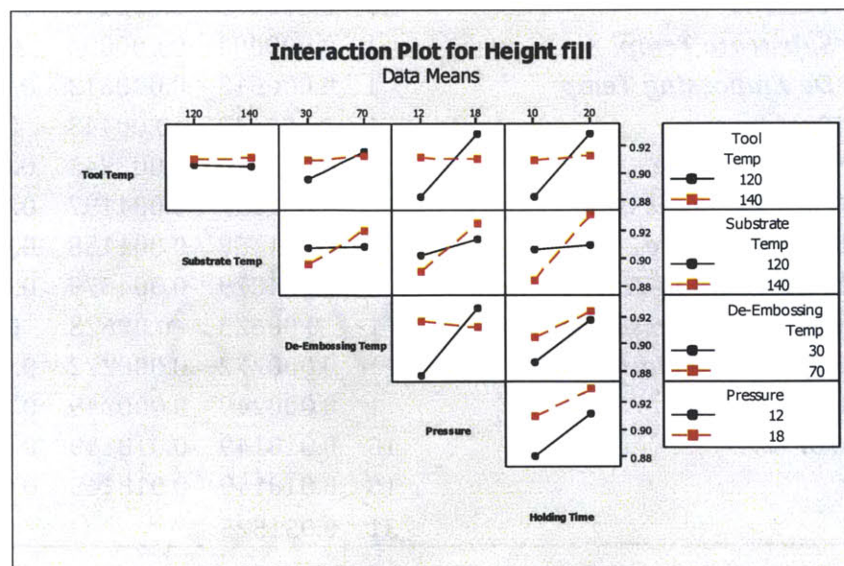

Figure 48 Interaction Effects for Height Fill

8.1.3 De-Embossing Defects

The Analysis of Variance (ANOVA) data for the De-Embossing Defects Response Variable in the Table 13 shows us that De-Embossing Temperature has a p value less than 0.05 which indicates that this main effect is the only significant factor in a 95% confidence interval. The R squared value for the model is 74.6% which indicates that the model is well utilized. To find the magnitude of the significance of each factor, we use the equation 4, which comes out to be 79% for De-Embossing Temperature. We clearly see that the only significant factor affecting the De-Embossing Defects Response Variable is the De-Embossing Temperature. Figure 49 clearly shows how the main effect of De-Embossing Temperature affects the response with a positive correlation.

Table 13 ANOVA for De-Embossing Defects

Analysis of Variance for De-embossing Defects						
R-Sq(adj) = 74.16%						
Source	***DF***	***Seq SS***	***Adj SS***	***Adj MS***	***F***	***P***
Main Effects	5	313.906	313.906	62.781	19.5	0.0000
Tool Temp	1	0.781	0.781	0.781	0.24	0.6290
Substrate Temp	1	3.781	3.781	3.781	1.17	0.2940
De-Embossing Temp	1	306.281	306.281	306.281	95.16	0.0000
Pressure	1	1.531	1.531	1.531	0.48	0.5000
Holding Time	1	1.531	1.531	1.531	0.48	0.5000
2-Way Interactions	10	20.812	20.812	2.081	0.65	0.7550
Tool Temp*Substrate Temp	1	0.281	0.281	0.281	0.09	0.7710
Tool Temp*De-Embossing Temp	1	0.781	0.781	0.781	0.24	0.6290
Tool Temp*Pressure	1	7.031	7.031	7.031	2.18	0.1590
Tool Temp*Holding Time	1	0.031	0.031	0.031	0.01	0.9230
Substrate Temp*De-Embossing Temp	1	2.531	2.531	2.531	0.79	0.3880
Substrate Temp*Pressure	1	0.031	0.031	0.031	0.01	0.9230
Substrate Temp*Holding Time	1	3.781	3.781	3.781	1.17	0.2940
De-Embossing Temp*Pressure	1	3.781	3.781	3.781	1.17	0.2940
De-Embossing Temp*Holding Time	1	2.531	2.531	2.531	0.79	0.3880
Pressure*Holding Time	1	0.031	0.031	0.031	0.01	0.9230
Residual Error	16	51.5	51.5	3.219		
Pure Error	16	51.5	51.5	3.219		
Total	31	386.219				

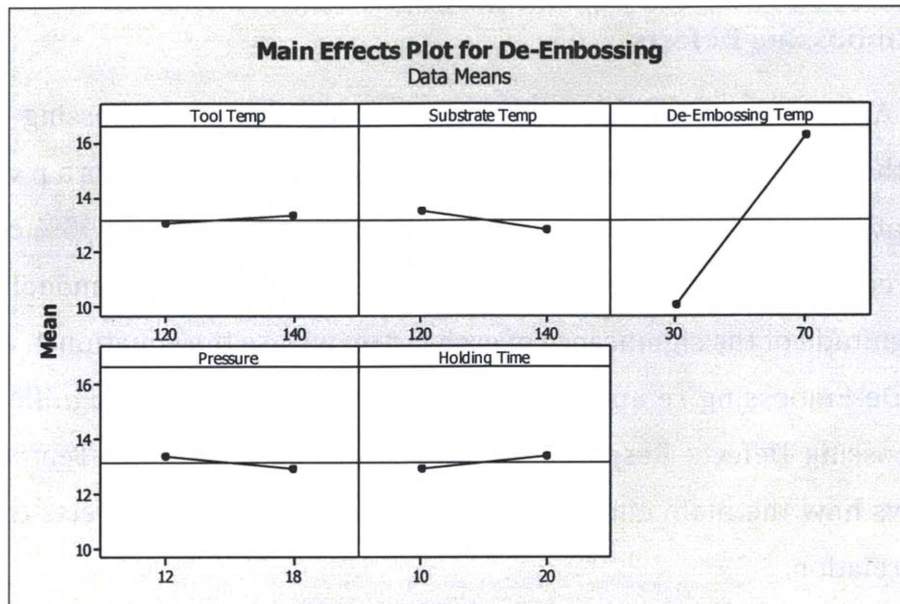

Figure 49 Main effects for De-Embossing Defects

8.2 Response Optimization and Analysis

In the fractional factorial model with 5 factors, we have analyzed the three responses of Height Fill, Width Fill and the De-Embossing Defects individually to find the most significant factors affecting each of them and the optimal level setting. For the solution to be optimal and get parts within tolerances we need to analyze the three responses together to find the global optimum. The optimal solution for the local response variable may directly contradict the global optimal setting of the factors. For this reason, we need to assign weights to the specific responses so we can resolve the conflict for the setting of the levels of the factors.

The process of optimization was done in MINITAB Version 16.0 which uses numerical optimization methods to calculate the optimal parameters with a predicted response. The MINITAB output is a contour plot with the factors and their effect on the responses. The software calculates the response using the regression model for each of the response output which is found using the Analysis of Variance (ANOVA) for individual factors. These equations are noted in derived from the co-efficients for each response variable as noted in Appendix B. MINITAB outputs a set of optimal parameters according to the weight assigned to each output variable and calculating the effective total response. One of the outputs is the "Composite

Desirability" which is a normalized measure of how optimal the set of parameters are for the global response with the specific weights and importance of each response variable. The factor levels can be changed to get the effective response at each set of levels by numerically solving the regression models for the response variables specific to the importance ratings.

For the response optimization of the Hot Embossing Process, we assign different weights to each of the three responses. The 'Width Fill' response is a measure of the radius as well as the draft angle of the corners and the wall. It is a better estimate of the filling of the corners of the ridge than the Height Fill which is a direct difference between the two flat surfaces. For this reason, the 'Width Fill' was given a higher weight rating than the 'Height Fill'. The De-embossing defects response is an attribute response and has the lowest rating as the defects do not impact the performance of the cuvette directly unless they are on a larger scale. Hence, a weight rating of 1 for the De-Embossing Defects, 3 for the Height Fill and 5 for the Width Fill were selected.

Figure 50 shows the response optimization contour plot as an output of MINITAB. We see that the composite desirability achieved is approximately 80% which is acceptable with a predicted value for the Height Fill Ratio of 0.9067 and the Width Fill Ratio at 0.9093. These optimal values achieved using numerical analysis are an estimate of the responses at the specific optimal levels for the factors. The result from this analysis is that these set of parameters do lead to a higher response set and hence are used as the optimal parameters for a confirmation run of experiments.

The optimal settings estimated were as follows: Tool temperature of 140 C, a substrate temperature of 130 C, a De-Embossing Temperature of 70 C, a Pressure (Force) of 16.6 mV (3500 N) and a holding time of 12 minutes.

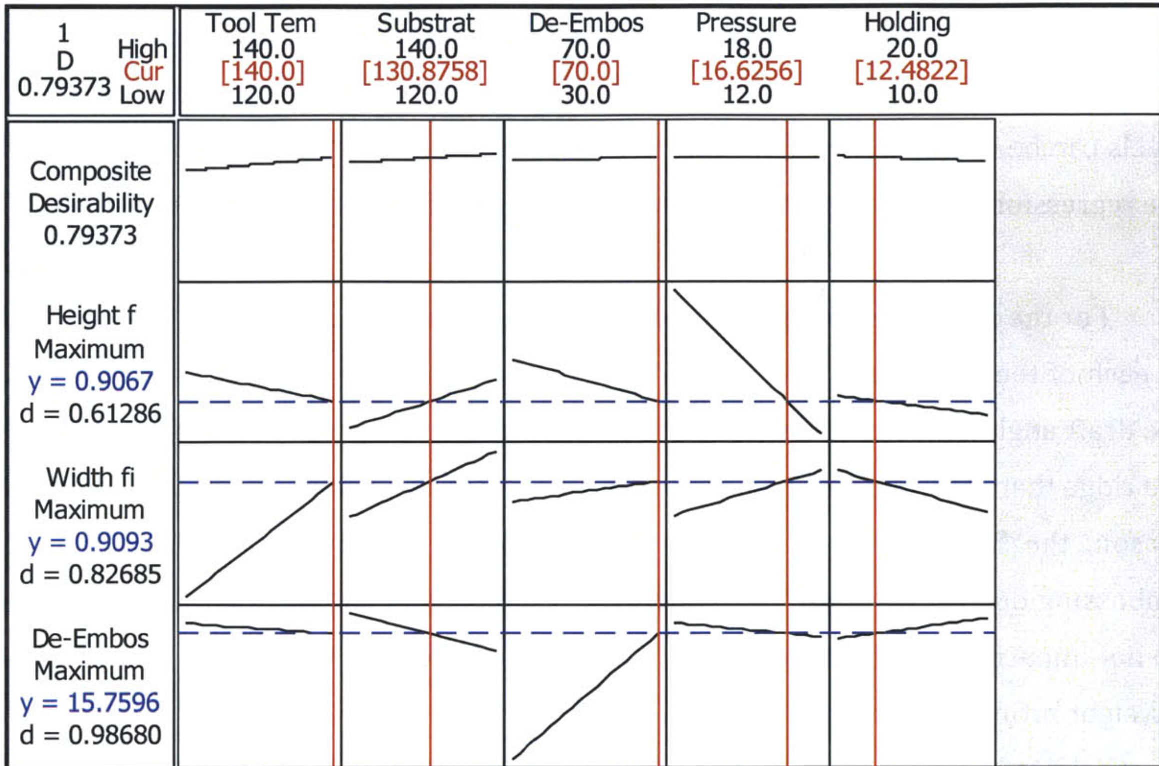

Figure 50 Response Optimization

8.3 Confirmation Experiments to find Process Capability

With the analysis of the experimental design and optimization, the optimal parameters were identified as the following:

Table 14 Optimal Parameters for Confirmation Runs

Tool Temp	140 C
Substrate Temp	130 C
De-Embossing Temp	70 C
Pressure	3500 N
Holding Time	12 min

The optimal parameters were used in a confirmation set of experiments to analyze the responses and characterize the capability of the process. The confirmation experiments were carried out in the same controlled environment of ambient temperature 23 C and humidity of 55% RH. The experiments were run with the same set of parameters with a standard operating procedure with a single operator. The measurements of the parts were taken on an

interferometer as described by Nicholas Ragosta [34]. The measurements for the height fill and the width fill were taken at the 3rd fiducial on the part which is approximately the center of the cuvette. Table 15 shows the operating parameters for the confirmation set of experiments and the responses of Height Fill and Width Fill for each run.

Table 15 Confirmation runs

Part No	*Tool Temp*	*Substrate Temp*	*De-Embossing Temp*	*Force*	*Holding Time*	*Height Fill*	*Width Fill*
C1	140	130	70	3500 N	12 min	0.915226661	0.897341954
C2	140	130	70	3500 N	12 min	0.976514811	0.918669181
C3	140	130	70	3500 N	12 min	0.974966338	0.870629041
C4	140	130	70	3500 N	12 min	0.975964991	0.925628592
C5	140	130	70	3500 N	12 min	0.981048025	0.880729167
C6	140	130	70	3500 N	12 min	0.986377917	0.851863326
C7	140	130	70	3500 N	12 min	0.980621634	0.905648348
C8	140	130	70	3500 N	12 min	0.986591113	0.902653556
C9	140	130	70	3500 N	12 min	0.970118941	0.870745779
C10	140	130	70	3500 N	12 min	0.979196589	0.892719558

The experiments show us that the Height Fill and the Width Fill is in process control and the Figure 51 depicts a run chart of the Height Fill and the Width Fill.

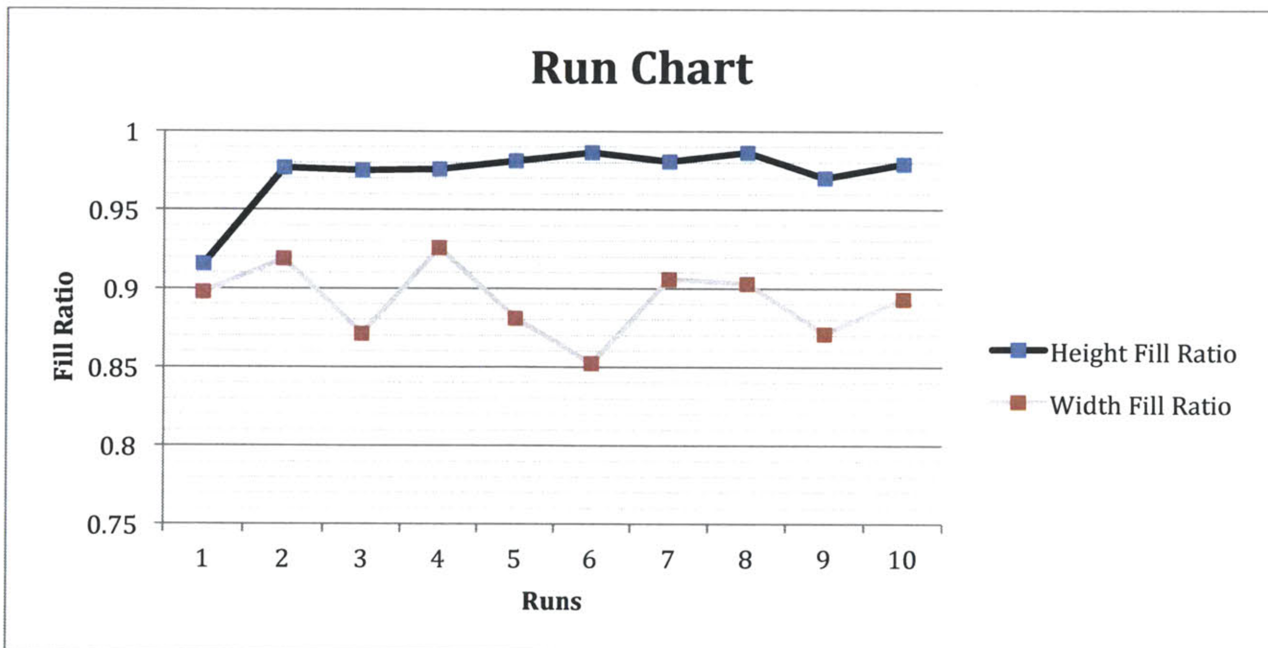

Figure 51Run Chart for Confirmation Run

For further analysis of the control and capability of the process we calculate the C_p and the C_{pk} for the process. The C_p or the process capability index is an indicator of the process' ability to meet a specification [41]. It is given by:

$$Cp = \frac{USL - LSL}{6\sigma} \tag{7}$$

Where, USL and LSL are the upper and lower specification limits and σ is the standard deviation. On the other hand, the C_{pk} is the position of the total process variation in relation to the specification mean [41]. The C_{pk}, associated with a process or a group of items, is either the value for the C_{pl} or the C_{pu} , whichever results in a smaller value, where C_{pl} index is the total process variation with respect to the lower specification limit and C_{pu} index is the total process variation with respect to the upper specification limit.

$$Cpk = \min\left(Cpl = \frac{\bar{X} - LSL}{3\sigma}, Cpu = \frac{USL - \bar{X}}{3\sigma}\right) \tag{8}$$

Where, LSL and USL are the upper and lower specification limits and $\bar{X}$ is the mean of the sample.

For the confirmation run experiments, the data for height used to calculate the Height Fill was analyzed to calculate the process capability using a tolerance of 1 micron. Figure 52 shows that the C_p is 4.71 and the C_{pk} is 2.34 and the process variation considering six standard deviations is well within the specification limits. One of the reasons why the C_{pk} is lower than the C_p is that the tolerance specification is that for the part itself but in case of hot embossing the height dimension can never be higher than height of the tool and therefore the data is not centered on the specification limits. Height is an easier dimension to achieve than the width and doesn't account for the draft angle or the radius on the corners and hence is relatively easier to replicate compared to the width of the ridge. Thus, we deduce that the process for height replication is under control and capable within a 6σ variation.

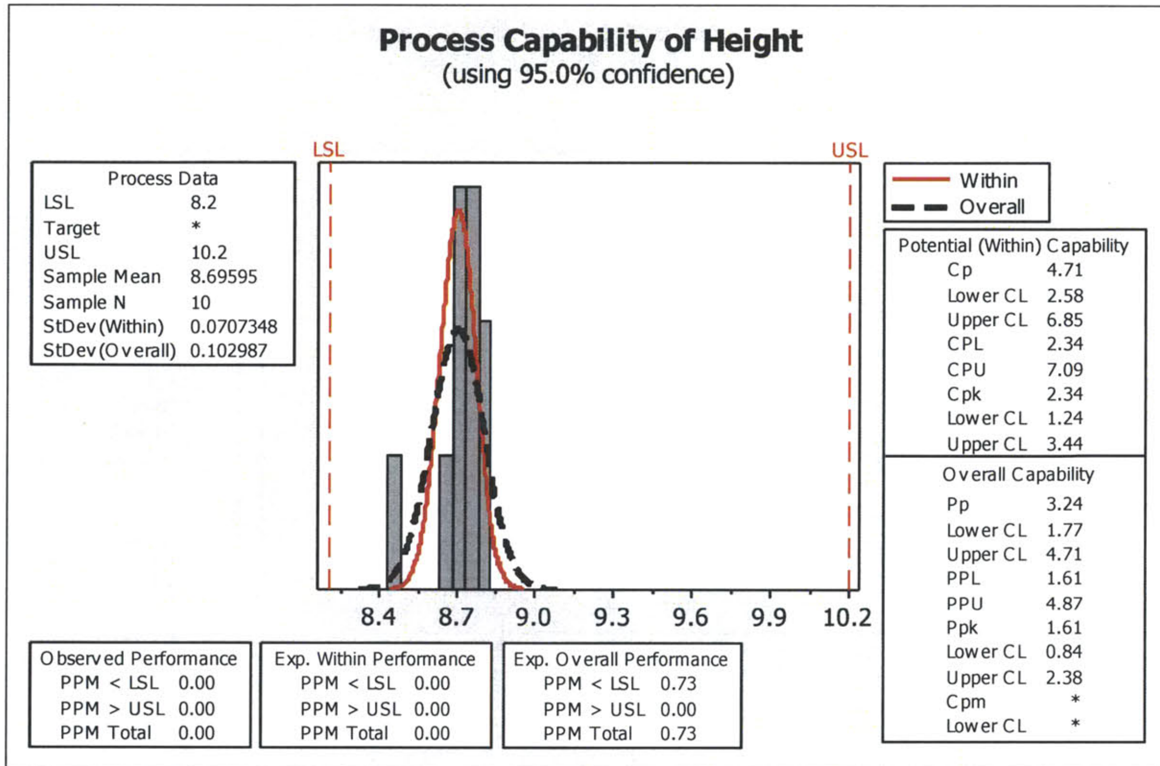

Figure 52 Process Capability Analysis of the Ridge Height

We analyze the Width data for the confirmation experiments using the MINITAB software to find the process capability and get an estimate of the control of the process. An important note when analyzing the width data is that the width is a measure of the radius and the draft angle of the wall on the part manufactured. The specification limit for this width is a $\pm$ 5 micron tolerance with a draft angle of 3^0. In an ideal case, the feature should be replicated exactly with a minimum a radius and the width would be equal to that on the tool. As the radius on the tool is of 5 micron with a $\pm$ 3 micron tolerance, the specification on the width will be estimated at $\pm$8 microns. Figure 53 notes the process capability analysis of the width dimension for the confirmation runs. The C_p value for the process is 1.97 which is indicative of the process being well within control. The width measurement and analysis is much more complex than the height because of the inclusion of error in measurement on the interferometer from radius and draft angle.

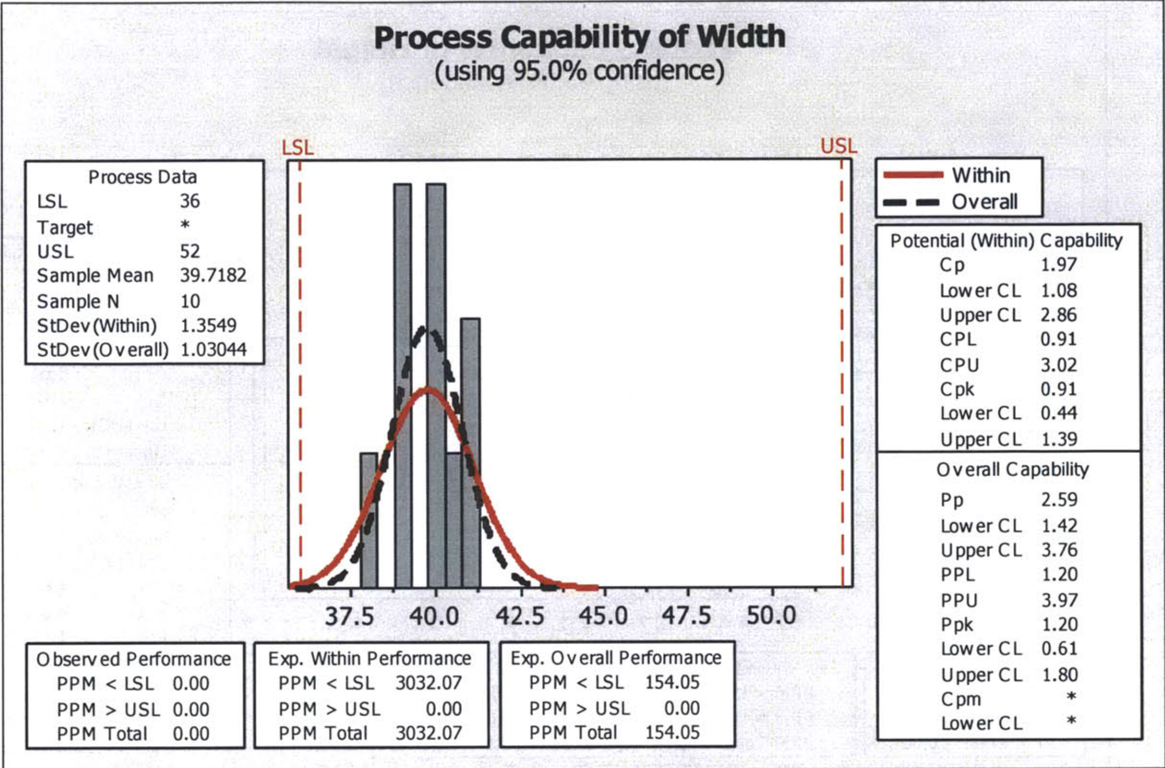

Figure 53 Process Capability Analysis of the Width fill

9 Recommendations

The cuvette is one of the most important parts on the cartridge backbone and is also one of the most difficult parts to emboss because of the high aspect ratios and the micro features. From the analysis and the results of the experimental data we will recommend Daktari to use the hot embossing process for the embossing of the microfluidic part. This research targeted a critical feature which could act as a gauge for analyzing the capability of the hot embossing process to be used as a suitable rapid prototyping method. The research suggests that the desired tolerances are achievable with the help of the process at the optimal parameters as discussed in the analysis. The optimal parameters for the individual cuvette have been identified according to the surface area being embossed and can be changed accordingly for a higher surface area. The parameters were the tool temperature, the substrate temperature, the de-embossing temperature, the pressure and the holding time.

The results suggest that the process for hot embossing with the current system is under process control and when optimized at the specific optimal parameters can produce the required tolerances. The process capability analysis suggests that the process variation of six standard deviations is well within the tolerance specifications for the features being embossed making it a six sigma process. Daktari can use the hot embossing process to manufacture the complete backbone of the cartridge which is 2inch X 3 inch with a relatively higher force as compared to the cuvette embossing. The response optimization of the process suggests that the

The system capability in terms of alignment and parallelism restricts the use of the current system to a 45 micron X Y repeatability tolerance and a 25 micron parallelism tolerance. These tolerances may not be sufficient in case of the use of the system to double emboss on both sides of the card and align the holes. Also, it may not be sufficient to emboss a feature on a partially manufactured cartridge if the tolerances for the X and Y repeatability are not met.

10 Conclusion and Future Work

This thesis is based on research conducted in association with Khanh Nguyen [40] and Nicholas Ragosta [34] to investigate the capabilities of hot embossing as a prototyping process for Daktari Diagnostics. This chapter will detail the conclusions drawn collectively from the team and present suggested next steps for Daktari.

10.1 Conclusion

The research concluded that hot embossing is a prototyping process capable of producing one of the critically toleranced features of Daktari's microfluidic backbone. When the process was optimized, fill rates of 98% and 91% were achieved for the height and width of the channel's smallest feature. To support this result the measurement system was validated using Gage R&R analysis. The precision-to-tolerance ratios of the critical measurements were between 0.30 and 0.50.

With optimal operating parameters, the 6σ process variation of this hot embossing system was within the specification limits of the assay channel. Surface roughness of the embossed part matched the surface roughness of the molding tool. In this work, micro-machined tools with surface roughness values of 150 nm and 350 nm were used. As an alternative to tooling multiple copies of a master, resin copies with less than a 2% change in overall feature dimensions could theoretically be used. The wear on the tool, containing just the assay feature, was seen to have a maximum dimensional loss of 3μm over the period of 40 uses. In summary, the quality of embossed parts is strongly dependent on the quality of the molding tool used.

The process is best suited for prototyping small (~10) to medium volume (~50) batches of parts. The tooling used for this study was purchased for roughly $1000 and took one week to machine. It is best to make this investment when multiple parts are necessary to evaluate a design. With the hot embossing machine detailed in this work, a cycle time of 20 minutes per part was achieved.

10.2 Future Work

This section will overview areas of work that could be pursued by Daktari to more fully understand the hot embossing process and increase the capability of the machine. First, possible improvements to the existing machine will be outlined. Next, suggestions for further experimentation will be suggested.

10.2.1 Machine Improvements

The machine designed for this research was suitable as a proof of concept device; however there are several improvements that should be made if Daktari will actively pursue hot embossing as a prototyping process. In general, these are improvements that would give greater control over the process and improve the repeatability of its operation.

Alignment

The maximum positional error of this machine was found to be 43 microns, and parallelism was found to be 20 microns over the width of the assay channel. Daktari is interested in the possibility of simultaneously embossing microfluidic features on the front and back of a part. Higher precision in x y positional repeatability is required from the embossing machine for it to be possible to align features on two sides of a part.

Force Control

The current system used for the prototyping of the microfluidic part using the hot embossing process uses displacement-control and it does not have a feedback control on the applied force. When a part is loaded for embossing above the glass transition temperature, the material starts flowing and the load relaxes over time, which is undesirable. A force-controlled system will also allow for control over embossing velocity. Analysis of the effect of this variable was not possible with the current system.

Cooling system control

The cooling system currently used is a recirculating pump with lines passing through the cold plates, which are in contact with the heating platens. The purpose of using the cooling system in this research was to reduce the cycle time by decreasing the time to cool down to the de-embossing temperature. A cooling system with control over the cooling rate would help in analyzing the effect of the cooling rate on the performance of the process.

Thermal insulation

Currently the machine uses an insulation material to isolate the force sensor and the air bladder from the heating platens. The middle plate and the top plate tend to heat up to 100 C after 4 cycles of heating and cooling the platens to around 150 C. In addition to the risk of damage to the load cell and air bladder, having a thermal path to the press frame drastically increases the thermal mass of the system and makes heating less efficient. A better insulation system using a more efficient insulator or using an air gap will be beneficial.

Tool alignment

If a better alignment system is integrated to make the embossing machine more precise with regards to the X and Y repeatability and parallelism, then a stage could be designed and integrated within the tool assembly to actively change the position of the tool for embossing. This may be a bigger issue when trying to emboss on both sides of the part or embossing on a part with pre-existing features.

Vacuum Control

The best width fill achieved by this system was 91%. The incomplete filling of width indicates that material is not flowing fully into the mold cavity. This results in a radius being left on edges of the channel. It may be possible to reduce the size of these edge radii by performing the embossing within a vacuum chamber. This would naturally complicate the embossing process and increase cycle time. Before this action is taken, the effect of larger edge radii on the end functionality of the part should be understood.

10.2.2 Further Experimentation

Further experimentation could be performed to better characterize the capabilities of hot embossing. These experiments could include studies to better understand variation in the process, to select optimal tooling options and to characterize the type of features that are well suited for the hot embossing process.

Robust Design

The current research focuses more upon the most significant factors and the main effects and interactions affecting the performance of the process. A further study using the Taguchi Array could be done to analyze the signal to noise ratio to characterize the robustness of the process. Another important future step would be to carry out a greater number of experiments with different optimal settings giving the same predicted response to find the most suitable set of parameters.

Feature Capability Tool

This work has demonstrated that the assay channel could be prototyped. More work could be done to catalogue the range of features that Daktari may have interest in prototyping and to study which of these features can be made with hot embossing. For example, a patterned tool could be designed such that it can be used to test hot embossing for a wide variety of features. Questions that could be answered by such a study are:

1. How closely can features be placed to one another?
2. What are the minimum and maximum feature sizes that can be embossed?
3. What aspect ratios of channels are achievable?
4. How can sharp and gradual changes in height be best prototyped?
5. Can features be placed on the edge of a part?

A further study of tool wear could be conducted with a higher quality tool so that measurement precision is not highly affected by defects on the tool. Characterizing the tool wear accurately is important to understanding the limits on tool use.

Experimentation with different Tools

Other tooling options should be considered and tested to compare the differences in their performance in terms of tooling accuracy, durability and feature transferring capability. For example, silicon tools may be able to provide a surface roughness below 100nm, but offer low durability. Titanium machined tools on the other hand can offer higher resistance to wear and complex feature geometries, but may have a higher surface roughness.

Future work on resin tools can be expanded to cover methods for combining qualities of different tools into an all-encompassing resin tool. The study in question could concern the methods and accuracy analysis of combining the low surface finishes of a silicon tools with complex geometries of a machined tools.

Appendix A

Engineering Drawings:

Assembly Drawing:

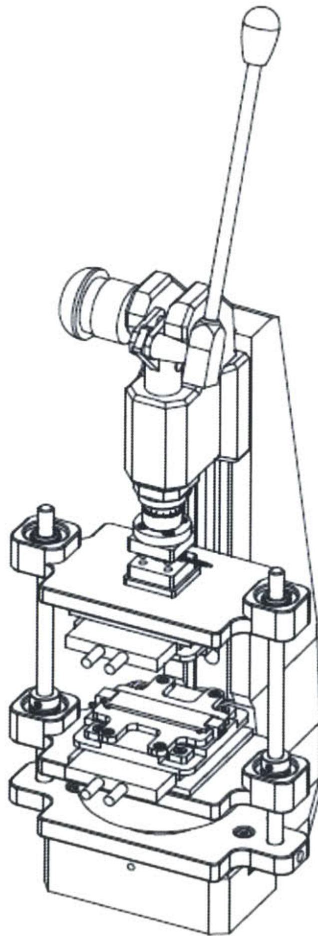

ITEM NO.	PART NUMBER	DESCRIPTION	QTY.
1	2-400105co	Schmidt Press Frame	1
2	92855A722	McMaster: M8—Pitch: 1.25 mm - 25mm	2
3	93615A510	McMaster: 3/8"-16 - 1/2"	4
4	AirSpring Valve - 9538K42	McMaster: AirSpring Valve	1
5	Rail Block		2
6	Half_in_rodx12in	SDP SI Rod	2
7	Bottom Heating plate		1
8	Corner Insulation Block		8
9	Cold Plate		2
10	MACOR		2
11	91253A251		8
12	Substrate plate ASMB		1
13	92220A161		4
14	heater		2
15	Sensor Block		2
16	Futek LCM200 Sensor		1
17	Sensor Insulator		1
18	Revised Top Heating plate		1
19	cuvette mold		1
20	91306A311		4
21	92855A522		5
22	Flange shaft		1
23	Small_Top		1
24	99642A229	McMaster: M12—Pitch: 1.5 mm - 12mm	2
25	94000A037		4
26	9414T11		2
27	Bottom ASMB		1
28	Airspring - 9539K41	McMaster: Airspring	1
29	Middle Plate		2
30	Bearing_S99LBC-050088	SDP SI Bearing	4
31	e clip_s73hw2-100-087	SDP SI e-clip for bearing	8
32	Top_Holder_New		1

Figure 54 Assembly Drawing

ITEM NO.	PART NUMBER	DESCRIPTION	QTY.
1	Bottom Heating plate		1
2	Corner Insulation Block		4
3	Cold Plate		1
4	MACOR		1
5	91253A251	10-24 1-1/4 inch flat head	4
6	Substrate plate ASMB		1
7	92220A161	10-24 1/4inch socket head	4
8	heater		1
9	Middle Plate		1

Figure 55 Bottom Sub-Assembly

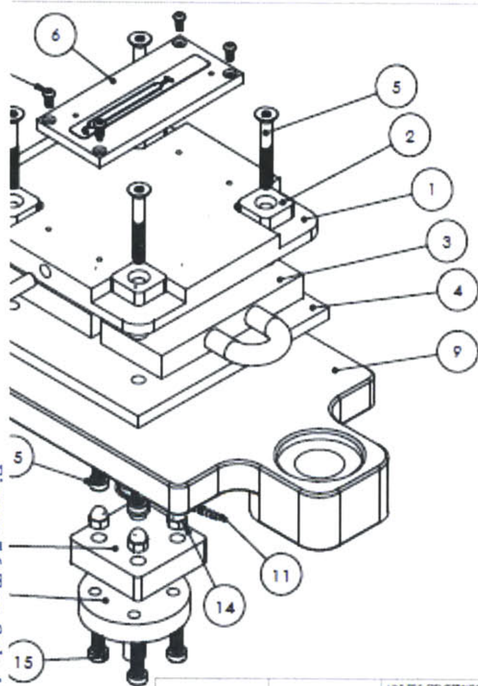

ITEM NO.	PART NUMBER	DESCRIPTION	QTY.
1	Revised Top Heating plate		1
2	Corner Insulation Block		4
3	Cold Plate		1
4	Insulation	Material MACOR	1
5	M5 0.8X25	Low Head Screw	4
6	cuvette mold		1
7	4-40 X 25 Screw	Button Head Screw	4
8	heater	Cartridge Heater	1
9	Top Plate		1
10	Sensor Insulator	Macor	1
11	Futek LCM200 Sensor	Load Cell	1
12	Sensor Block		2
13	Flange shaft		1
14	M5 0.8X25 Nut	Acron Nut	8
15	M5 0.8X25	Low Head Screw	8

UNLESS OTHERWISE SPECIFIED:
DIMENSIONS ARE IN INCHES
TOLERANCES:
FRACTIONAL ±
ANGULAR: MACH ± BEND ±
TWO PLACE DECIMAL ±
THREE PLACE DECIMAL ±
INTERPRET GEOMETRIC TOLERANCING PER:
MATERIAL
FINISH
DO NOT SCALE DRAWING

NEXT ASSY | USED ON
APPLICATION

NAME | DATE
DRAWN
CHECKED
ENG APPR.
MFG APPR.
Q.A.
COMMENTS:

TITLE:

SIZE A | DWG. NO. Top Complete Assembly | REV

SCALE: 1:8 | WEIGHT: | SHEET 1 OF 1

PROPRIETARY AND CONFIDENTIAL
...RMATION CONTAINED IN THIS ...G IS THE SOLE PROPERTY OF ... COMPANY NAME HERE>. ANY ...UCTION IN PART OR AS A WHOLE ... THE WRITTEN PERMISSION OF ... COMPANY NAME HERE> IS ...ED.

5 4 3 2 1

Figure 56 Top Sub-Assembly

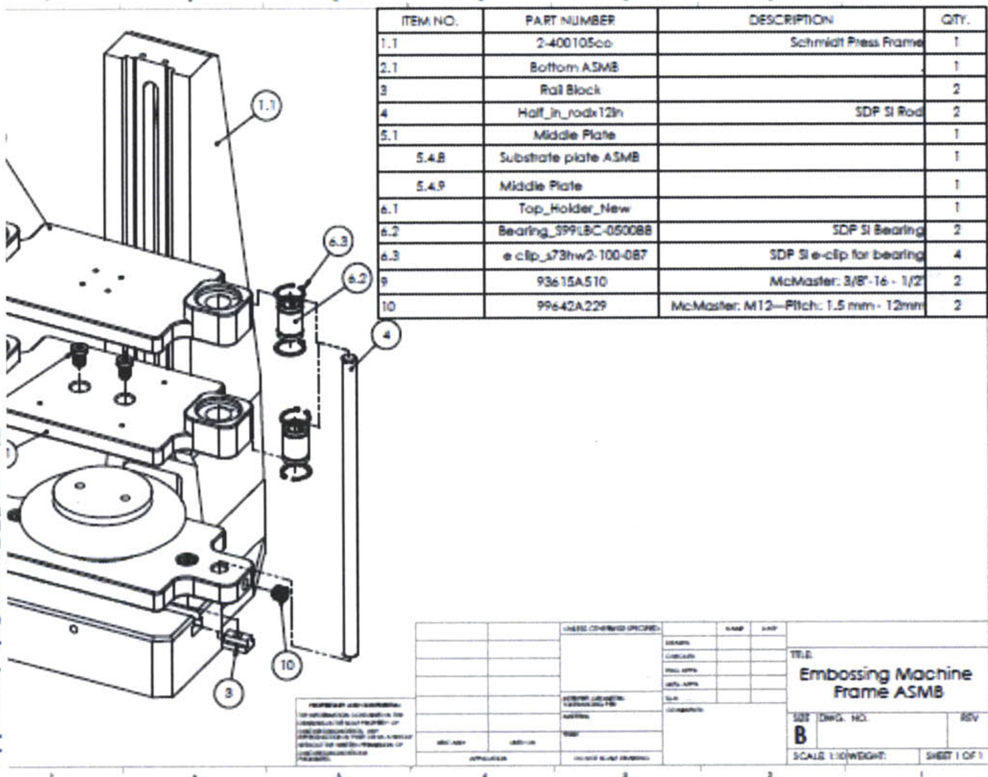

ITEM NO.	PART NUMBER	DESCRIPTION	QTY.
1.1	2-400105co	Schmidt Press Frame	1
2.1	Bottom ASMB		1
3	Rail Block		2
4	Half_in_rodx12in	SDP SI Rod	2
5.1	Middle Plate		1
5.4.8	Substrate plate ASMB		1
5.4.9	Middle Plate		1
6.1	Top_Holder_New		1
6.2	Bearing_S99LBC-05008B	SDP SI Bearing	2
6.3	e clip_s73hw2-100-087	SDP SI e-clip for bearing	4
9	93615A510	McMaster: 3/8"-16 - 1/2"	2
10	99642A229	McMaster: M12—Pitch: 1.5 mm - 12mm	2

Figure 57 Frame Sub-Assembly

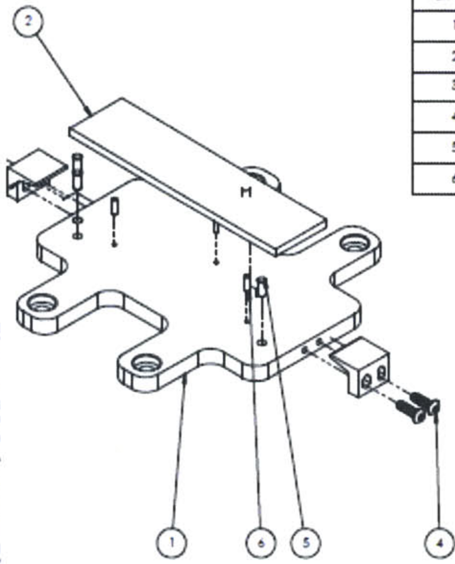

ITEM NO.	PART NUMBER	DESCRIPTION	QTY.
1	Substrate plate		1
2	PMMA sheet model		1
3	Substrate Flange		2
4	91306A315	4-40 3/8inch steel cap screw	4
5	97395A439	1/8 inch diameter dowel pin	3
6	97395A401	1/16 inch diameter dowel pin	3

Substrate plate ASMB

Figure 58 Substrate Plate Sub-Assembly

Bill of Materials

Table 16 Bill of Materials

Part	Vendor	Part No.	Material	Quantity	Unit Cost	Total
Top Assembly						
Flange	First Cut		Aluminum	1	$353.00	$353.00
Top Sensor Block	First Cut		Aluminum	1	$75.00	$75.00
Force Sensor	FUTEK			1	$575.00	$575.00
Ceramic Insulator	In house		Macor	1	$179.00	$179.00
Top Plate	Zero Hour Parts		Aluminum	1	$620.00	$620.00
Cold Plate	Mcmaster		Aluminum	1	$100.00	$100.00
Heating Plate	In house		Aluminum	1	$37.00	$37.00
Catridge Heaters	Mcmaster			1	$18.57	$18.57
Hose Pipes	Mcmaster			1	$29.00	$29.00
Tool	Atometric		Aluminum	2	$975.00	$1,950.00
Bearings	SDP-SI	S99LBC-050088		2	$17.12	$34.24
Shafts	SDP-SI	A 7X 1-1612A	Aluminum	2	$22.82	$45.64
Bottom Assembly						
Substrate Plate	First Cut		Aluminum	1	$198.00	$198.00
Substrate Flanges	First Cut		Aluminum	2	$42.00	$84.00
Heating Plate	In house		Aluminum	1	$0.00	$0.00
Cartridge Heater	Mcmaster			1	$18.57	$18.57
Cold Plate	Mcmaster		Aluminum	1	$100.00	$100.00
Ceramic Insulator	In House		Macor	1	$0.00	$0.00
Bottom Plate	Zero Hour Parts		Aluminum	1	$675.00	$675.00
Bearings	SDP-SI		Steel	2	$17.12	$34.24
Air Spring	Mcmaster	9539K41		1	$94.50	$94.50
Valve	Mcmaster	9538K42		1	$11.39	$11.39

Base Plate	Zero Hour Parts		Aluminum	1	$375.00	$375.00
Fasteners	Mcmaster					$0.00
Fasteners						
8mm hex bit	Mcmaster Carr	*7397A48*	Stainless Steel	1	$5.76	$5.76
M8-1.25 D5 Tap	Mcmaster Carr	*25235A43*	Stainless Steel	1	$27.86	$27.86
M8-1.25 rod	Mcmaster Carr	*94185A160*	Stainless Steel	1	$12.86	$12.86
Metric M8 Bolt 25mm	Mcmaster Carr	*92855A722*	Stainless Steel	1	$7.86	$7.86
M5 Size, 60 mm Length	Mcmaster Carr	*92855A543*	Stainless Steel	1	$9.51	$9.51
Hose Clamp for the piping of the cooling system for the hot embossing project	Mcmaster Carr	*45945K63*	Stainless Steel	8	$3.61	$28.88
M5x18 - Metric Class 12.9 Alloy Steel	Mcmaster Carr	*91290A238*	Stainless Steel	1	$11.66	$11.66
18-8 Stainless Steel Low Head Sckt Cap Screw 3/8"-16 Thread, 1/2" Length, packs of 5	Mcmaster Carr	*93615A510*	Stainless Steel	1	$7.72	$7.72
Alloy Steel Cup Point Set Screw M12 Size, 12mm Long, 1.5mm Pitch, packs of 5	Mcmaster Carr	*99642A229*	Stainless Steel	1	$12.18	$12.18
Alloy Steel Flat Head Socket Cap Screw 10-24 Thread, 1-1/2" Length, Black, packs of 25	Mcmaster Carr	*91253A251*	Stainless Steel	1	$10.36	$10.36
Alloy Steel Low Head Socket Cap Screw 10-24 Thread, 1/4" Length, packs of 25	Mcmaster Carr	*92220A161*	Stainless Steel	1	$7.31	$7.31
Zinc-Plated STL Button Head Socket Cap Screw 4-40 Thread, 1/4" Length, packs of 50	Mcmaster Carr	*91306A311*	Stainless Steel	1	$8.31	$8.31

Zinc-Plated STL Button Head Socket Cap Screw 4-40 Thread, 3/8" Length, packs of 50	Mcmaster Carr	*91306A315*	Stainless Steel	1	$8.63	$8.63
Corrosion Resistant Dowel Pin Type 316 SS, 1/8" Diameter, 5/16" Length, packs of 10	Mcmaster Carr	*97395A606*	Stainless Steel	1	$6.95	$6.95
Metric 18-8 Stainless Steel Acorn Nut M5 Size, .8mm Pitch, 8mm Width, 10mm Height, packs of 25	Mcmaster Carr	*94000A037*	Stainless Steel	1	$4.95	$4.95
Metric 18-8 SS Low Head Socket Cap Screw M5 Size, 25 mm Length, .8 mm Pitch, packs of 25	Mcmaster Carr	*92855A522*	Stainless Steel	1	$8.89	$8.89
E clips	Mcmaster Carr	*S73HW2-100-087*	Stainless Steel	8	$1.72	$13.76
Dowel Pins 1/8th dia 1/4 th length	Mcmaster Carr	*97395A439*	Stainless Steel	1	$6.14	$6.14
Corrosion Resistant Dowel Pin Type 316 SS, 1/16" Diameter, 1/4" Length, packs of 25	Mcmaster Carr	*97395A401*	Stainless Steel	1	$10.48	$10.48

PARTS

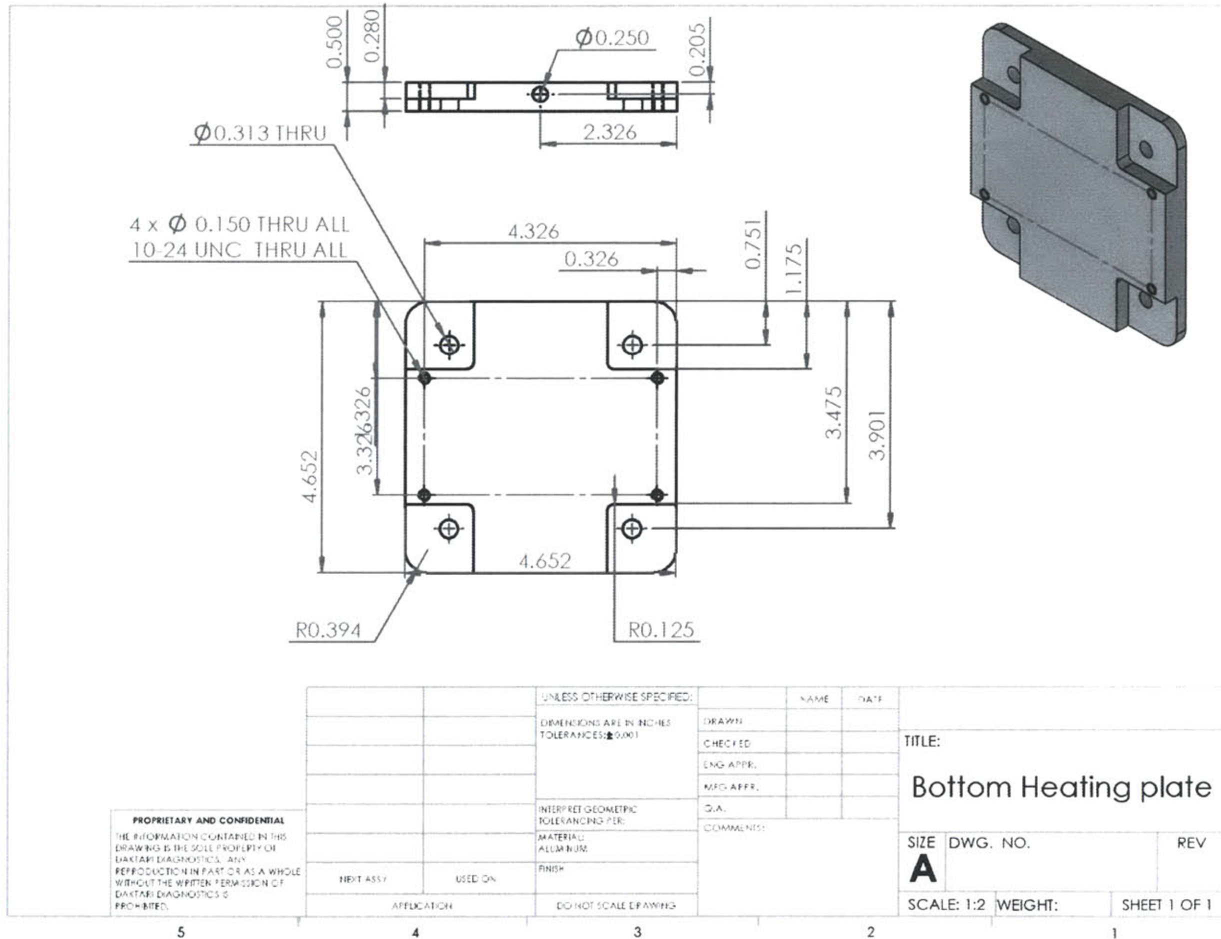

Figure 59 Bottom Heating Plate

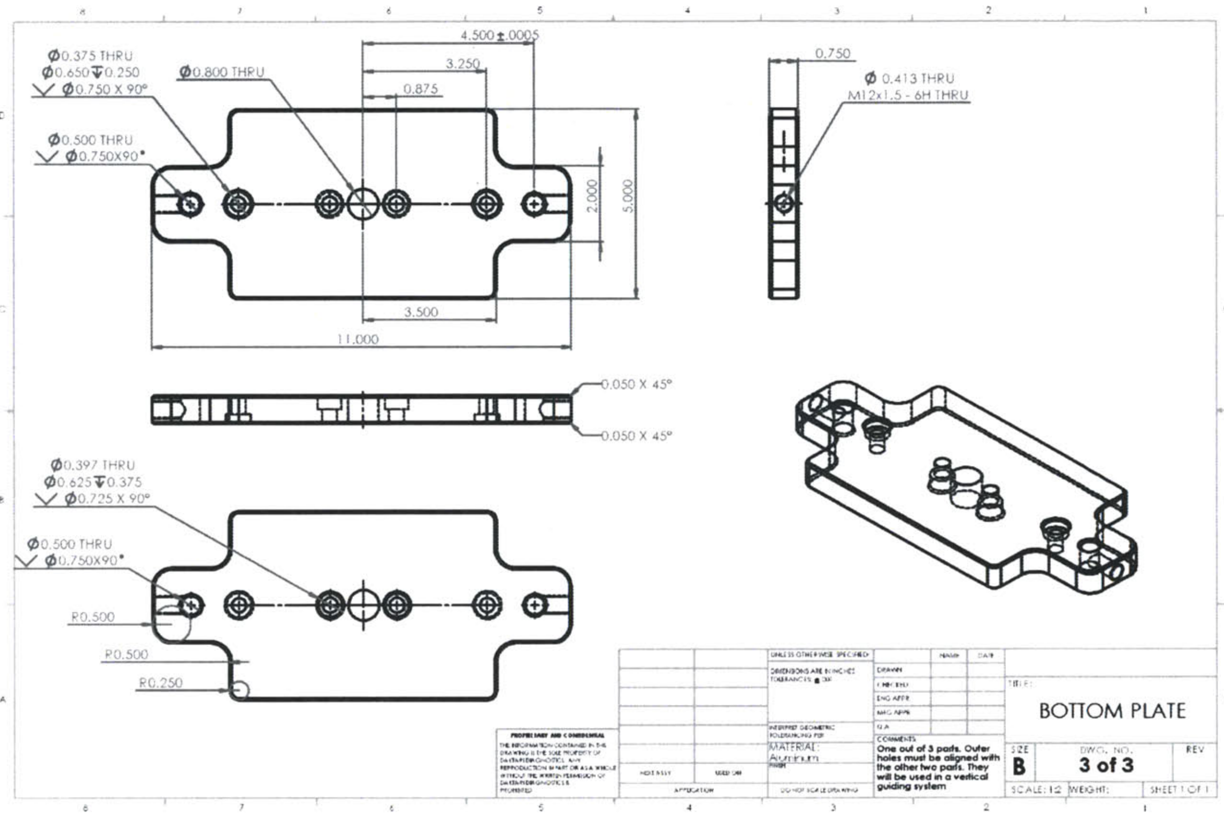

Figure 60 Bottom Plate

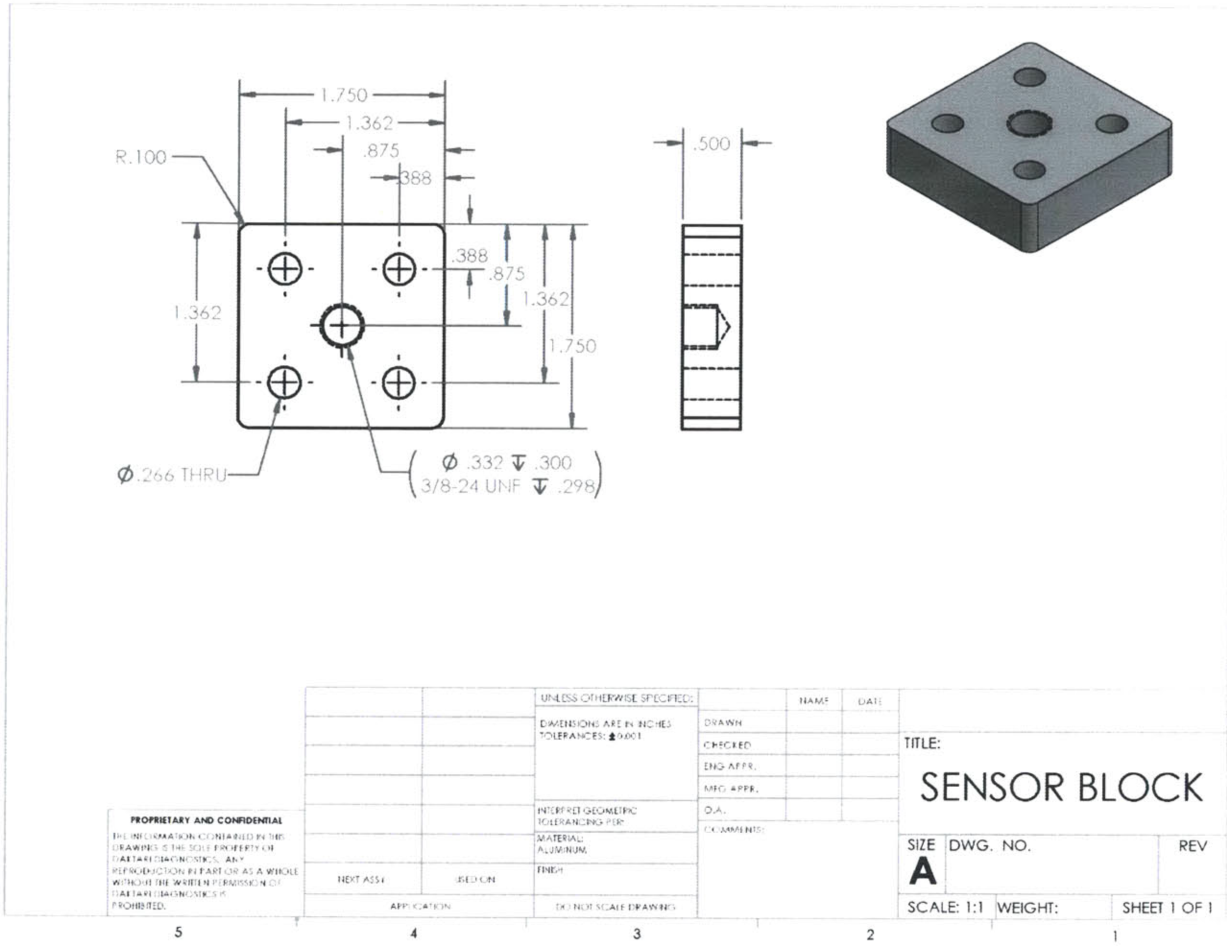

Figure 61 Sensor Block

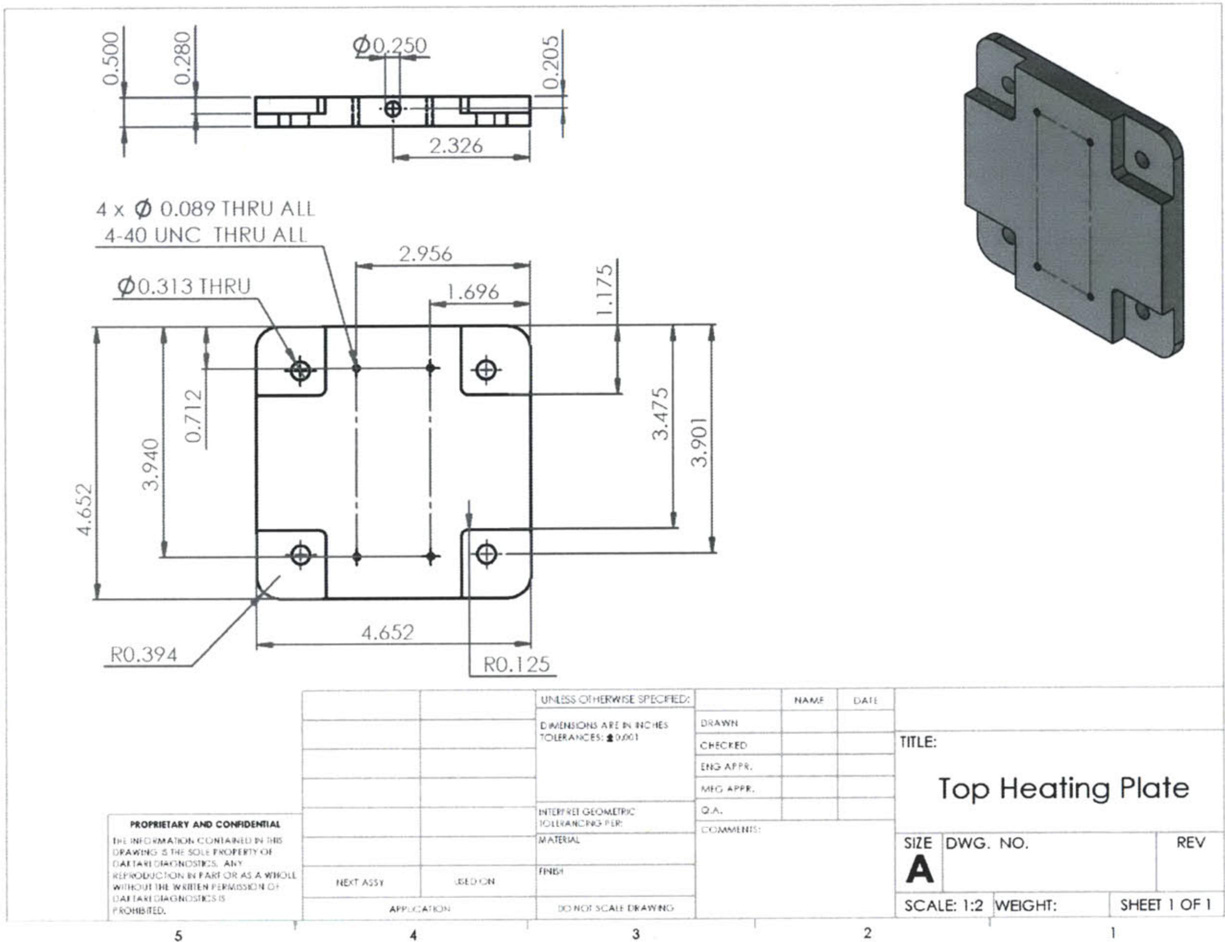

Figure 62 Top Heating Plate

4 x Ø 0.150 ↧ 0.400
10-24 UNC ↧ 0.380

Ø0.397 THRU
⌴ Ø0.625 ↧ 0.375
⌵ Ø0.725 X 90°

Ø0.872 THRU
+.00083
-.00000

⌴ Ø1.500 ↧ .190
⌵ Ø0.725X 90°

4.500 ± .0005
1.575
0.875
1.575
2.000
5.000
2.000
11.000

SECTION A-A

1.250
0.650
.0005
.0005
0.050 X 45°
0.050 X 45°
0.050 X 45°

⌴ Ø1.500 ↧ .190
⌵ Ø0.725X 90°

R0.500
R0.500
R0.250

TITLE:
Middle Plate

MATERIAL:
Aluminum

COMMENTS:
One out of 3 parts. Outer holes must be aligned with the other two parts. They will be used in a vertical guiding system

SIZE B
DWG. NO.
2 of 3
REV

SCALE: 1:2 WEIGHT: SHEET 1 OF 1

Figure 63 Middle Plate

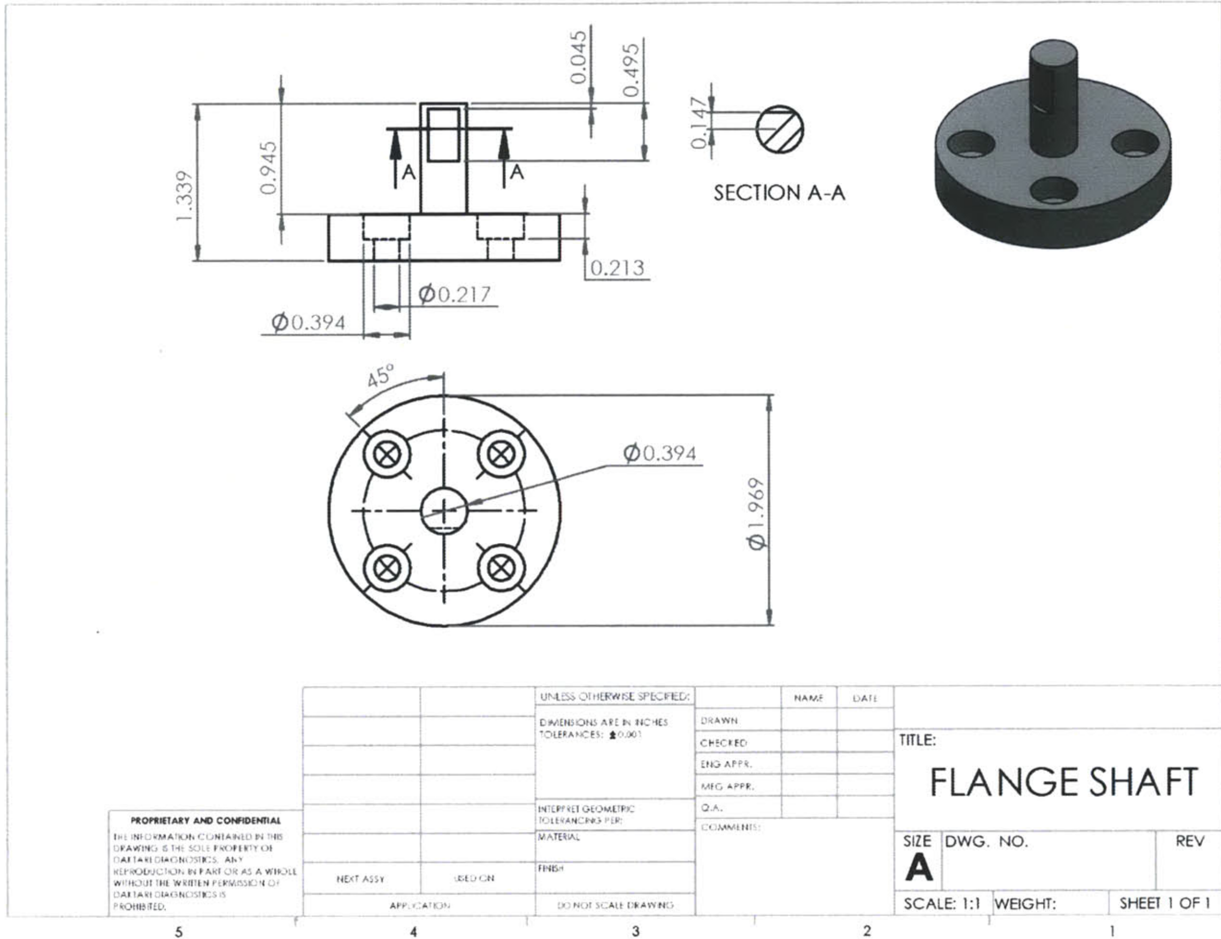

Figure 64 Flange Shaft

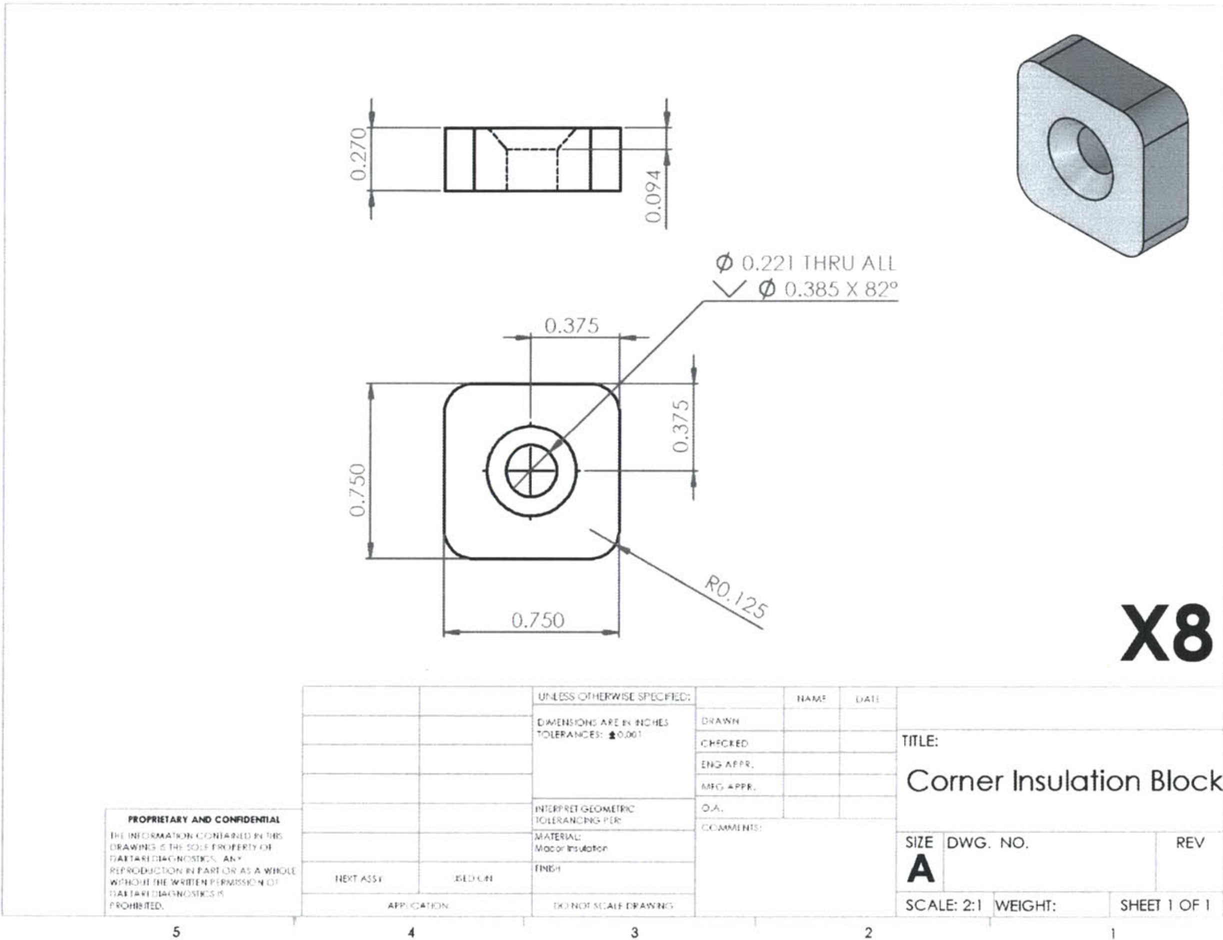

Figure 65 Corner Insulation Block

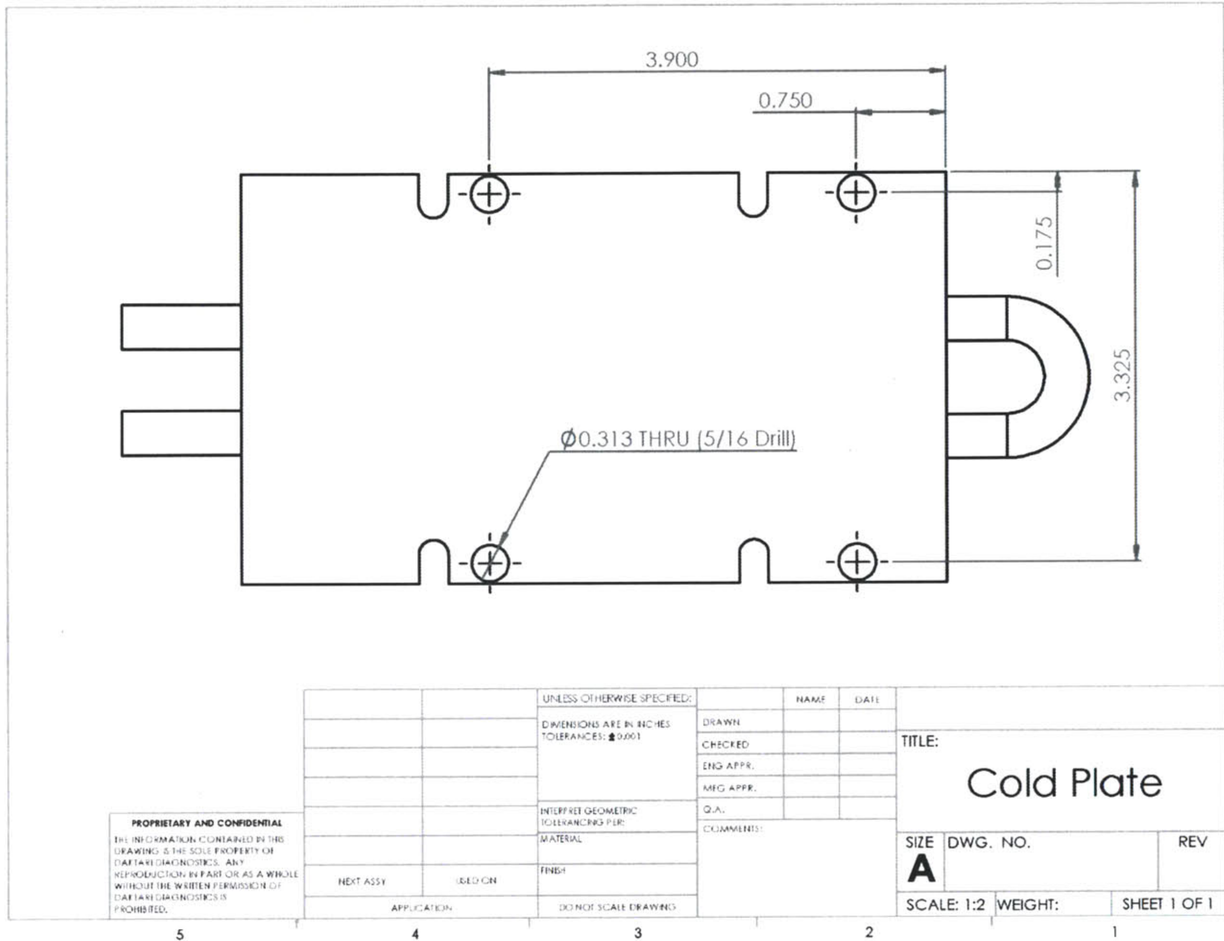

Figure 66 Cold Plate

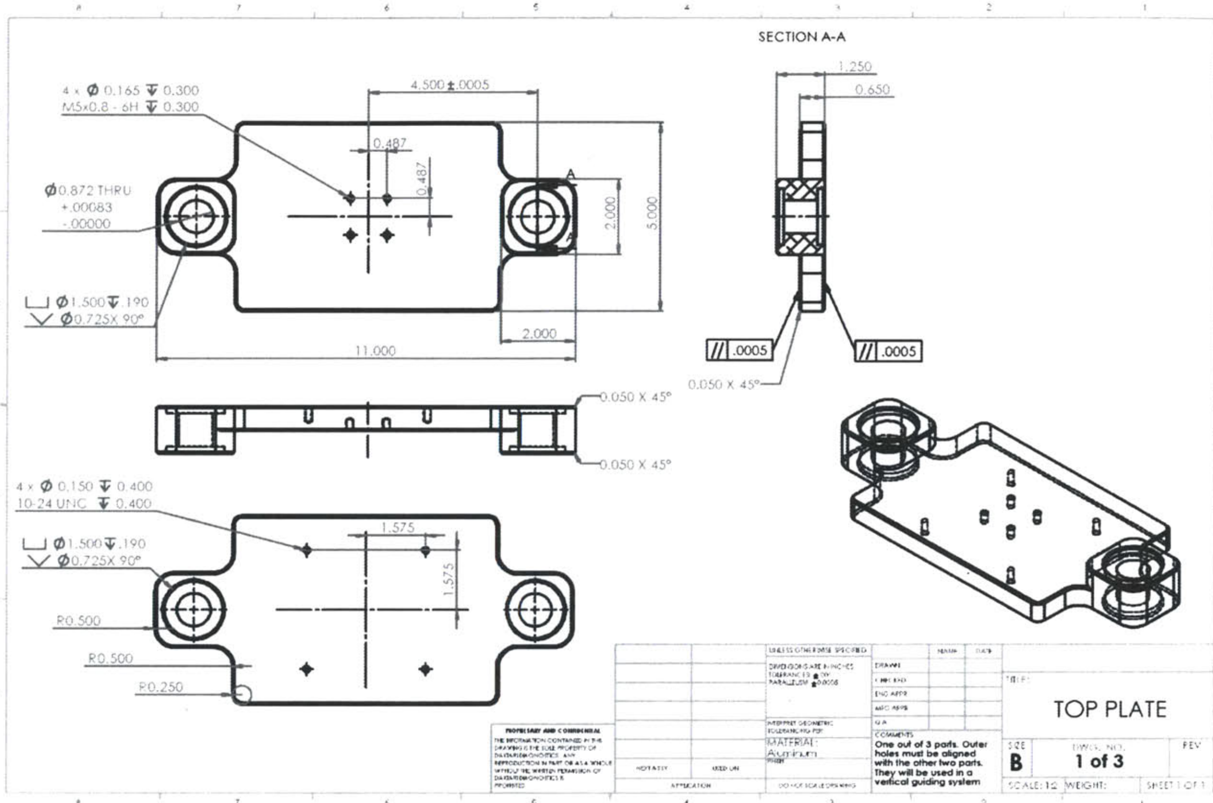

Figure 67 Top Plate

Product Information

DOW CORNING

Encapsulants

Dow Corning® 184 Silicone Elastomer

Transparent encapsulant with good flame resistance

FEATURES

- Flowable
- RT and heat cure
- High tensile strength
- Same as Sylgard 182 but with RT cure capability
- UL and Mil Spec tested

BENEFITS

- Rapid, versatile cure processing controlled by temperature
- High transparency allows easy inspection of components
- Can be considered for uses requiring UL and Mil Spec requirements

COMPOSITION

- 2-part
- 10:1 mix ratio
- Polydimethylsiloxane elastomer

APPLICATION METHODS

- Automated metered mixing and dispensing
- Manual mixing

APPLICATIONS

- General potting applications
- Power supplies
- Connectors
- Sensors
- Industrial controls
- Transformers
- Amplifiers
- High voltage resistor packs
- Relays
- Adhesive/encapsulant for solar cells
- Adhesive handling beam lead integrated circuits during processing

TYPICAL PROPERTIES

Specification Writers: These values are not intended for use in preparing specifications. Please contact your local Dow Corning sales office or your Global Dow Corning Connection before writing specifications on this product.

Property	Unit	Value
Viscosity (Part A)	cP	5175
	mPa-sec	5175
	Pa-sec	5.2
Viscosity (Mixed)	cP	3500
	mPa-sec	3500
	Pa-sec	3.5
Specific Gravity (Uncured Base)	-	1.03
Specific Gravity (Cured)	-	1.04
Working Time at 25°C (Pot Life - hours)	hr	1.4
Cure Time at 25°C	hrs	48
Heat Cure Time @ 100°C	minutes	35
Heat Cure Time @ 125°C	minutes	20
Heat Cure Time @ 150°C	minutes	10

Figure 68 PDMS

DESCRIPTION

Dow Corning® silicone encapsulants are supplied as two-part liquid component kits. When liquid components are thoroughly mixed, the mixture cures to a flexible elastomer, which is well suited for the protection of electrical/electronic applications. Dow Corning silicone encapsulants cure without exotherm at a constant rate regardless of sectional thickness or degree of confinement. Dow Corning silicone elastomers require no post cure and can be placed in service immediately following the completion of the cure schedule. Standard silicone encapsulants require a surface treatment with a primer in addition to good cleaning for adhesion while primerless silicone encapsulants require only good cleaning. Underwriters Laboratory (UL) 94 recognition is based on minimum thickness requirements. Please consult the UL Online Certifications Directory for the most accurate certification information.

MIXING AND DE-AIRING

The 10:1 mix ratio these products are supplied in gives one latitude to tune the modulus and hardness for specific application needs and production lines. In most cases de-airing is not required.

PREPARING SURFACES

In applications requiring adhesion, priming will be required for many of the silicone encapsulants. See the Primer Selection Guide for the correct primer to use with a given product. For best results, the primer should be applied in a very thin, uniform coating and then wiped off after application. After application, it should be thoroughly cured prior to application of the silicone elastomer. Additional instructions for primer usage can be found in the information sheets specific to the individual primers.

PROCESSING/CURING

Thoroughly mixed Dow Corning silicone encapsulant may be poured/dispensed directly into the container in which it is to be cured. Care should be taken to minimize air entrapment. When practical, pouring/dispensing should be done under vacuum, particularly if the component being potted or encapsulated has many small voids. If this technique cannot be used, the unit should be evacuated after the silicone encapsulant has been poured/dispensed. Dow Corning silicone encapsulants may be either room temperature (25°C/77°F) or heat cured. Room temperature cure encapsulants may also be heat accelerated for faster cure. Ideal cure conditions for each product are given in the product selection table. Two-part condensation cure encapsulants should not be heat accelerated above 60°C (140°F).

TYPICAL PROPERTIES, continued

Property	Unit	Value
Tensile Strength	psi	1025
	MPa	7.1
	kg/cm2	71
Elongation	%	120
Tear Strength (Die B)	ppi	5
	N/cm	2
Durometer Shore A	-	44
Dielectric Strength	volts/mil	475
	kV/mm	19
Volume Resistivity	ohm*cm	2.9E+14
Dielectric Constant at 100 Hz	-	2.72
Dielectric Constant at 100 kHz	-	2.68
Dissipation Factor at 100 hz	-	0.00257
Dissipation Factor at 100 kHz	-	0.00133
Mil Specification	NA	Mil Spec
Agency Listing	-	UL 94V-0
Shelf Life at 25ºC	months	24
Refractive Index @ 589 nm	-	1.4118
Refractive Index @ 632.8 nm	-	1.4225
Refractive Index @ 1321 nm	-	1.4028
Refractive Index @ 1554 nm	-	1.3997

Figure 69 PDMS

CYTEC

TECHNICAL DATA SHEET CONAP®

CONAPOXY® FR-1080

CONAPOXY FR-1080 is a two-part high temperature epoxy potting system designed to meet Class H (180°C) operating requirements.

TYPICAL PRODUCT CHARACTERISTICS

	Resin Properties Part A	Curative Properties Part B
Viscosity @ 25°C	4,000 cps	300 cps
Specific Gravity @ 25°C	1.03	1.23
Color	Amber	Dark Brown

TYPICAL CURED PROPERTIES

	25°C	105°C
Hardness, Shore D		90
Tensile Strength, psi		8200
Elongation, %		2
Tear Strength, pli		250
Shrinkage, %		1.42
Volume Resistivity, ohm-cm	9.7×10^{16}	2.9×10^{14}
Surface Resistivity, ohms	5.5×10^{16}	5.7×10^{14}
Dielectric Constant @ 1 KHz	3.12	3.29
Dissipation Factor @ 1 KHz	0.004	0.004
Dielectric Strength, vpm	600	450
Flexural Strength, psi		12,789
Flexural Modulus, psi		388,650
Compressive Strength, psi		4230

RECOMMENDED PROCESSING PARAMETERS

Parameter	Value
Mix Ratio by Weight, Resin/Curative	100/83
Mix Ratio by Volume, Resin/Curative	100/67
Initial Mixed Viscosity @ 25°C	2500 cps
Work Life @ 25°C	>2 hours
Gel Time @ 100°C	1-2 hours
Cure @ 120°C	4-16 hours
Post Cure @ 180°C (for maximum properties)	2 hours

STORAGE AND HANDLING

The shelf life of CONAPOXY FR-1080 resin and hardeners is 18 months from date of manufacture when stored in the original unopened containers.

Some settling of fillers may occur in the resin. Mix resin thoroughly before each use.

CAUTION: FOR INDUSTRIAL USE ONLY!

Epoxy resins and hardeners can cause skin rashes, dermatitis, and eye irritation. Use only in well ventilated areas. The use of appropriate clothing and safety glasses is recommended. Avoid breathing of vapors and protect skin and eyes from contact with material. Should skin contact occur, immediately clean with suitable hand cleaner, then scrub with soap and water. For eye contact, immediately flush with water for at least 15 minutes and obtain medical attention.

FOR COMPLETE SAFETY AND HEALTH INFORMATION, REFER TO THE MATERIAL SAFETY DATA SHEET (MSDS) FOR THIS PRODUCT.

AVAILABILITY

CONAPOXY FR-1080 is available in gallon, 5-gallon, and 55-gallon containers. An evaluation kit of CONAPOXY FR-1080 is available for a nominal fee.

CAUTION

Responsible handling of Cytec products requires a thorough preview of safety, health, and environmental issues prior to use. Review the Material Safety Data Sheets(s) for the specific Cytec product(s) and container label information before opening containers. Ensure that employee exposure issues are understood, communicated to all workers, and controls are in place to prevent exposures above Permissible Exposure Limits (P.E.L.'s). Review safety and environmental issues to be certain controls are in place to prevent injury to employees, the community, or the environment, and ensure compliance with all applicable Federal, State, and Local laws and regulations. For assistance in this review process, please call your Cytec representative or our office noted below.

www.cytec.com/conap

• Email: custinfo@cytec.com Worldwide Contact Info: www.cytec.com/conap Tel: 716.372.9650 Fax: 716.372.1594 •

Cytec Industries Inc. in its own name and on behalf of its affiliated companies (collectively, "Cytec") decline any liability with respect to the use made by anyone of the information contained herein. The information contained herein represents Cytec's best knowledge thereon without constituting any express or implied guarantee or warranty of any kind (including, but not limited to, regarding the accuracy, the completeness or relevance of the data set out herein). Cytec is the sole owner or authorized user of the intellectual property rights relating to the information communicated. The information relating to the use of the products is given for information purposes only. No guarantee or warranty is provided that the product is adapted for any specific use. The user or purchaser should perform its own tests to determine the suitability for a particular purpose. The final choice of use of a product remains the sole responsibility of the user.
©2009 Cytec Industries Inc. All Rights Reserved.

TRADEMARK NOTICE: The ® indicates a Registered Trademark in the United States and the ™ or * indicates a Trademark in the United States. The mark may also be registered, the subject of an application for registration or a trademark in other countries.

UPT-P-206C

Figure 70 Epoxy Resin

FUTEK MODEL LCM200

ULTRA LIGHT MINIATURE UNIVERSAL THREADED LOAD CELL

Drawing Number: FI1064-B

INCH [mm] | R.O.= Rated Output

WIRING CODE (WC1)			
+Excitation	-Excitation	+Signal	-Signal
RED	BLACK	GREEN	WHITE
Shield			
FLOATING			

+OUTPUT
(TENSION)
-OUTPUT
(COMPRESSION)

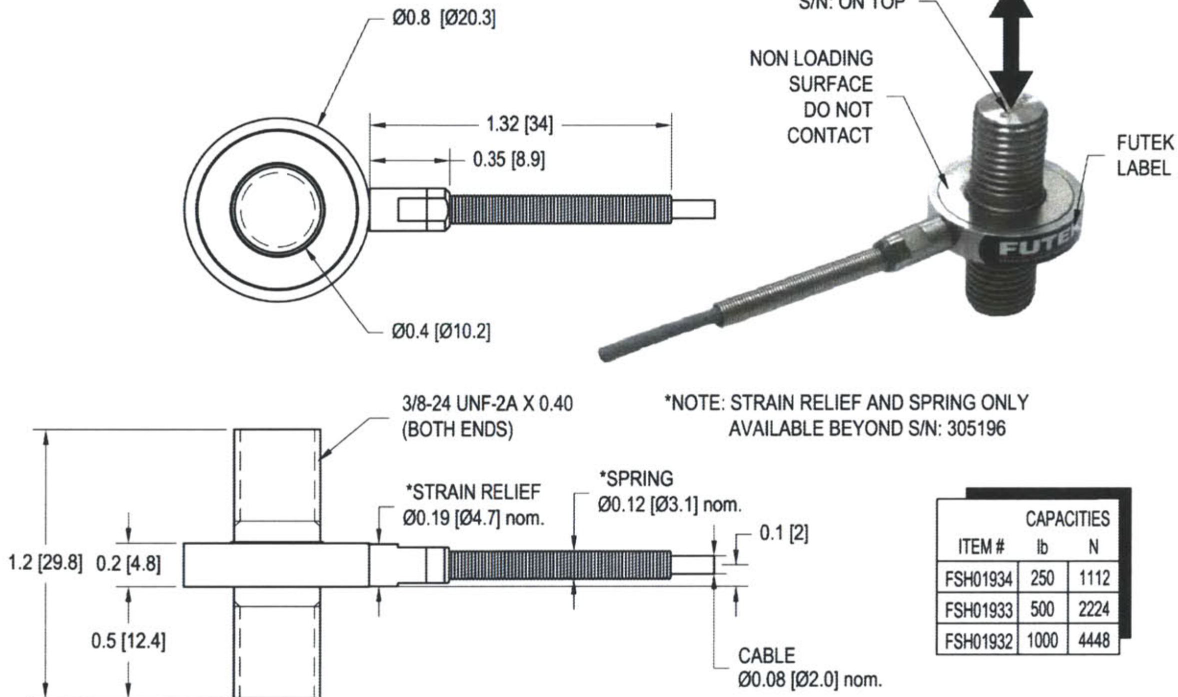

ITEM #	CAPACITIES lb	N
FSH01934	250	1112
FSH01933	500	2224
FSH01932	1000	4448

SPECIFICATIONS:

RATED OUTPUT	*1 mV/V nom (250 lb); 2 mV/V nom.*
SAFE OVERLOAD	*150% of R.O.*
ZERO BALANCE	*±3% of R.O.*
EXCITATION (VDC OR VAC)	*15 MAX*
BRIDGE RESISTANCE	*350 Ω nom.*
NONLINEARITY	*±0.5% of R.O.*
HYSTERESIS	*±0.5% of R.O.*
NONREPEATABILITY	*±0.1% of R.O.*
TEMP. SHIFT ZERO	*±0.01% of R.O./°F [0.018% of R.O./°C]*
TEMP. SHIFT SPAN	*±0.02% of LOAD/°F [0.036% of LOAD/°C]*
COMPENSATED TEMP.	*60 to 250°F [15 to 121°C]*
OPERATING TEMP.	*-60 to 285°F [-50 to 140°C]*
WEIGHT	*0.6 oz [17 g]*
MATERIAL	*17-4PH S.S.***
DEFLECTION	*0.002 [0.05] nom.*

CABLE: #29 AWG, 4 Conductor, Spiral Shielded Teflon Cable 10 ft [3 m] Long

ACCESSORIES AND RELATED INSTRUMENTS AVAILABLE

CALIBRATION (STD)	*5 pt. TENSION; 60.4 KΩ SHUNT CAL. VALUE* *100 KΩ FOR 250 lb SHUNT CAL. VALUE*
CALIBRATION (AVAILABLE)	*COMPRESSION*
CALIBRATION TEST EXCITATION	*10 VDC*

This drawing is submitted solely for the information and exclusive use of the original addressee. It is not to be divulged in whole or in part, by any firm or individual without written permission from FUTEK

10 THOMAS
IRVINE, CA 92618 USA
1-800-23-FUTEK (38835)

INTERNET:
http://www.futek.com

Figure 71 Load Sensor

1/32 DIN Ramp/Soak Controllers

CN7500 Series

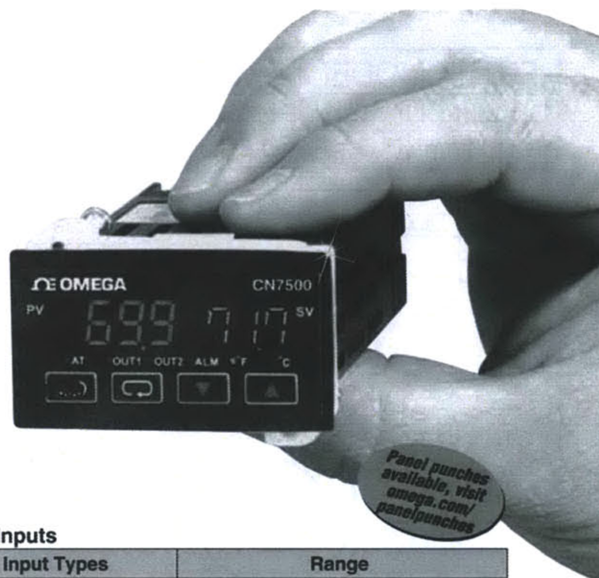

- Dual 4-Digit LED Display
- 8 Ramp/Soak Programs, 8 Segments Each
- Universal Inputs
- Autotune
- Dual Control Outputs
- RS485 Communications Standard
- Alarm Functions
- Free Software

The CN7500 Series temperature/process controller's advanced control features can handle the most demanding temperature or process applications. Enclosed in a compact 1/32 DIN housing, the CN7500 has dual, 4-digit LED displays for local indication of process value and setpoint. Control methods include on/off, PID, autotune, and manual tune. PID control is supported with 64 temperature and time (ramp/soak) control actions. The dual-loop output control allows simultaneous heating and cooling. The second output can be configured as an alarm mode using one of the 13 built-in alarm functions.

RS485 communications is standard. Up to 247 communication addresses are available, with transmission speeds of 2400 to 38,400 bps. Other features include universal inputs, selectable temperature units (°C/°F), selectable resolution, quick sampling rate, and security protection.

Specifications

Inputs: Thermocouple, RTD, DC voltage or DC current
Display: Two 4-digit, 7 segment 6.35 mm H (25") LEDs;
PV: red
SV: green
Accuracy: ±0.25% span, ±1 least significant digit
Supply Voltage: 100 to 240 Vac, 50/60 Hz
Power Consumption: 5 VA max
Operating Temperature: 0 to 50°C (32 to 122°F)
Memory Backup: Non-volatile memory
Control Output Ratings:
Relay: SPST, 5A @ 250 Vac resistive
Voltage Pulse: 14 V, 10 to -20% (max 40 mA)
Current: 4 to 20 mA
Communication: RS485 MODBUS® A-5-11/RTU communication protocol
Weight: 114 g (4 oz)
Panel Cut-Out: 45 x 22.5 mm (1.772 x 0.886")
Maximum Panel Thickness: 3.40 mm (0.14")
Panel Depth: 99.80 mm (3.86")

Inputs

Input Types	Range
K	-200 to 1300°C (-328 to 2372°F)
J	-100 to 1200°C (-148 to 2192°F)
T	-200 to 400°C (-328 to 752°F)
E	0 to 600°C (32 to 1112°F)
N	-200 to 1300°C (-328 to 2372°F)
R	0 to 1700°C (32 to 3092°F)
S	0 to 1700°C (32 to 3092°F)
B	100 to 1800°C (212 to 3272°F)
L	-200 to 850°C (-328 to 1562°F)
U	-200 to 500°C (-328 to 932°F)
Pt100 RTD	-200 to 600°C (-328 to 1112°F)
0 to 50 mV	-999 to 9999
0 to 5 V	-999 to 9999
0 to 10 V	-999 to 9999
0 to 20 mA*	-999 to 9999
4 to 20 mA*	-999 to 9999

** Requires external 250 Ω precision shunt resistor, **OMX-R250** (sold separately).*

To Order *Visit omega.com/cn7500 for Pricing and Details*

Model No.	Description
CN7523	Dual output, DC pulse/relay, RS485*
CN7533	Dual output, relay/relay, RS485*
CN7553	Dual output, 4 to 20 mA/relay, RS485*

Accessories (Field Installable)

Model No.	Description
CNQUENCHARC	Noise suppression RC snubber (2 leads),110 to 230 Vac
OMX-R250	250 Ω precision resistor
CN7-485-USB-1	RS485 to USB mini-node converter

Comes complete with operator's manual.
** Free CN7-A software download available at **omega.com/cn7500***
***Ordering Example: CN7523,** dual-output controller, DC pulse and a mechanical relay output, RS485 communications.*

P-23

Figure 72 Temperature Controller

NEW

Inch Inch Inch Inch Inch Inch Inch

SDP/SI

Linear Ball Bearings – Closed Type

Stock Drive Products/Sterling Instrument ■ Phone: 516-328-3300 ■ Fax: 516-326-8827

■ LOW FRICTION COEFFICIENT ■ HIGH POSITIONING ACCURACY
■ HIGH LOAD CAPACITY ■ QUIET MOVEMENT ■ LONG TRAVEL LIFE

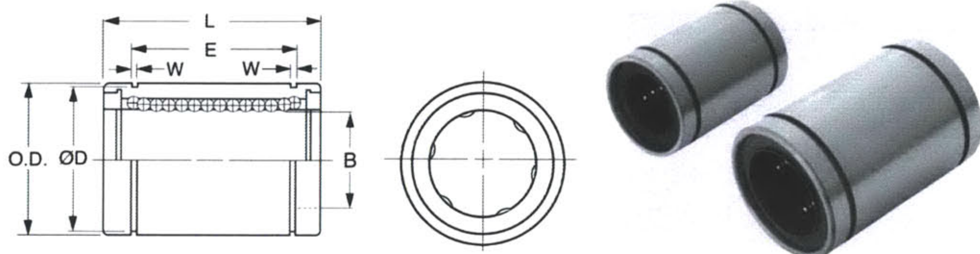

MATERIAL: **Sleeve and Balls** – AISI 52100 Steel
Retainer – Duracon M90

Catalog Number	Ball Circuit	B* Bore	O.D.□	L$^{\Delta}$ Length	E§ Groove Distance	W Groove Width	D Groove	Load Capacity Dynamic lbf	Load Capacity Static lbf
S99LBC-025075□	4	.2500	.5000	.750	.511	.0390	.4687	46	60
S99LBC-038063□		.3750	.6250	.875	.636		.5880	51	71
S99LBC-050088□	4	.5000	.8750	1.250	.963	.0459	.8209	115	176
S99LBC-063113□		.6250	1.1250	1.500	1.104	.0559	1.0590	174	265
S99LBC-075125□	5	.7500	1.2500	1.625	1.166	.0559	1.1760	194	308
S99LBC-100156□	6	1.0000	1.5625	2.250	1.755	.0679	1.4687	220	353
S99LBC-125200□	6	1.2500	2.0000	2.625	2.005	.0679	1.8859	353	616
S99LBC-150238□		1.5000	2.3750	3.000	2.412	.0859	2.2389	490	904

NOTE: To order bearings with no seals, use catalog numbers as they are. To order bearings with seals at both ends, add **"S"** to the end of catalog number.

BEARING TOLERANCES

* **B Tolerance:**	.2500, .3750, .5000 & .6250	+.0000 / -.00025
	.7500 & 1.0000	+.0000 / -.00030
	1.2500 & 1.5000	+.0000 / -.00035
□ **O.D. Tolerance:**	.5000	+.0000 / -.00045
	.6250, .8750 & 1.1250	+.0000 / -.00050
	1.2500 & 1.5625	+.0000 / -.00065
	2.0000 & 2.3750	+.0000 / -.00075
$^{\Delta}$ **L Tolerance:**	.750, .875, 1.250, 1.500 & 1.625	+.000 / -.008
	2.250, 2.625 & 3.000	+.000 / -.012
§ **E Tolerance:**	.511, .636, .963, 1.104 & 1.166	+.000 / -.008
	1.755, 2.005 & 2.412	+.000 / -.012

72

Figure 73 Bearings

UNDERSIZE, NOMINAL AND OVERSIZE DIAMETERS

PHONE: 516.328.3300 • FAX: 516.326.8827 • WWW.SDP-SI.COM

› MATERIAL:
303 Stainless Steel

Other lengths and diameters available on special order.

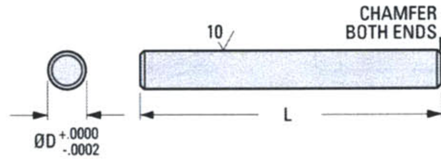

INCH COMPONENT

Catalog Number	D Diameter +.0000 -.0002	L Length ±.125 in.
A 7X 1-0112B	.0311	12
A 7X 1-0112	.0313	12
A 7X 1-0112A	.0317	12
A 7X 1-0212	.0622	12
A 7X 1-0212A	.0626	12
A 7X 1-0212B	.0630	12
A 7X 1-0312	.0778	12
A 7X 1-0312A	.0781	12
A 7X 1-0312B	.0786	12
A 7X 1-0312C	.0934	12
A 7X 1-0312F	.0935	12
A 7X 1-0312D	.0938	12
A 7X 1-0312E	.0942	12
A 7X 1-0424	.1247	24
A 7X 1-0424A	.1250	24
A 7X 1-0424B	.1252	24
A 7X 1-0424C	.1255	24
A 7X 1-0524	.1560	24
A 7X 1-0524A	.1562	24
A 7X 1-0524B	.1567	24
A 7X 1-0624	.1872	24
A 7X 1-0624A	.1875	24
A 7X 1-0624B	.1877	24
A 7X 1-0724	.2184	24
A 7X 1-0724A	.2187	24
A 7X 1-0724B	.2192	24

Catalog Number	D Diameter +.0000 -.0002	L Length ±.125 in.
A 7X 1-0824	.2497	24
A 7X 1-0836	.2497	36
A 7X 1-0824A	.2500	24
A 7X 1-0836A	.2500	36
A 7X 1-0824B	.2502	24
A 7X 1-0836B	.2505	36
A 7X 1-1024	.3122	24
A 7X 1-1016	.3123	16
A 7X 1-1016A	.3125	16
A 7X 1-1024A	.3125	24
A 7X 1-1016B	.3127	16
A 7X 1-1024B	.3130	24
A 7X 1-1216	.3747	16
A 7X 1-1236	.3747	36
A 7X 1-1216A	.3750	16
A 7X 1-1236A	.3750	36
A 7X 1-1216B	.3752	16
A 7X 1-1236B	.3755	36
A 7X 1-1616	.4997	16
A 7X 1-1636	.4997	36
A 7X 1-1612A	.5000	12
A 7X 1-1616A	.5000	16
A 7X 1-1636A	.5000	36
A 7X 1-1616B	.5002	16
A 7X 1-1636B	.5005	36
A 7X 1-2412A	.7500	12

Figure 74 Guiding Rods

Appendix B

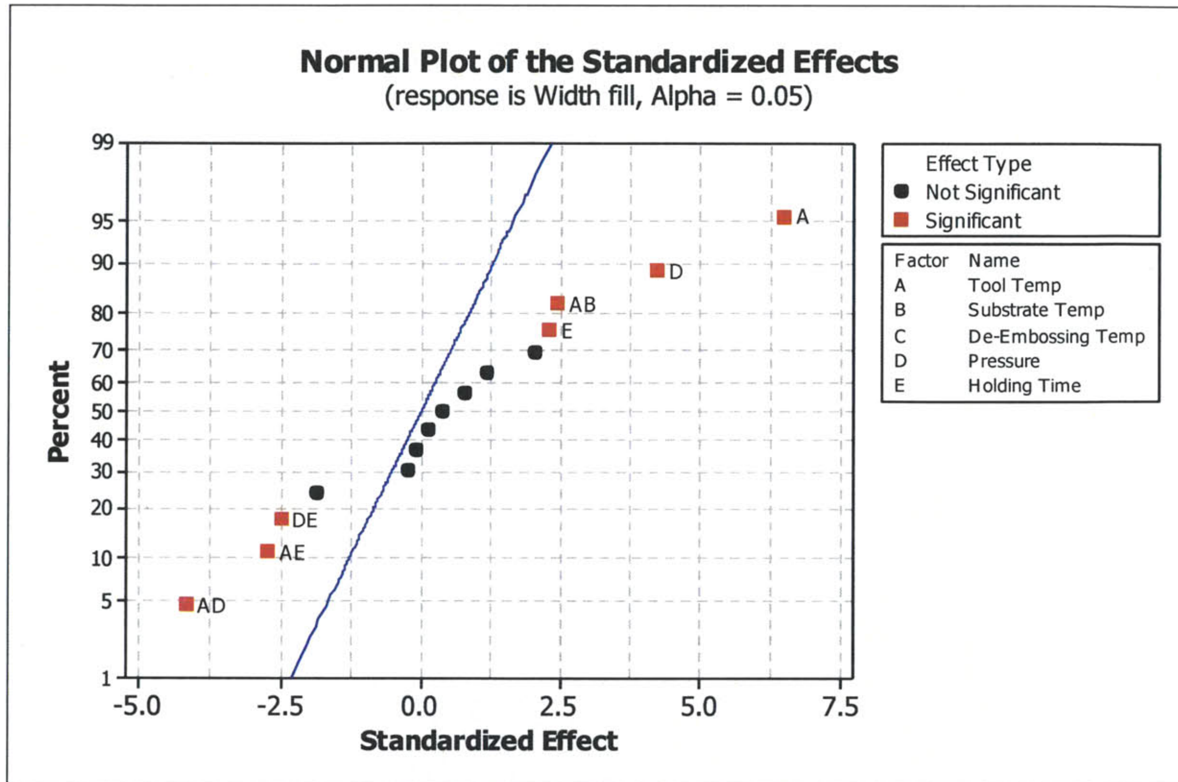

Figure 75 Normal Plot for Width Fill

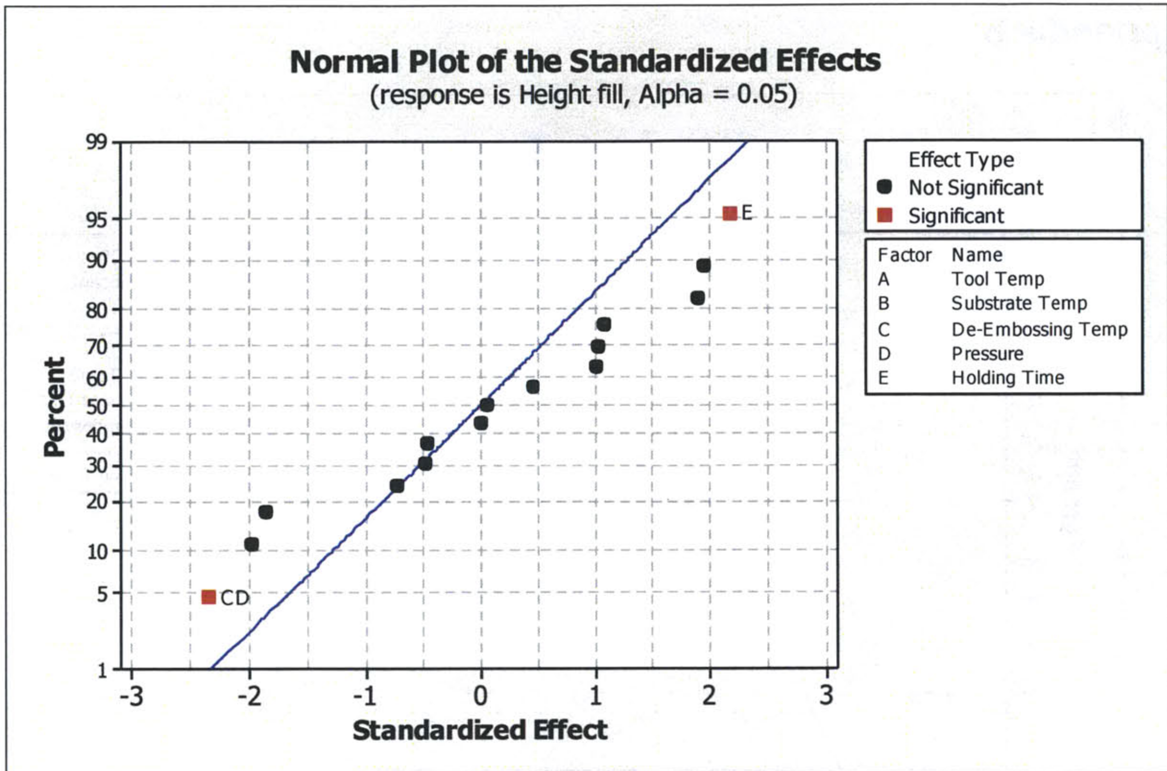

Figure 76 Normal Plot for Height Fill

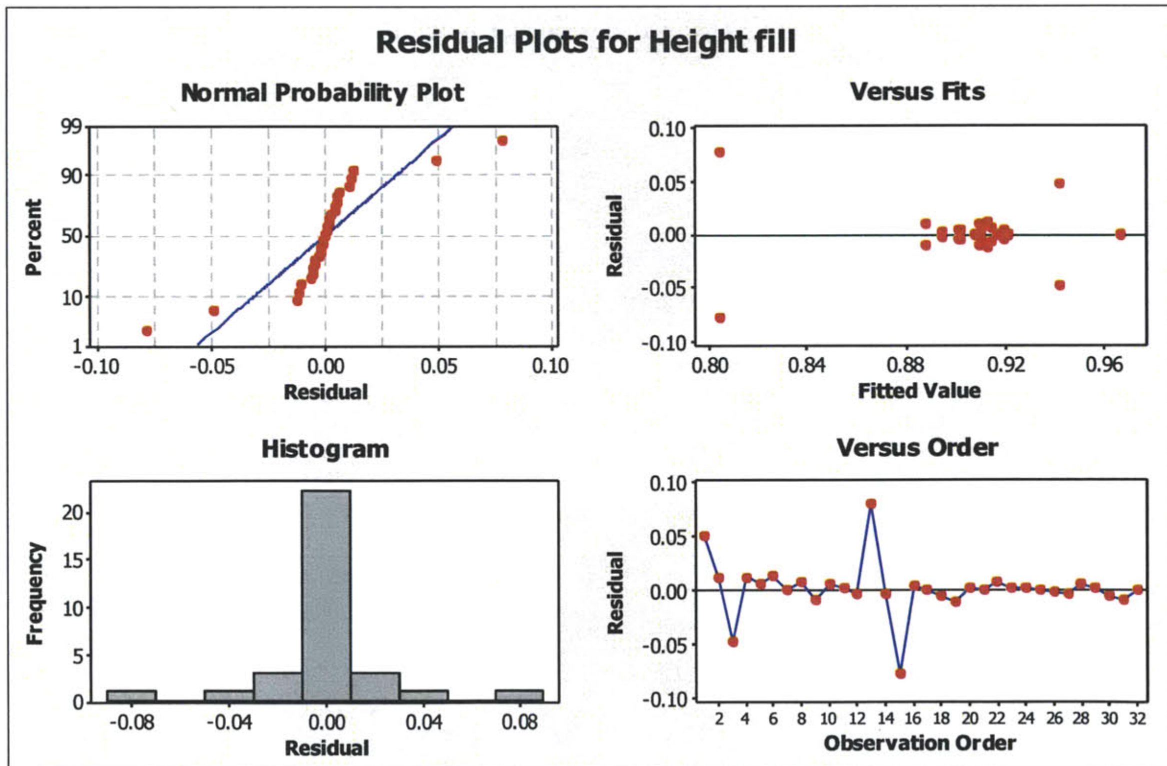

Figure 77 Residual Plot for Height Fill

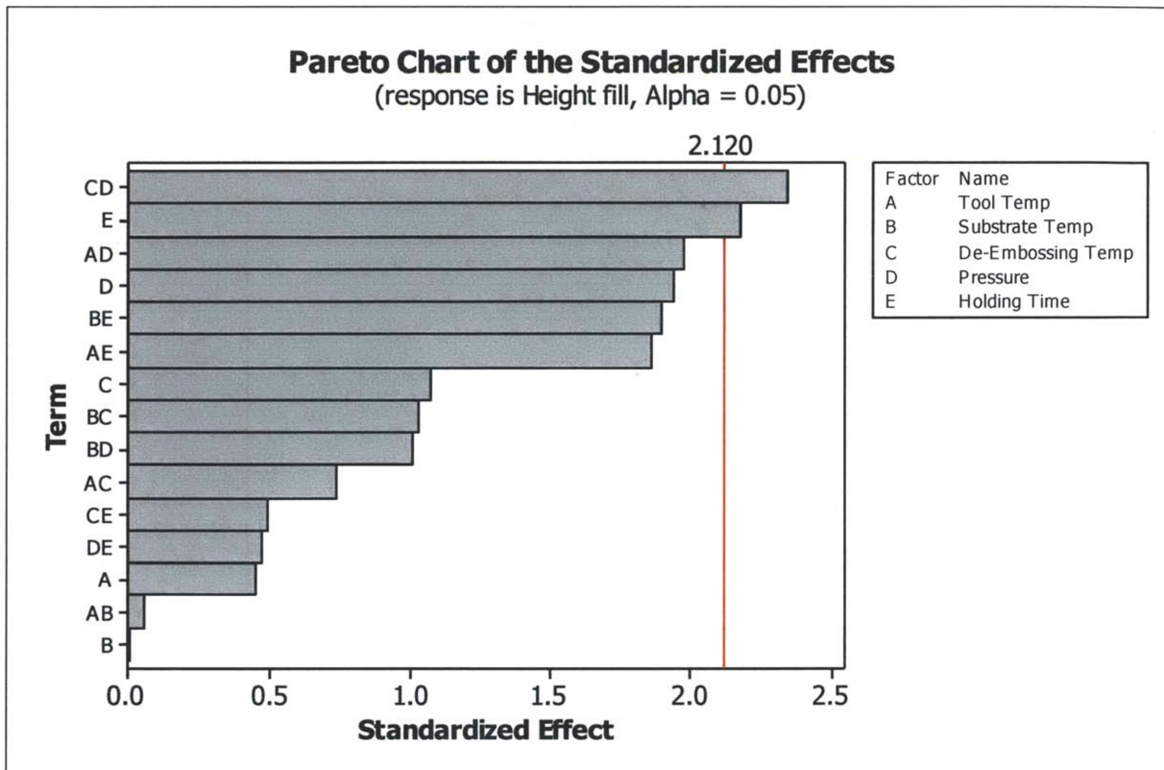

Figure 78 Pareto Chart for Height Fill

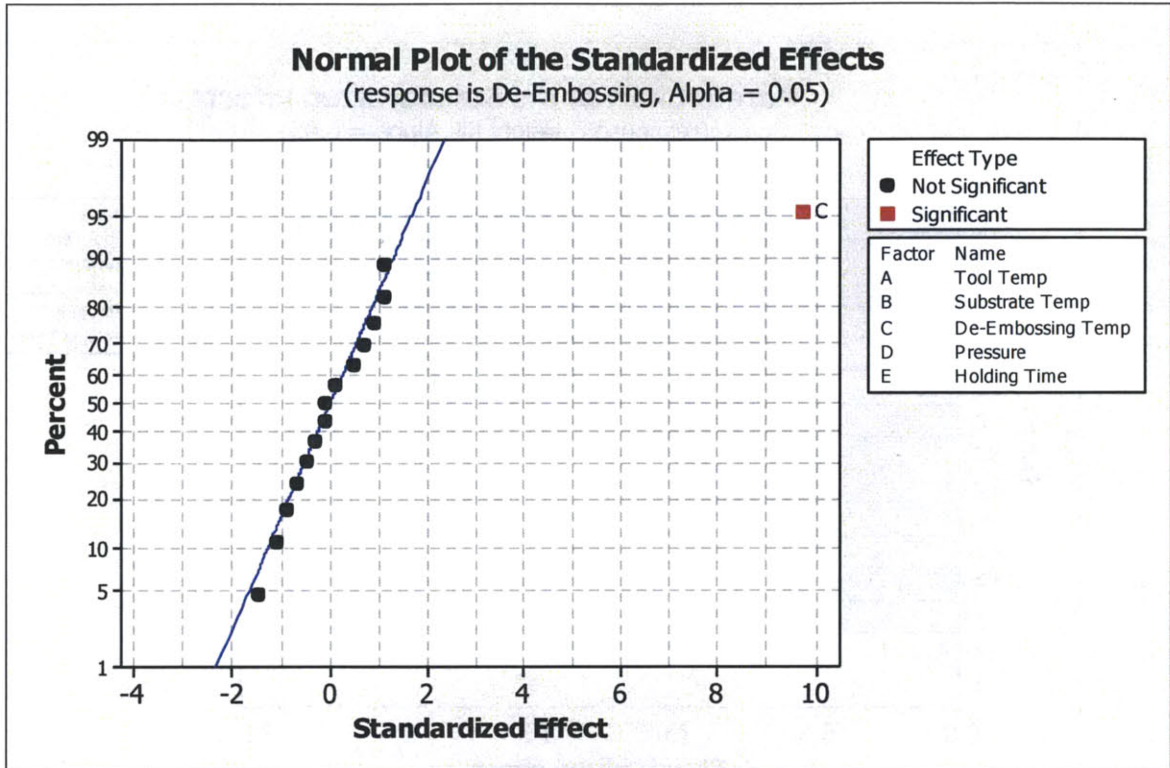

Figure 79 Normal Plot for De-Embossing Defects

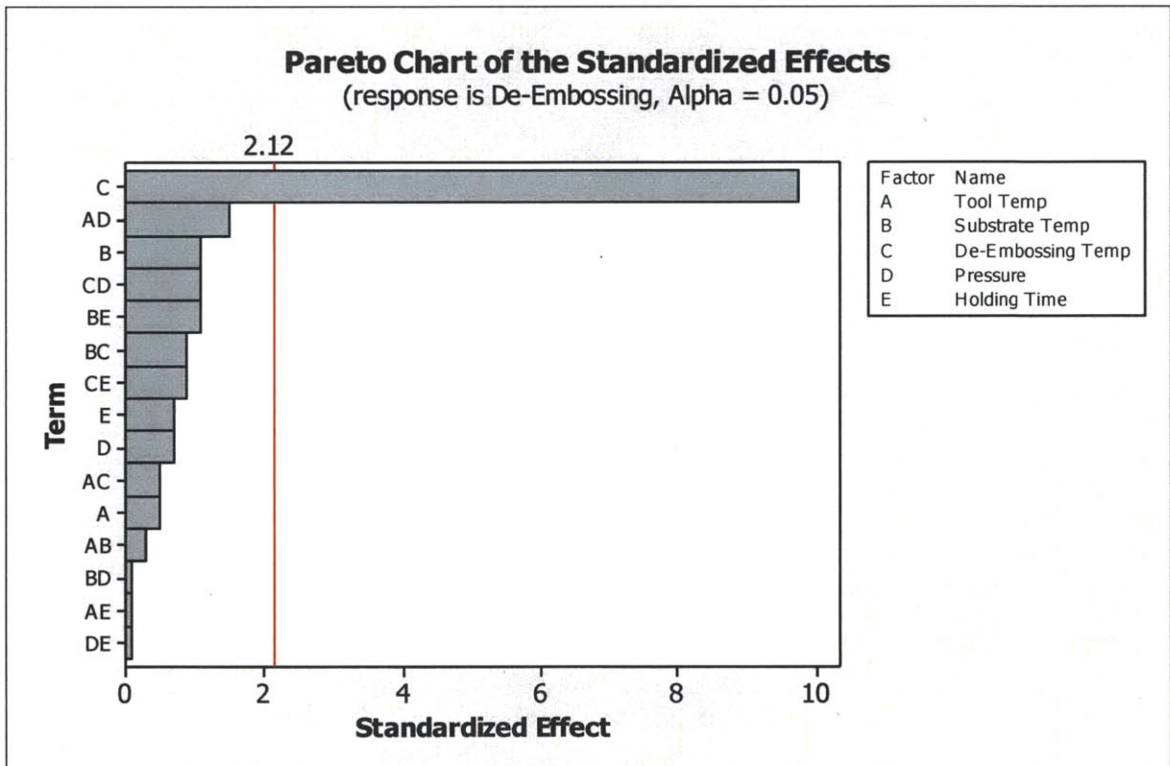

Figure 80 Pareto Chart for De-Embossing defects

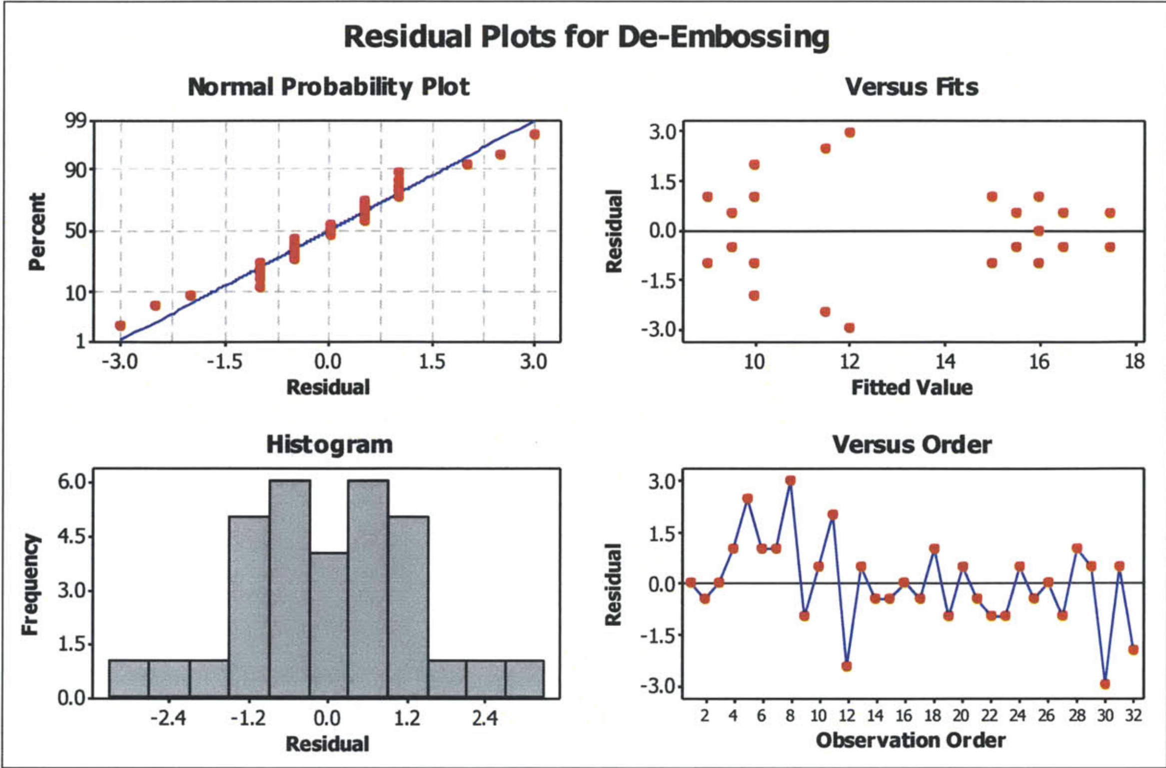

Figure 81 Residual Plot for De-embossing defects

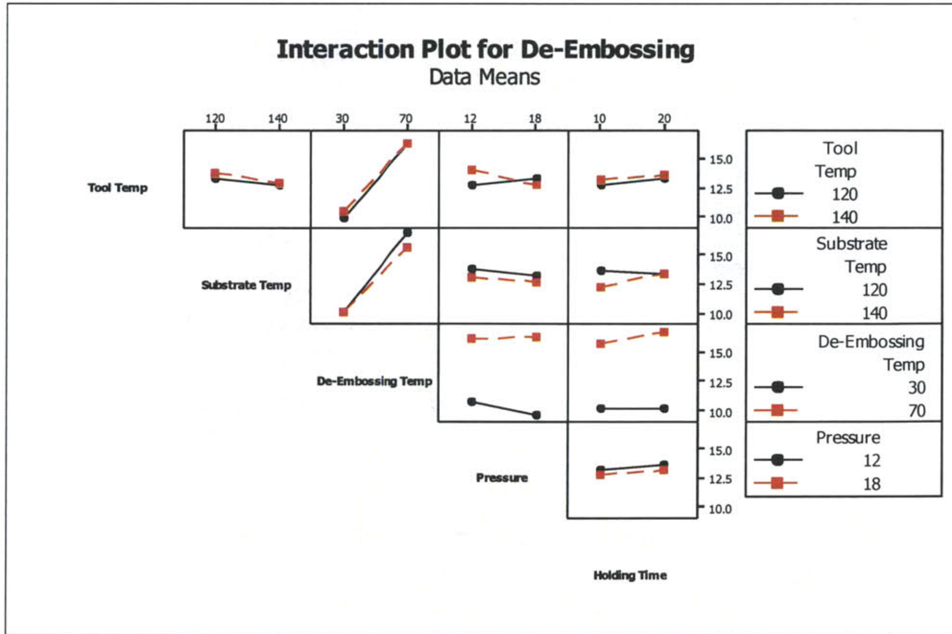

Figure 82 Interaction Effects for De-Embossing Defects

Factorial Fit: De-Embossing versus Tool Temp, Substrate Temp, ...

Estimated Effects and Coefficients for De-Embossing (coded units)

Term	Effect	Coef	SE Coef	T	P
Constant		13.1563	0.3172	41.48	0.000
Tool Temp	0.3125	0.1563	0.3172	0.49	0.629
Substrate Temp	-0.6875	-0.3437	0.3172	-1.08	0.294
De-Embossing Temp	6.1875	3.0937	0.3172	9.75	0.000
Holding Time	0.4375	0.2188	0.3172	0.69	0.500
Pressure	-0.4375	-0.2187	0.3172	-0.69	0.500
Tool Temp*Substrate Temp	-0.1875	-0.0937	0.3172	-0.30	0.771
Tool Temp*De-Embossing Temp	-0.3125	-0.1563	0.3172	-0.49	0.629
Tool Temp*Holding Time	-0.0625	-0.0312	0.3172	-0.10	0.923
Tool Temp*Pressure	-0.9375	-0.4687	0.3172	-1.48	0.159
Substrate Temp*De-Embossing Temp	-0.5625	-0.2813	0.3172	-0.89	0.388
Substrate Temp*Holding Time	0.6875	0.3437	0.3172	1.08	0.294
Substrate Temp*Pressure	0.0625	0.0313	0.3172	0.10	0.923
De-Embossing Temp*Holding Time	0.5625	0.2812	0.3172	0.89	0.388
De-Embossing Temp*Pressure	0.6875	0.3437	0.3172	1.08	0.294
Holding Time*Pressure	-0.0625	-0.0312	0.3172	-0.10	0.923

Figure 83 Co-efficient for the regression model for De-embossing defects

Estimated Coefficients for Height fill using data in uncoded units

Term	Coef
Constant	0.27178
Tool Temp	0.0101158
Substrate Temp	-0.00837953
De-Embossing Temp	0.00311641
Holding Time	0.0063541
Pressure	0.0431901
Tool Temp*Substrate Temp	3.53125E-06
Tool Temp*De-Embossing Temp	-2.18906E-05
Tool Temp*Holding Time	-2.22063E-04
Tool Temp*Pressure	-3.92188E-04
Substrate Temp*De-Embossing Temp	3.05781E-05
Substrate Temp*Holding Time	0.000225813
Substrate Temp*Pressure	0.000200521
De-Embossing Temp*Holding Time	-2.91562E-05
De-Embossing Temp*Pressure	-2.32552E-04
Holding Time*Pressure	-1.86042E-04

Figure 84 Co-efficient for the regression model for Height Fill

Estimated Coefficients for Width fill using data in uncoded units

Term	Coef
Constant	1.69792
Tool Temp	0.0051975
Substrate Temp	-0.0627141
De-Embossing Temp	-0.0195291
Holding Time	0.136196
Pressure	0.224761
Tool Temp*Substrate Temp	0.000340875
Tool Temp*De-Embossing Temp	-7.31250E-06
Tool Temp*Holding Time	-7.56250E-04
Tool Temp*Pressure	-0.00192417
Substrate Temp*De-Embossing Temp	0.000142781
Substrate Temp*Holding Time	0.000037375
Substrate Temp*Pressure	0.000541458
De-Embossing Temp*Holding Time	-3.53125E-05
De-Embossing Temp*Pressure	0.000180938
Holding Time*Pressure	-0.00230875

Figure 85 Co-efficient for Regression Model for Width Fill

References

[1] WHO, 2006, AIDS Epidemic Update.

[2] Cheng X., Irimia D., Dixon M., Ziperstein J. C., Demirci U., Zamir L., Tompkins R. G., Toner M., and Rodriguez W. R., 2007, "A Microchip Approach for Practical Label-Free CD4+T-Cell Counting of HIV-Infected Subjects in Resource-Poor Settings," Basic Science, **45**(3), pp. 257–261.

[3] Peter T., Badrichani A., Wu E., Freeman R., Ncube B., Ariki F., Daily J., Shimada Y., and Murtagh M., 2008, "Challenges in implementing CD4 testing in resource-limited settings.," Cytometry. Part B, Clinical cytometry, **74 Suppl 1**(January), pp. S123–30.

[4] Pratt E. D., Huang C., Hawkins B. G., Gleghorn J. P., and Kirby B. J., 2011, "Rare Cell Capture in Microfluidic Devices.," Chemical engineering science, **66**(7), pp. 1508–1522.

[5] Dirckx M. E., and Hardt D. E., 2011, "Analysis and characterization of demolding of hot embossed polymer microstructures," Journal of Micromechanics and Microengineering, **21**(8), p. 085024.

[6] Lin M., Yeh J., Chen S., Chien R., Hsu C., and Chuck B., 2013, "Study on the replication accuracy of polymer hot embossed microchannels ⍰ Baffle," **42**, pp. 55–61.

[7] Becker H., and Heim U., 2000, "Hot embossing as a method for the fabrication of polymer high aspect ratio structures," Sensors and Actuators A: Physical, **83**(1-3), pp. 130–135.

[8] Tran N. K., Lam Y. C., Yue C. Y., and Tan M. J., 2010, "Manufacturing of an aluminum alloy mold for micro-hot embossing of polymeric micro-devices," Journal of Micromechanics and Microengineering, **20**(5), p. 055020.

[9] Hale M., 2009, "Development of a Low Cost, Rapid-Cycle Hot Embossing System for Microscale Parts."

[10] Koerner T., Brown L., Xie R., and Oleschuk R. D., 2005, "Epoxy resins as stamps for hot embossing of microstructures and microfluidic channels," Sensors and Actuators B: Chemical, **107**(2), pp. 632–639.

[11] Figeys D., and Pinto D., 2004, Lab-on-a-Chip : A Revolution in Biological and Medical Sciences A look at some of the basic concepts and.

[12] Beebe D. J., Mensing G. a, and Walker G. M., 2002, "Physics and applications of microfluidics in biology.," Annual review of biomedical engineering, **4**, pp. 261–86.

[13] Schudel B. R., Choi C. J., Cunningham B. T., and Kenis P. J. a, 2009, "Microfluidic chip for combinatorial mixing and screening of assays.," Lab on a chip, **9**(12), pp. 1676–80.

[14] Leu T.-S., and Chang P.-Y., 2004, "Pressure barrier of capillary stop valves in micro sample separators," Sensors and Actuators A: Physical, **115**(2-3), pp. 508–515.

[15] Love J. C., Wolfe D. B., Jacobs H. O., and Whitesides G. M., 2001, "Microscope Projection Photolithography for Rapid Prototyping of Masters with Micron-Scale Features for Use in Soft Lithography," Langmuir, **17**(19), pp. 6005–6012.

[16] Sia S. K., and Whitesides G. M., 2003, Microfluidic devices fabricated in poly(dimethylsiloxane) for biological studies.

[17] Singleton L., 2003, "Manufacturing Aspects of LIGA Technologies," Journal of Photopolymer Science and Technology, **16**(3), pp. 413–422.

[18] Berkeley U. C., and David A., 2004, "A Study of Surface Roughness in the Micro-End-Milling Process," Consortium on Deburring and Edge Finishing,.

[19] Lee K. S., and Kim K., 2010, "Analysis of unavoidable geometric errors in the side wall of end-milled parts for corner surface," Journal of Mechanical Science and Technology, **23**(2), pp. 525–535.

[20] Attia U. M., Marson S., and Alcock J. R., 2009, "Micro-injection moulding of polymer microfluidic devices," Microfluidics and Nanofluidics, **7**(1), pp. 1–28.

[21] Niggemann M., Ehrfeld W., and Weber L., "Fabrication of miniaturized biotechnical devices," SPIE - The International Society for Optical Engineering, Santa Clara, CA, pp. 204–213.

[22] Pirskanen, Immonen, Kalima, Pietarinen, Siitonen, Kuittinen, Mönkkönen, Pakkanen, Suvanto, Pääkkönen E. J. ., 2005, "Replication of sub-micrometre features using microsystems technology," Plastics, Rubber and Composites, **34**(5-6), pp. 222–226.

[23] Lorenz H., Despont M., Vettiger P., and Renaud P., 1998, "Fabrication of photoplastic high-aspect ratio microparts and micromolds using SU-8 UV resist," Microsystem Technologies, **4**(3), pp. 143–146.

[24] Wang Q., 2006, "Process Window Characterization and Process Variation Identification of Micro Embossing Process."

[25] Tran N. K., Lam Y. C., Yue C. Y., and Tan M. J., 2010, "Manufacturing of an aluminum alloy mold for micro-hot embossing of polymeric micro-devices," Journal of Micromechanics and Microengineering, **20**(5), p. 055020.

[26] Chien R.-D., 2006, "Hot embossing of microfluidic platform," International Communications in Heat and Mass Transfer, **33**(5), pp. 645–653.

[27] Mekaru H., Yamada T., Yan S., and Hattori T., 2004, "Microfabrication by hot embossing and injection molding at LASTI," Microsystem Technologies, **10**(10), pp. 682–688.

[28] Hale M., 2009, "Development of a Low Cost, Rapid-Cycle Hot Embossing System for Microscale Parts."

[29] Sun H. L., Liu C., Li M. M., Liang J. S., and Chen H. H., 2009, "Study on Replication of Densely Patterned, High-Depth Channels on a Polymer Substrate Using Hot Embossing Techniques," Materials Science Forum, **628-629**, pp. 411–416.

[30] Leveder T., Landis S., Davoust L., Soulan S., and Chaix N., 2007, "Demolding strategy to improve the hot embossing throughput," **6517**, p. 65170N–65170N–8.

[31] Guo Y., Liu G., Xiong Y., and Tian Y., 2007, "Study of the demolding process—implications for thermal stress, adhesion and friction control," Journal of Micromechanics and Microengineering, **17**(1), pp. 9–19.

[32] Guo Y., Liu G., Xiong Y., and Tian Y., 2007, "Study of the demolding process—implications for thermal stress, adhesion and friction control," Journal of Micromechanics and Microengineering, **17**(1), pp. 9–19.

[33] Liu C., Li J. M., Liu J. S., and Wang L. D., 2010, "Deformation behavior of solid polymer during hot embossing process," Microelectronic Engineering, **87**(2), pp. 200–207.

[34] Ragosta N., 2013, "Design and Measurement Analysis of a Hot Embossing Machine for High Aspect Ratio Mico-Features."

[35] Chien R.-D., 2006, "Hot embossing of microfluidic platform," International Communications in Heat and Mass Transfer, **33**(5), pp. 645–653.

[36] Hale M., 2009, "Development and Testing of a Low-Cost Rapid-Cycle Hot Embossing System for Manufacturing Microscale Parts," Massachusetts Institute of Technology.

[37] Heckele M. W. 2006, "Modeling and optimization of the hot embossing process for micro- and nanocomponent fabrication," Journal of Micro/Nanolithography, MEMS, and MOEMS, **5**(1).

[38] M. Heckele, W. Bacher K. D. M., 1998, "Hot embossing - The molding technique for plastic microstructures," Microsystem Technologies, **4**(3), pp. 122–124.

[39] Dirckx M. E., 2010, "Demolding of Hot Embossed Polymer Microstructures."

[40] Nguyen K., 2013, "Design of a Hot Embossing Machine and Tool Design for micro-features with High Aspect Ratios."

[41] Montgomery D. C., 2009, Introduction to Statistical Process Control.